ACCOUNT AND AADHAAR NUMBER AS A POLYNOMIAL

Megha Manoharan[1], M. Yamuna[2]

[1,2] *VIT University, Vellore,(India)*

ABSTRACT

With everything becoming online, there is an urgent need to ensure security of the information. The data security can be exponentially increased if the data is sent through secure transfer protocols and encryption. We all have so much different data that require remembering as well as safe data transfer. In this paper we propose a method of encrypting the bank account number and aadhaar number together as a polynomial.

Keywords*: *Decryption, Encryption, Account Number, Aadhaar Number.

I. INTRODUCTION

Account numbers are unique numbers given to all individuals who have an account in a bank. It requires to be kept safely with that particular individual himself. The aadhaar number is also an identity number which is unique for each and every individual in our country and should be kept safe and private. These numbers can reveal your identity to anyone. It can also reveal all your personal details. Hence it should be maintained safe. In this paper we propose a method of encrypting an account number and an aadhaar number together. In [1] a doubly secured authentication scheme which uses RKO technique to login is proposed. [1]. In [2] Venn diagrams are used as tool for encryption. Many mathematics concepts are used as a tool for encryption. In this paper we propose a method where a polynomial is used as a tool for encryption.

II. PRELIMINARY NOTE

In this section we provide few discussions used in the encryption of the aadhaar number and the account number

2. 1 Account Number

A bank account is a financial account between a bank customer and a financial institution. A bank account can be a deposit account, a credit card, or any other type of account offered by a financial institution. The financial transactions which have occurred within a given period of time on a bank account are reported to the customer on a bank statement and the balance of the account at any point in time is the financial position of the customer with the institution [3].

2.2 Aadhaar Number

Adhaar is a 12 digit individual identification number issued by the Unique Identification Authority of India on behalf of the Government of India. This number will serve as a proof of identity and address, anywhere in India[4].

III PROPOSED METHOD

In this paper we propose a method of encrypting details of aadhaar number and bank account number. We convert the details of these numbers into a polynomial which is then encrypted.

3. 1 Polynomial Construction

We basically have a string of numbers. The variable of the polynomial is taken as x. An account number of maximum length 10 which are numbers 0 – 9. The account number is many times of length less than 12. In such cases we shall assign a value 10 to the last characters.

We shall use alphabets a, b, …, k to indicate the numbers 0 – 10 in the account number.

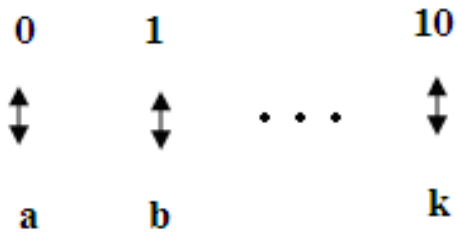

Chart – 1

An aadhaar number is of length 12 containing the numbers 0 – 9. We shall assign the values x, x^2, …., x^{10} to these numbers.

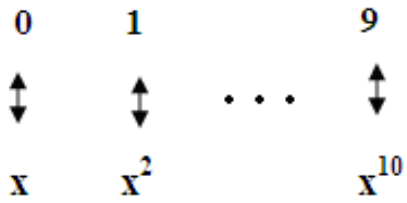

Chart – 2

Let the string of account number be denoted by a1, a2, …,a12 and the string of the aadhaar number be represented by b1, b2,…., b12. Concatenating these two strings we generate a single string a1, b1, a2,b2,…., a12 , b12. We now divide them into segments of size two as (a1 b1) (a2 b2)… (a12 b12). We then replace this string by the corresponding values from Chart – 1 and Chart – 2. We finally add them to generate a polynomial.

3. 2 Graph Construction

Using Chart – 1 and Chart – 2 we can construct a graph as follows

X – axis Label the coordinates of the X – axis as a, b, c,…, k

Y – axis Label the coordinates of the Y – axis as x, x^2,…, x^{10}

Draw a graph as follows

For the points (a1 b1) (a2 b2)… (a12 b12) generated in Sec 3. 1draw lines directed from ai to bi, i = 1, 2,… , 12 and label the line values as 1, 2, …., 12.

Let the account number and aadhaar number to be encrypted be

ACCOUNT NUMBER: 6 1 2 8 6 7 7 9 0 6

AADHAAR NUMBER: 2 6 1 7 5 4 2 5 5 4 9 3

The account number is of length 10 so we replace it by a string of length 10 as 6 1 2 8 6 7 7 9 0 6 10 10

3. 3 Encryption Algorithm

Step 1 Combine both the account number and aadhaar number as a single string S ie., alternate Characters represent account and aadhaar numbers respectively starting with the account number.

For the picked example the string generated is

S: 6 2 1 6 2 1 8 7 6 5 7 4 7 2 9 5 0 5 6 4 10 9 10 3

Step 2 Convert the string S into a polynomial as explained in Sec 3. 1

For the string S we first divide it into segments of size 2 as

(6 2), (1 6), (2 1), (8 7), (6 5), (7 4), (7 2), (9 5), (0 5), (6 4), (10 9), (10 3)

Replacing them by the corresponding values from Chart – 1 and Chart – 2 we generate

(f x^3), (b x^7), (c x^2), (i x^8), (g x^6), (h x^5), (h x^3), (j x^6), (a x^6), (g x^5), (k x^{10}), (k x^4).

Combining them we generate the polynomial

$f x^3 + bx^7 + c x^2 + i x^8 + g x^6 + h x^5 + h x^3 + j x^6 + a x^6 + g x^5 + k x^{10} + k x^4$.

Step 3 Construct the graph as given in Sec 3.2.

Step 4 Send the polynomial or the graph to the receiver.

We finally send the following polynomial to the receiver

$\mathbf{f x^3 + bx^7 + c x^2 + i x^8 + g x^6 + h x^5 + h x^3 + j x^6 + a x^6 + g x^5 + k x^{10} + k x^4.}$

Suppose the received message is

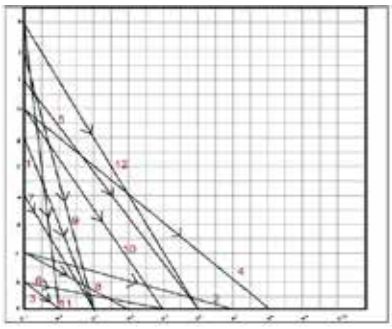

Splitting them into string of length 2 we get

First pick the lines with labels 1, 2, …, 12. From the graph graph it is seen that the lines are directed as

(g x^3), (c x^7), (b x^2), (h x^8), (i x^6), (b x^5), (e x^3), (c x^4), (j x^3), (h x^5), (k x^2), (k x^6)

Using Chart – 1 and Chart – 2 the string get converted as

(6 2), (2 6), (1 1), (7 7), (8 5), (1 4), (4 2), (2 3), (9 2), (7 4), (10 1), (10 5)

So the message is decrypted as

Account Number: 6 2 1 7 8 1 4 2 9 7 10 10

Aadhaar Number: 2 6 1 7 5 4 2 3 2 4 1

IV CONCLUSION

Account and aadhaar number are encrypted as a single string. A polynomial is a mathematical expression and it has nothing related to account or aadhaar numbers. The polynomial has no meaning on its own. If encrypted as a graph, then the one will try to decrypt the details using the labeling of the X and Y axis. But the data provided in these axis have nothing to do with the encrypted data and hence tough to be decrypted. Moreover numerous details related to polynomials and graphs are available in public domain such that it is tough to find the difference between original and fake polynomials. So the proposed method is efficient for encryption of aadhaar and account number.

REFERENCES

[1] Moushmee Kuri, Tanuja Sarode, Doubly Secured Authentication Scheme using RKO technique of Visual Cryptography, International Journal of Engineering And Science Vol.4, Issue 5 (May 2014), PP 16-20.

[2] Parijit Kedia, Sumeet Agrawal, Encryption using Venn-Diagrams and Graph, International Journal of Advanced Computer Technology, VOLUME 4, NUMBER 1, 94 – 99

[3] http://en.wikipedia.org/wiki/Bank_account

[4] http://uidai.gov.in/what-is-aadhaar.html

MATLAB PROGRAM FOR MINIMUM WEIGHTED SPANNING TREE USING DOMINATING SET

M. Yamuna[1] and K. Karthika[2]

[1,2]*School of Advanced Sciences, VIT University, Vellore, (India)*

ABSTRACT

Finding a minimum weighted spanning tree is an important problem as it has many applications. Finding minimum weighted spanning tree using graph properties is not in much use. In this paper we provide a MATLAB Programme, for generating a minimum weighted spanning tree using adjacency matrix.

Keywords: Adjacency matrix, Dominating set, Graph domination, Spanning tree

I INTRODUCTION

In the 1950's, many people contributed to the minimum spanning tree problem. Among them were R. C. Prim and J. B. Kruskal, whose algorithms are very widely used today. Prims algorithm grows a spanning tree from a given tree from a given vertex of a connected weighted graph G, iteratively adding the cheapest edge from a vertex already reached to a vertex not yet reached, finishing when all the vertices of *G* have been reached [1]. Kruskal's algorithm maintain an acyclic spanning subgraph H, enlarging it by edges with low weight to form a spanning tree, by considering edges in non decreasing order of weight, breaking ties arbitrarily [2].

In [3], M. Yamuna et al have provided a procedure for generating a minimum weighted spanning tree by using minimum domination set and adjacency matrix. In this paper we provide a MATLAB Programme, for generating a minimum weighted spanning tree using adjacency matrix.

II MATERIALS AND METHODS

A spanning tree of G is a subgraph of G that is a tree containing every vertex of G. A spanning forest of a graph G is forest that contains every vertex of G such that two vertices are in the same tree of the forest when there is a path in G between these two vertices.

A graph G is said to be a weighted graph if its edges are assigned some weight. A minimum weighted spanning tree in a connected weighted graph is a spanning tree that has the smallest possible sum of weights of its edges.

An adjacency matrix of a graph G with n vertices that are assumed to be ordered from v_1 to v_n is defined by,

$$A = [\, a_{ij} \,]_{n \times n} = \begin{cases} 1 & \text{if there exist an edge between } v_i \text{ and } v_j \\ 0 & \text{otherwise} \end{cases}$$

Adjacency matrix is also used to represent weighted graphs. If $[\, a_{ij} \,] = w$, then there is an edge from vertex v_i to vertex v_j with weight w. For properties related to graph theory we refer to [4].

A set of vertices D in a graph G = (V, E) is a dominating set if every vertex of V − D is adjacent to some vertex of D. If D has the smallest possible cardinality of any dominating set of G, then D is called a minimum

dominating set. The cardinality of any minimum dominating set for G is called the domination number of G and it is denoted by γ (G). γ – set denotes a dominating set for G with minimum cardinality.The open neighborhood of vertex v Î V (G) is denoted by N (v) = { u Î V (G) | (uv) Î E (G) }, while its closed neighborhood is the set N [v] = N(v) È { v }. The private neighborhood of v Î D is denoted by pn [v, D], is defined by pn [v, D] = N (v) – N (D − { v }). For properties related to domination theory we refer to [5].

Graph Domination

In [3], M. Yamuna et al have defined a γ - set D Î V as a graph domination set if D covers all the vertices and edges of G. A γ – set D of G that satisfies this property is denoted by γ_G(G).

In all the graphs circled vertices represent a g - set D.

Example

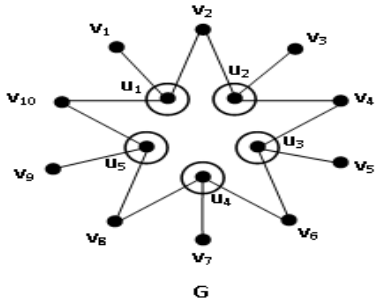

Fig. 1

The graph G in Fig. 1 is a graph domination graph. The γ – set { u_1, u_2, u_3, u_4, u_5 } covers all the edges and vertices of G.

In [3], they have proved the following result

R1. Let G be a weighted connected graph with n vertices and D be a γ - set for G that covers all the edges of G. Then there is a spanning tree T for G such that

1. γ (G) = γ (T).
2. T is minimum weighted.

Given any weighted graph G a minimum weighted spanning tree can be obtained using the following steps.

Step 1 Consider the vertices in D, where D is a graph dominating g - set for G.

Step 2 Include the private neighbor of every vertex in D.

Step 3 Include the 2 dominated vertices (taking care to pick the edge with smallest weight).

Step 4 Combine the spanning forest into a spanning tree by including an edge with minimum weight each time.

Spanning tree generation using the above steps is given in the following example for the graph in Fig. 2.

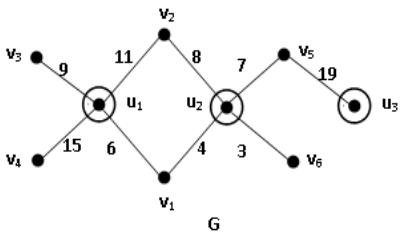

Fig. 2

By using R1 and the steps, we can generate a minimum weighted spanning tree from a weighted graph.

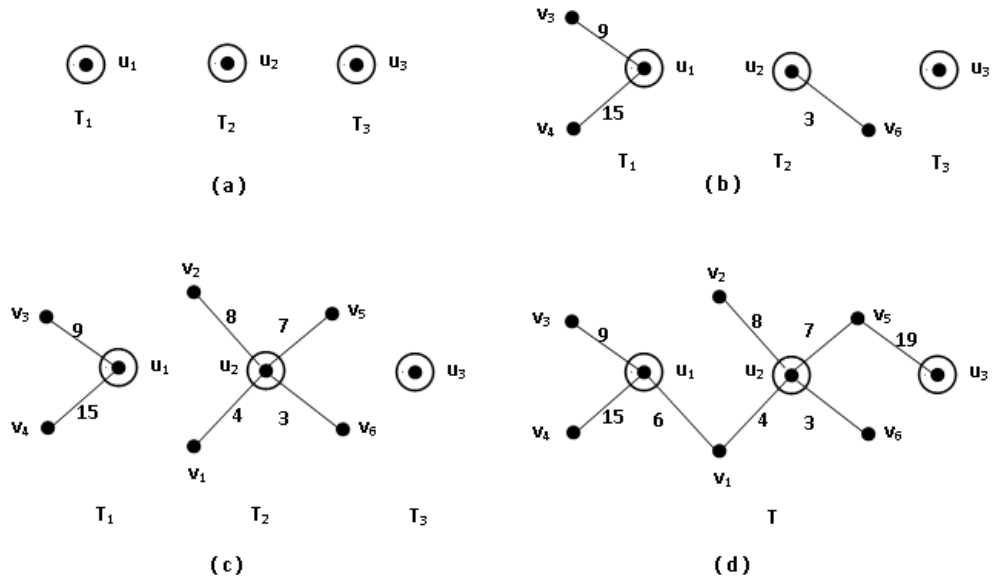

Fig. 3

In Fig. 3,

(a) The graph represents the spanning forest that contain vertices in D = { u_1, u_2, u_3 } only.

(b) The tree partially constructed by adding minimum weighted edges belonging to pn[u_1, D] and pn [u_2, D], where pn [u_1, D] = { v_3, v_4 }, pn [u_2, D] = { v_6 }.

(c) The tree partially constructed by adding minimum weighted edges belonging to 2 – dominated vertices.

(d) Minimum weighted spanning tree generated from D. The weight of this spanning tree is equal to 71.

Adjacency Matrix Using γ - set

In this procedure from [3], G is a weighted connected, graph domination graph with n vertices. Let D = {u_1, u_2, . . . , u_k }, and V − D = {v_1, v_2, . . . , v_m}, k + m = n. Let X be the adjacency matrix of G. For comfort of discussion, let us arrange the rows and columns of X as follows

$$X = \begin{bmatrix} X_{11} & X_{12} \\ X_{21} & X_{22} \end{bmatrix}$$

where X11 represents adjacency between vertices in D, X12 and X21 between vertices in D and V – D and X22 between vertices in V − D. In a graph domination graph, since V − D is independent, X22 is a null matrix. Using these notations and procedure we have developed the MATLAB code.

MATLAB Code for Generating Minimum Weighted Spanning Tree

Using the above explained procedure and adjacency matrix X we have developed a MATLAB program for the same. The coding part of the program is given inn snapshots 1,2.

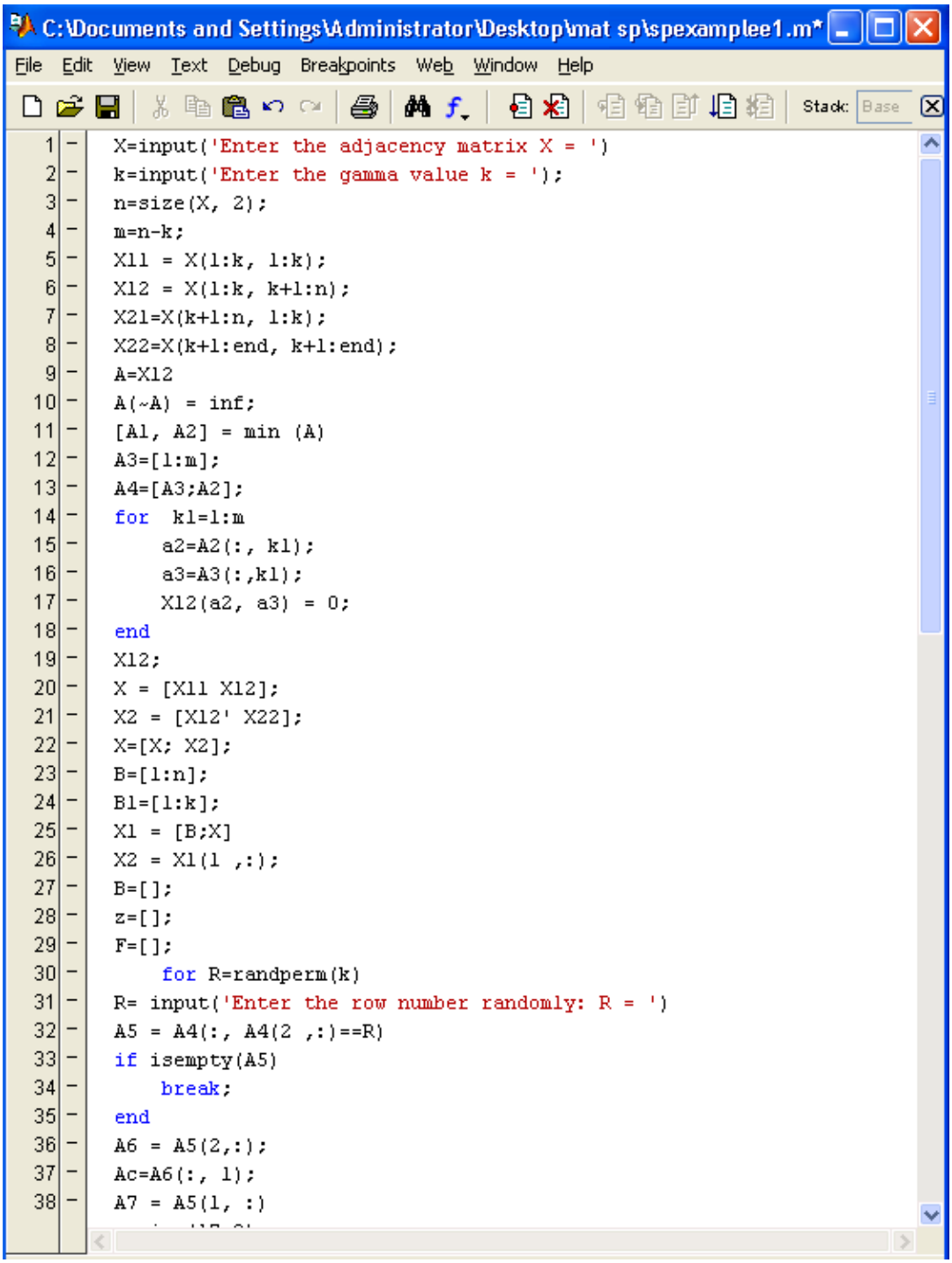
C:\Documents and Settings\Administrator\Desktop\mat sp\spexamplee1.m*
File Edit View Text Debug Breakpoints Web Window Help
Stack: Base
X=input('Enter the adjacency matrix X = ')
k=input('Enter the gamma value k = ');
n=size(X, 2);
m=n-k;
X11 = X(1:k, 1:k);
X12 = X(1:k, k+1:n);
X21=X(k+1:n, 1:k);
X22=X(k+1:end, k+1:end);
A=X12
A(~A) = inf;
[A1, A2] = min (A)
A3=[1:m];
A4=[A3;A2];
for k1=1:m
a2=A2(:, k1);
a3=A3(:,k1);
X12(a2, a3) = 0;
end
X12;
X = [X11 X12];
X2 = [X12' X22];
X=[X; X2];
B=[1:n];
B1=[1:k];
X1 = [B;X]
X2 = X1(1 ,:);
B=[];
z=[];
F=[];
for R=randperm(k)
R= input('Enter the row number randomly: R = ')
A5 = A4(:, A4(2 ,:)==R)
if isempty(A5)
break;
end
A6 = A5(2,:);
Ac=A6(:, 1);
A7 = A5(1, :)

Snapshot 1

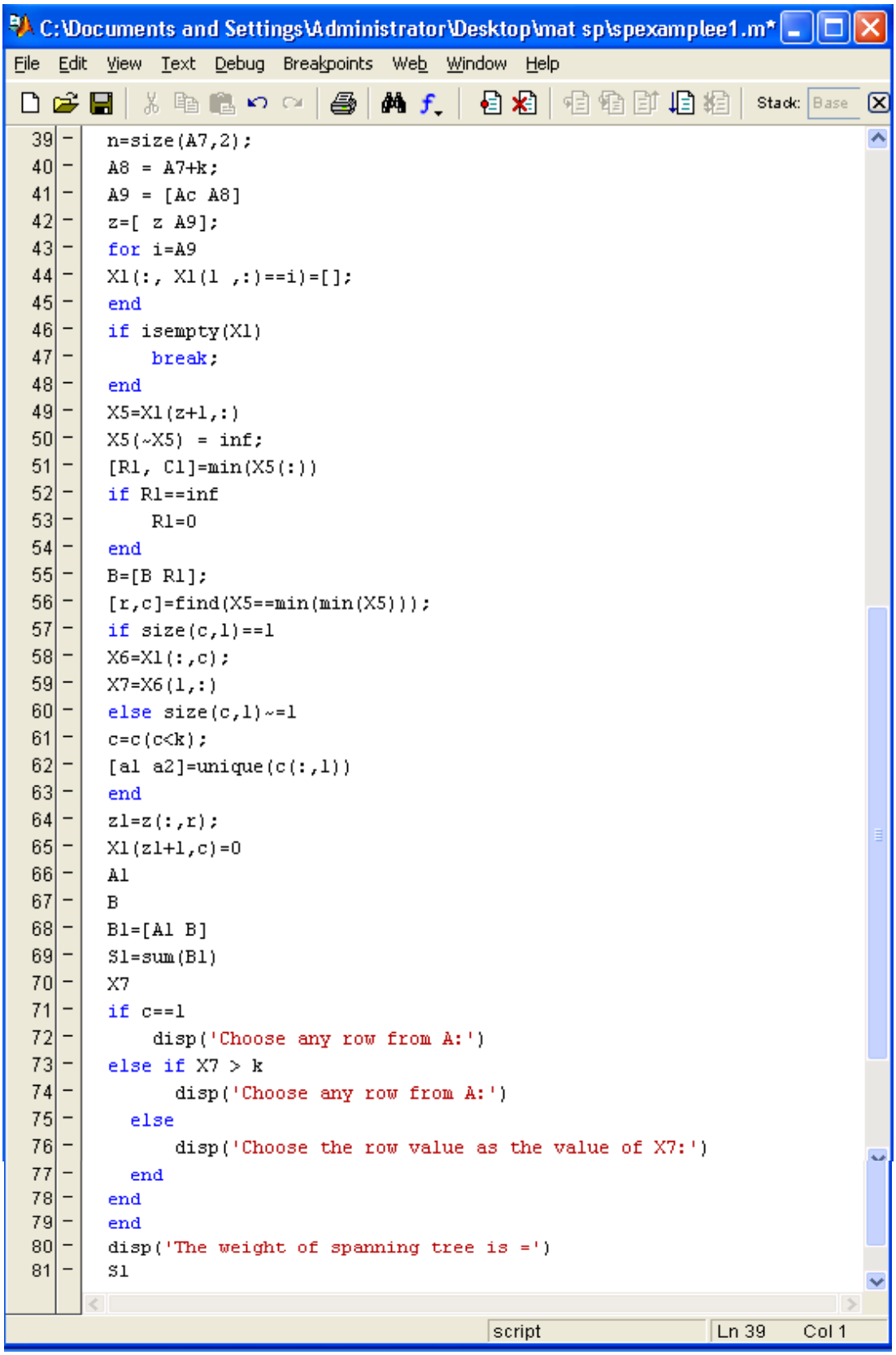
C:\Documents and Settings\Administrator\Desktop\mat sp\spexamplee1.m*
File Edit View Text Debug Breakpoints Web Window Help
Stack: Base
n=size(A7,2);
A8 = A7+k;
A9 = [Ac A8]
z=[z A9];
for i=A9
Xl(:, Xl(l ,:)==i)=[];
end
if isempty(Xl)
break;
end
X5=Xl(z+l,:)
X5(~X5) = inf;
[Rl, Cl]=min(X5(:))
if Rl==inf
Rl=0
end
B=[B Rl];
[r,c]=find(X5==min(min(X5)));
if size(c,l)==l
X6=Xl(:,c);
X7=X6(l,:)
else size(c,l)~=l
c=c(c<k);
[al a2]=unique(c(:,l))
end
zl=z(:,r);
Xl(zl+l,c)=0
Al
B
Bl=[Al B]
Sl=sum(Bl)
X7
if c==l
disp('Choose any row from A:')
else if X7 > k
disp('Choose any row from A:')
else
disp('Choose the row value as the value of X7:')
end
end
end
disp('The weight of spanning tree is =')
Sl
script
Ln 39 Col 1

Snapshot 2

III RESULTS AND DISCUSSION

Output Verification

In this section we provide verification for few graphs using the above coding.

Example 1

We consider the adjacency matrix of Fig. 2. and verify the weight of spanning tree.

Snap shot 3 provides the input matrix for the graph in Fig. 2.

Snapshot 3

Snapshot 4 provides the out put matrix for the matrix in snapshot 3. Here the cardinality of the g - value is 3. So when k = 3, the submatrix A generated is also seen in snapshot 4.

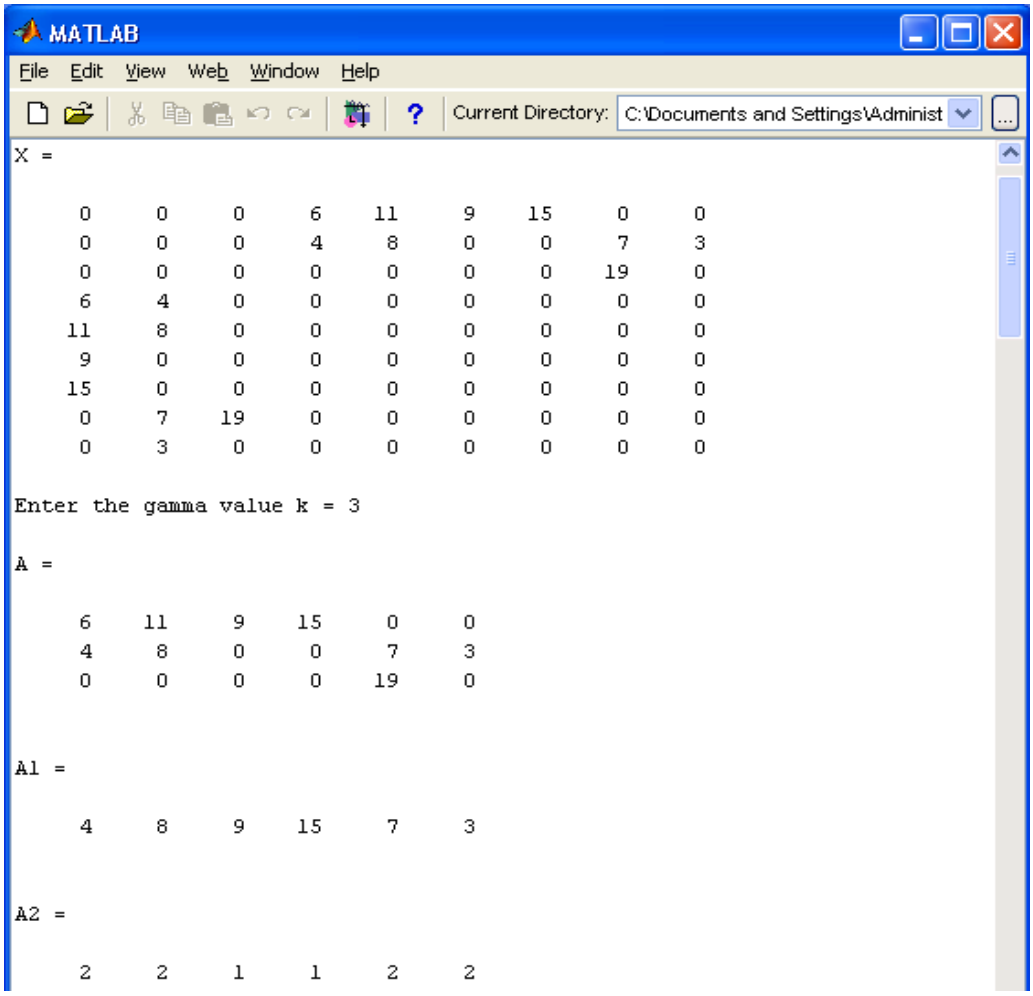

Snapshot 4

In the following snapshots 5 – 7, Xi represents the reduced matrix obtained in each stage, R represents the row selected in each execution, R1 the minimum value in each stage.

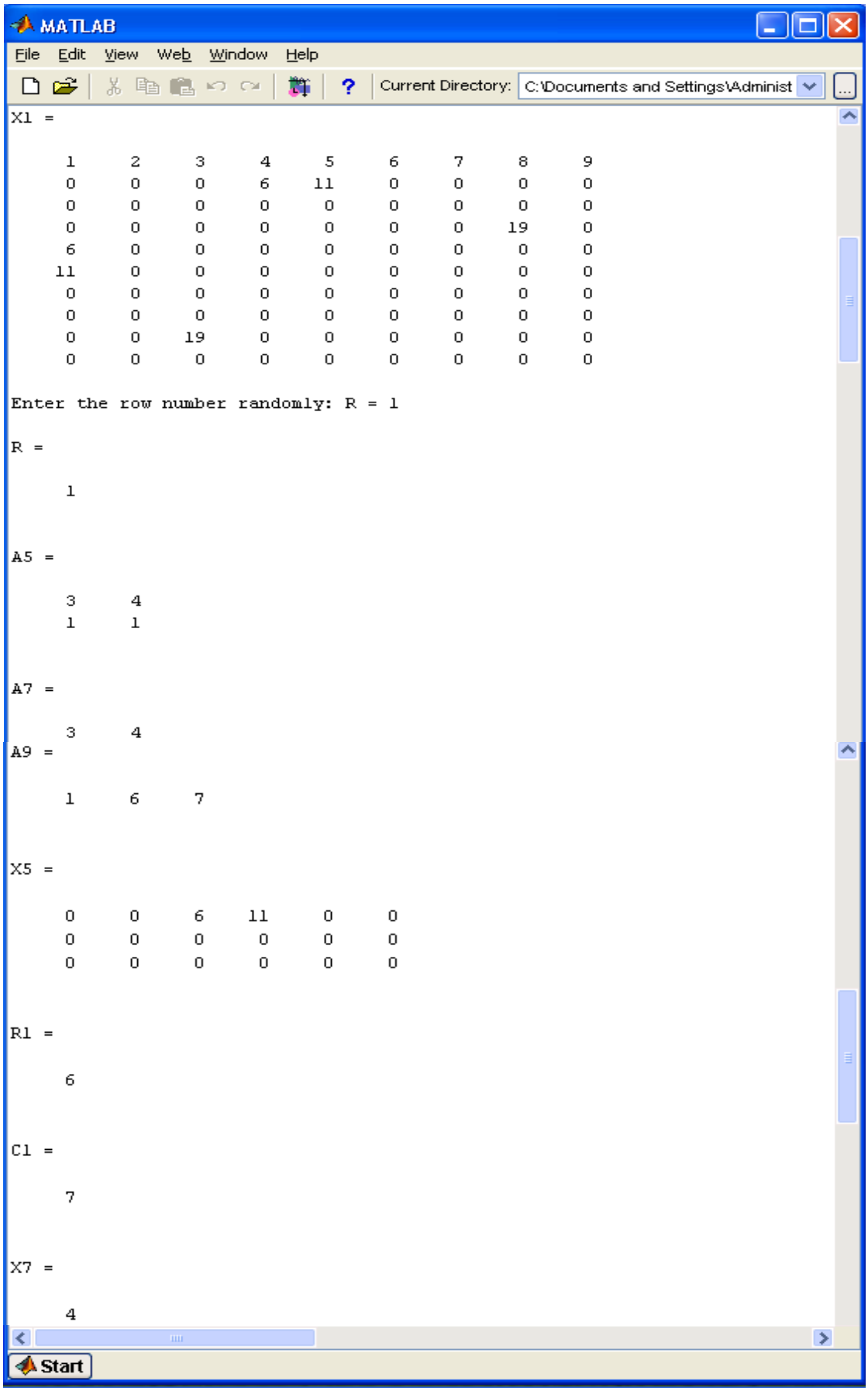
MATLAB
File Edit View Web Window Help
Current Directory: C:\Documents and Settings\Administ
X1 =
1 2 3 4 5 6 7 8 9
0 0 0 6 11 0 0 0 0
0 0 0 0 0 0 0 0 0
0 0 0 0 0 0 0 19 0
6 0 0 0 0 0 0 0 0
11 0 0 0 0 0 0 0 0
0 0 0 0 0 0 0 0 0
0 0 0 0 0 0 0 0 0
0 0 19 0 0 0 0 0 0
0 0 0 0 0 0 0 0 0
Enter the row number randomly: R = 1
R =
1
A5 =
3 4
1 1
A7 =
3 4
A9 =
1 6 7
X5 =
0 0 6 11 0 0
0 0 0 0 0 0
0 0 0 0 0 0
R1 =
6
C1 =
7
X7 =
4
Start

Snapshot 5

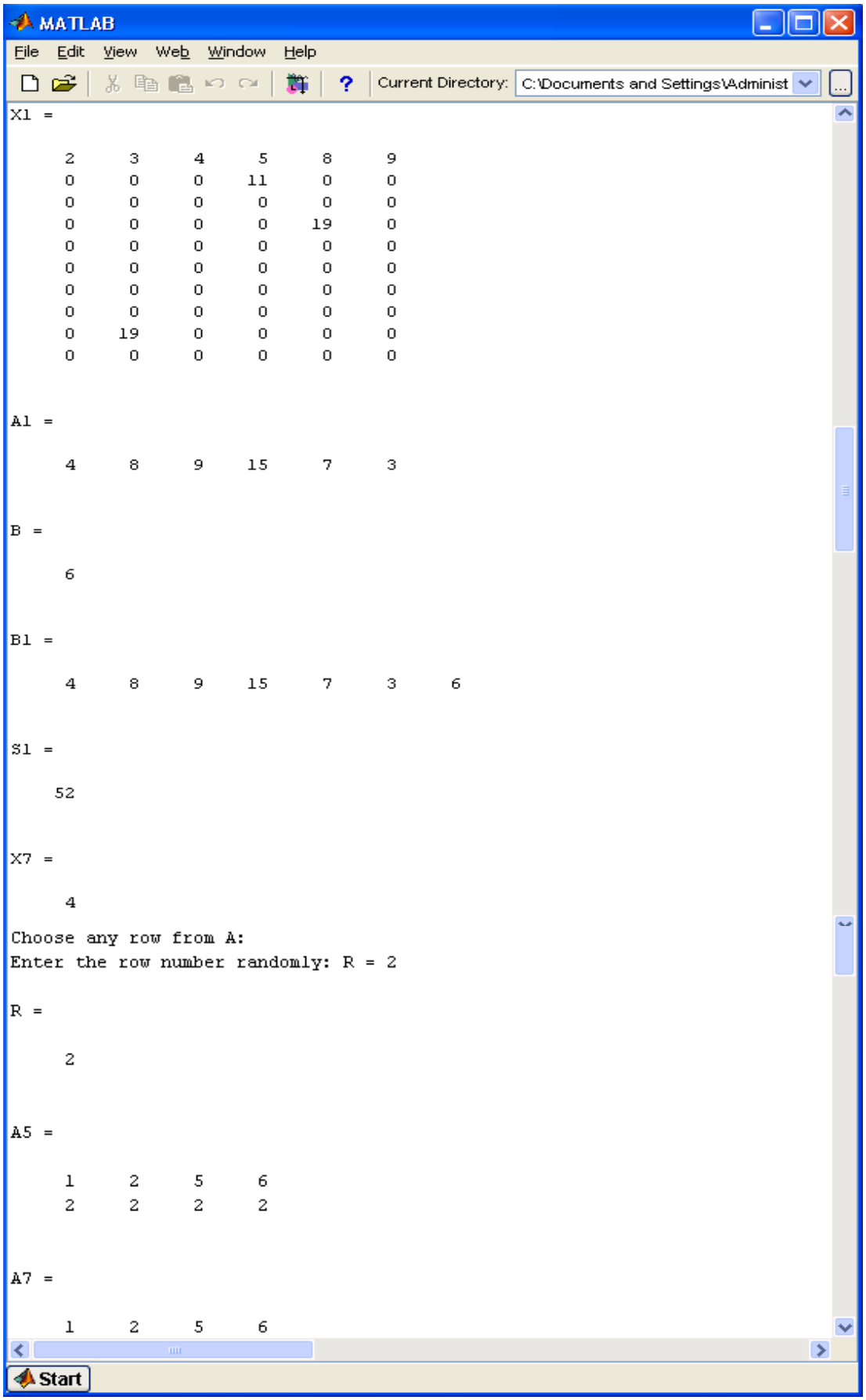
MATLAB
File Edit View Web Window Help
Current Directory: C:\Documents and Settings\Administ
X1 =
2 3 4 5 8 9
0 0 0 11 0 0
0 0 0 0 0 0
0 0 0 0 19 0
0 0 0 0 0 0
0 0 0 0 0 0
0 0 0 0 0 0
0 0 0 0 0 0
0 19 0 0 0 0
0 0 0 0 0 0
A1 =
4 8 9 15 7 3
B =
6
B1 =
4 8 9 15 7 3 6
S1 =
52
X7 =
4
Choose any row from A:
Enter the row number randomly: R = 2
R =
2
A5 =
1 2 5 6
2 2 2 2
A7 =
1 2 5 6
Start

Snapshot 6

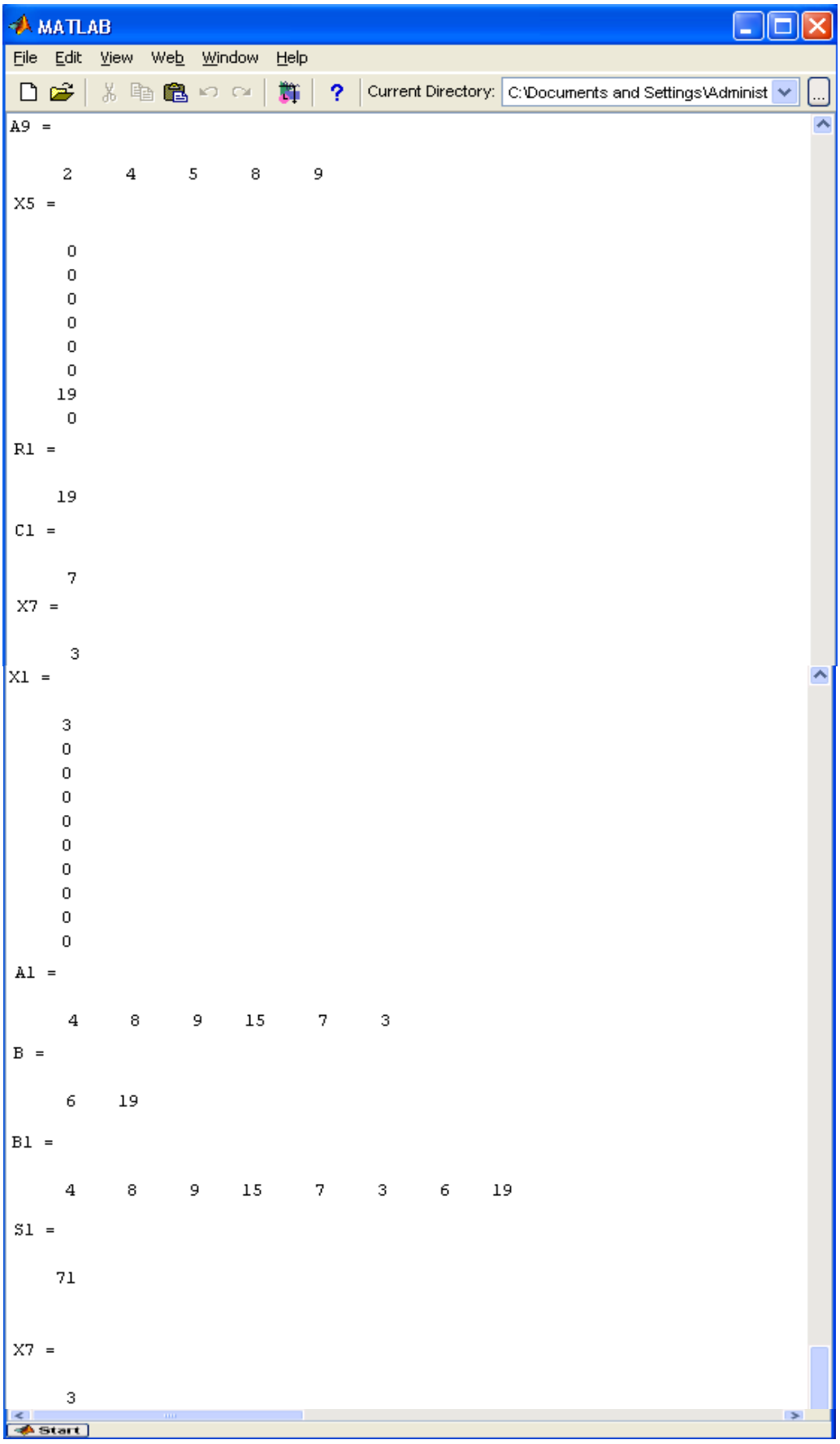
MATLAB
File Edit View Web Window Help
Current Directory: C:\Documents and Settings\Administ
A9 =
2 4 5 8 9
X5 =
0
0
0
0
0
0
19
0
R1 =
19
C1 =
7
X7 =
3
X1 =
3
0
0
0
0
0
0
0
0
0
A1 =
4 8 9 15 7 3
B =
6 19
B1 =
4 8 9 15 7 3 6 19
S1 =
71
X7 =
3
Start

Snapshot 7

In snapshot 8 the final output is 71, which matches with the weight of the sapnning tree, for the graph in Fig . 2.

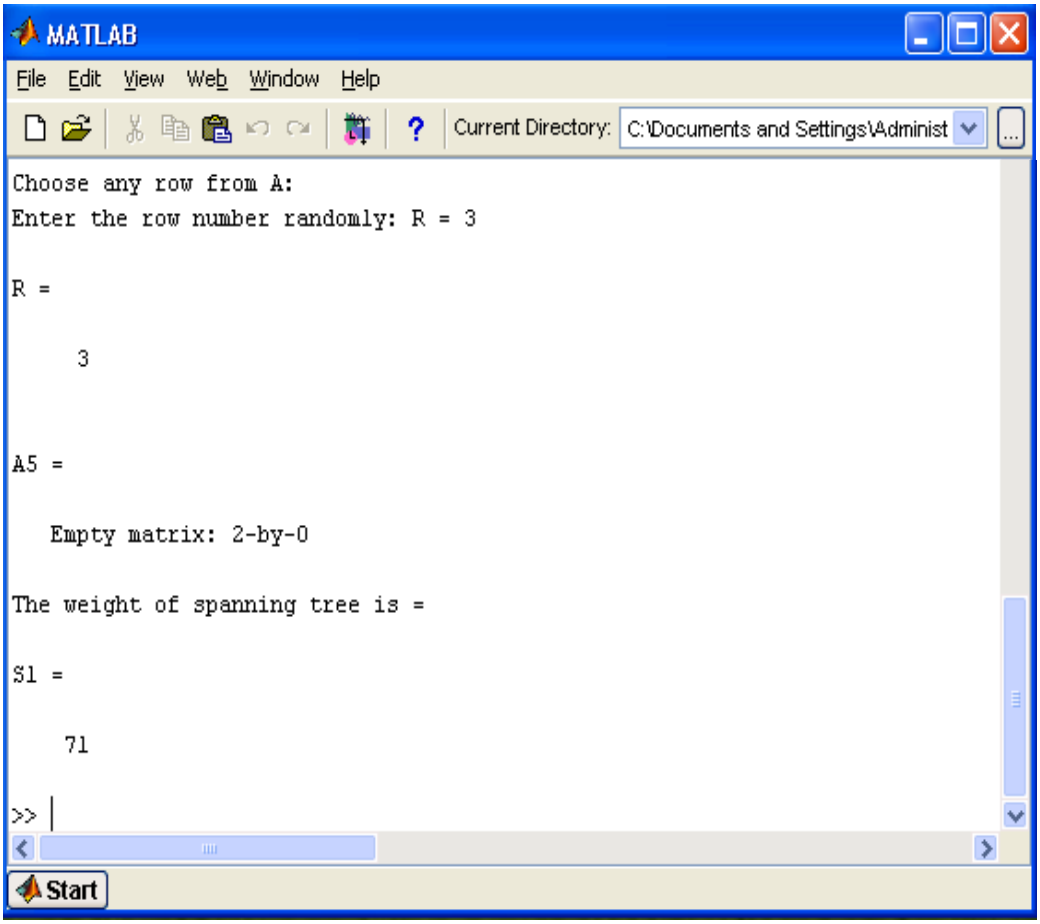

Snapshot 8

Example 2

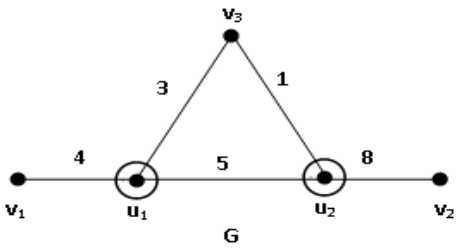

Fig. 4

OUTPUT

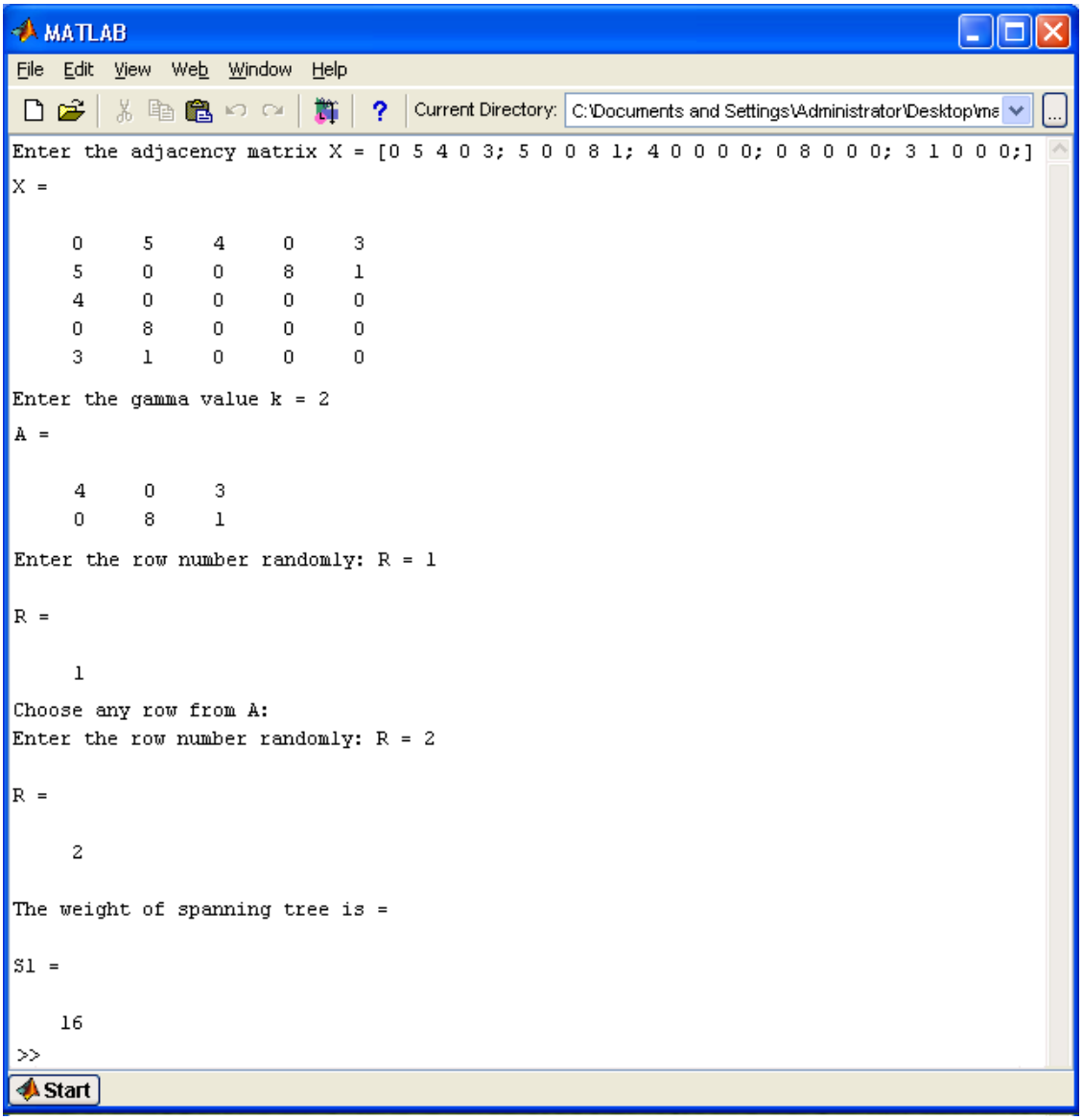

Snapshot 9

The minimum weight of the spanning tree for the graph in Fig. 4 is 16, which matches with the value obtained in snapshot 9.

IV CONCLUSION

The above procedure generates the minimum weight of the spanning tree using dominating set. The program developed enables us to calculate the minimum weight of the spanning tree easily since MATLAB is user friendly. We just need to input the adjacency matrix to obtain the minimum weight of the tree. So this procedure can be adopted for generation of spanning trees.

REFERENCES

[1] R. C. Prim. Shortest Connection Networks and Some Generalizations, Bell Syst. Tech. J., 36, 1957, pp.1389 – 1401.

[2] J. B. Kruskal. On the Shortest Spanning Sub tree of a Graph and the Traveling Salesman Problem, Proc. Am. Math. Soc., l.7, 1956, pp.48 – 50.

[3] M. Yamuna and K. Karthika. Minimal Spanning Tree from a Minimum Dominating Set, WSEAS Transactions on Mathematics, 12 (11), 2013, pp. 1055 – 1064.

[4] D. B. West. Introduction to Graph Theory, second ed., Prentice - Hall, New Jersey, 2007.

[5] T. W. Haynes, S. T. Hedetniemi, and P. J. Slater. Fundamentals of Domination in Graphs, Marcel Dekker, New York, 1998.

GLOBAL TRENDS IN INNOVATION OF BUSINESS EDUCATION & INDIAN BUSINESS SCHOOLS

Dr. Ajay Singh

Assistant Professor, College of Business Administration,

University of Hail, Kingdom of Saudi Arabia

ABSTRACT

The purpose of this paper is to study the global trends in business education and its impact on country's overall growth through studying and analyzing the present scenario and trends of business schools in India and their impact on overall system and also analyze that how these business schools are competent in maintaining total quality management with the global industry expectation at national and global level. The research examines through statistical tests such as Chi-square Goodness of fit tests for hypothesis testing and Spearman correlation is used to find the correlation among distinguished variables. Principal Component Analysis (PCA) and Regression analysis is also used for further extension of the research. As the globalization of business education is the way to fulfil the future demand for the skilled managers through making creative change in course structure as per industry demand and pattern of management education. Our samples have adapted a strategy of multiple Business schools and an attempt has been made for analysing different patterns of globalization & innovation and assessing the appropriate mechanisms to business education in various business schools of India. The research pays a significant role to understand the sophisticated methodology and business curriculum worldwide with Industry's changing demand in global business environment.

Keywords: Globalization, B Schools, Business Schools, Management Education, Business Management Education, India

I. INTRODUCTION

1.1. Global Trends in Business Education

Globalization of Education means integration of economies and societies through cross country flows of information, knowledge, ideas, technologies, and people etc. such type integration can have several dimensions likewise cultural, social, political and economic. The world is more connected to each other than ever before in the past. Flow of the information takes place quickly than ever. Also the flow of goods and services are increasing rapidly thorough out the world. International traveling and communication become very easy. The world is very challenging today and it became very crucial for managers to stay in competition and sustain it as the power is shifted to the customer, collaborations across firms and across country's geographical boundaries. There is a need to maintain a high level of business talent in respective nations. This is possible through providing high level business programs across the country to cope with the external global competitive pressure. Globalization of management education is on the way to fulfill the demand for the skilled managers through making creative change in course structure as per industry demand and pattern of management education.

Management education is in the process of globalization. The demands on the skills of present and future managers are changing. It has become essential to re-examine the entire structure, content, purpose and pattern of business management education. Ongoing and rapid change in the world economy and increasing competitiveness has have a central role in enhancing the scope of business management education lead success of personnel and corporations worldwide. The growing relationship between business education and corporates are continuously leading to change in technology as well as economic conditions worldwide along with constant learning. The management education has become essential for every nation and attracting every corporate business across the world.

The focus of professors of business school should be to creating good managers who have excellent business ethics, values, knowledge to increase the efficiency and effectiveness. We should focus on the key issues and challenges of the nation's management education system and try to uplift it as per world class. Business education does not teach us to shaping a student's capability as entrepreneur to help an organization nor to become an entrepreneur and this is not on result of degree or diploma in business management but it should be focus on real business skills development and creating self-sustainability for the nation.

The present management education system is alienated to some level in various countries from real life. This is due to the gap between subjectivity and objectivity in benchmarking for Quality in Management Education, so as to create an enduring Indian corporation. Professionalism in business management Education needs qualified and competent professors, good infrastructure facilities, world level Course curriculum etc.

The things that any one might be thinks at the time of searching a right school are the quality and reputation of the business school, cost of the business school, location and personal fit. If we talk about the cost, there are two types of people, one who hardly can pay the cost and want to get a reputed degree as much as lower cost, on the other side there are some people who paid a lot for the degree. Most of the people take help of published rankings in various business magazines to choose their business school but they definitely not investigate the quality and the course curriculum that they really want. It is very important for anyone who wants to join a good business school must make sure about the infrastructure, faculty, library facilities, quality of services that can fulfill the career goals as per need and expectations. So it is very important at very early stage to find the good business school that matches your needs will enhance the likelihood of your being one of the majorities students must delivers on its promise.

Graduate Management Admission Council (GMAC) revealed the findings of its annual global survey which revealed that jobs have rebound by a considerable number in 2011(54%) from last year (32%) and also pointed out that internships are important after graduation (GMAC Alumni Perspective Survey 2011 Survey Report).

1.2. Parameters of Benchmarking for Quality Education

Benchmarking in business education for quality purpose is the world best means of teaching the knowledge for today and technology for tomorrow providing the best knowledge to the students. It should be creative and innovative. Benchmarking guide the students in right direction and provide the opportunity for employment and also guide the institution from academics to corporates. This may be happen when:

- © Skill Development of the students as per industry expectations
- © Maintaining Total Quality Management in business management education.
- © Apply sophisticated methods & skills required in teaching

Benchmarking suggest us the best Quality Management Systems in every areas such as assurance of quality standards, designing course curriculum, teaching methodology, faculty and staff, training & development, lecture delivery, performance measurement, student support and guidance, other student and faculty allied material.

1.3. Business Education and Professionalization

Generally, It is known that there are many differences in assessing the quality of business school's education but one important reason is that there should be a body to set and assess the level of standard likewise AACSB in USA which defines the basic quality framework for quality in management education and also approves the entry and expansion of various institutions worldwide. In the same way, in order to maintain the quality in the field of business education in India, the apex body of the country focus on quality assurance, competent faculty & staff, state-of-the art infrastructure, accountability and responsibility of the universities, ethics and values, role of government and professional bodies etc. through:

- © Adaptation of modern and scientific method of management.
- © Development of professional body to govern and promote business schools education objectives and functions for the nation.
- © Develop business education as a powerful tool for industry and economy.
- © Cope with latest changes in the field of business education principles and practices and incorporate these changes to provide new way to industry and economy.
- © Ensure the exercise of best business ethics and values in the profession.
- © Ensure development & participation of new ideas through seminars, workshops and conferences for the purpose of professional growth.
- © Exercise research and publication activities, publishing books in the field of business and economy.

1.4. Business Education and Contemporary Global Trends

Business transactions, consulting, products offering through internet are changing the trends in business education and it became essential to make changes. Increasing industry interface, student faculty interaction and managing student knowledge with the current business environment. Knowledge creation is very important mission for business schools not only in ivory towers but also in business organizations. The global forces have brought some fundamental changes for managing business organizations.

- © Globalization of curriculum and removing barrier to curriculum.
- © Benefit to society.
- © Industry-wide initiation.
- © Enhancing capability through strategic partnership and collaboration of business models.
- © Building faculty global caliber.
- © Performance management & implication for management educators.

II. REVIEW OF LITERATURE

As per GMAC (2013)[1] Application Trends survey, source of comprehensive statistics for graduate management education worldwide, a career enhancements and exposure to new professional and business opportunities of top

graduate business school and its outcomes among prospective students for future employment success depends on many factors such as regional variations and industry demand depending upon different types of business degree candidates. This study explores the early job search success for 5,331 graduating students in the class of 2013 from 159 business schools located in 33 countries worldwide. This survey examines information relating to volume trends of applicant, recruitment strategies of companies as well as increasing demand for management education worldwide.

Prospective Students Survey Report (2012 mba.com)[2] examines the individual motivations, their behaviours, choices of program, and career outcomes who expressed a desire to further their education in a graduate business program from more than 16,000 prospective students who are preparing for the GMAT examination for applying to a graduate business school program worldwide. The report was based on the data collected in 2011 from mba.com registrants worldwide over 16,358 respondents.

The GMAC (2013)[3] Corporate Recruiters Survey was conducted at 158 business schools worldwide through partnership with the European Foundation for Management Development (EFMD) and the MBA Career Services Council (MBA CSC). This survey was based on responses taken form than 900 employers in 50 countries around the world, including the Asia-Pacific region, Europe, and the United States of America. The result from the survey examines and analyzes the demand and the hiring of graduate business students based on the distinguished variable such as salaries, job functions, industry and worldwide job placement.

The Alumni Perspectives Survey (2013)[4] is a product of the Graduate Management Admission, a global non-profit education organization of leading graduate business schools and the owner of the Graduate Management Admission Test (GMAT). The survey results of 2013 Alumni Perspectives Survey report explains address the current economic and regional trends affecting alumni of MBA and other business graduate programs.

Mohammed Abdullah Mamun & Ariffin Bin Mohamad (2009)[5] explains in his research that the business organizations have been giving pressures to universities to be perfect professional otherwise it becomes difficult for their success and survival as well as creating intelligent professionals to face the challenges of today's business environment. According to this study, management education has to be shaped to fulfil the needs of the industries and send a clear message to the business management schools about their role to play in this regard to face the challenges of today's business environment have got proven records of maintaining standards in regard to vision, program design and offerings. Some leading business schools of the USA and Asia has to contributing very well into the needs of changing business situations by providing better management education and to producing managers as per today's business environment.

In a study by M. Mahmood Shah Khan & Nandita Sethi (2009)[6] investigates the perception of future managers towards Corporate Governance and further explores its scope for business schools. In the primary study the relation and impact of corporate governance in the management education has studied and the issues relating to management, stockholders, customers and corporate governance has taken for analysis keeping in view the major part as culture, society and business in environment. The study also examines the gap between the modern training needs of business graduates and the globalized, complex environment of corporates in the field in Corporate Governance.

W. Peng (2008)[7] a distinguished professor of Global Strategy at University of Texas, Dallas of School of Management examines a wide divide between the elites and the public to view globalization. As per him, it seems important to know the attitude of future business leaders toward globalization being educated currently

and will shape the global economy in the future. The finding of the study discussed are relating to managers and management educators.

In 'Principles for Responsible Management Education' (2007)[8] the UN Global Compact is the largest corporate citizenship initiative in the world. By May 2007 more than 3,000 companies from 100 countries, as well as over 700 hundred civil society, international labour organizations and academic institutions are engaged in the initiative. These all are working to promote responsible corporate citizenship, ensuring that business is part of the solution to the challenges of globalization.

Henry Grunfield (2005)[9] chaired professor of Investment Banking and Dean, INSEAD, Fontainebleau, France, in a study made on "The future of business schools Gabriel Hawawini" examines that the traditional business school model in rapidly markets will most likely successful and survive, assuming to meet strong and standard demand for management education as well as in mature countries it will have to satisfy the demand from both students and their employers in a complex and challenging environment. The paper examines some of the most challenging issues facing business schools and made a few suggestions on how they could meet the challenges with the current business environment, opportunities for new and established schools.

Deanne Butchey (2005)[10] in "Globalization of Tertiary Business Education" describes that AACSB is committed to the concept that the educational experience in every management education program should promote diversity and early exposure to other cultures and concepts can grow this diversity. One method for achieving this goal is to encourage diversity among participants in the educational process among the students and academicians. The global challenge involves expansion of universities across geographical regions to maintain academic standards and ensure the credibility of the degree.

By Jonathan Crichton, Michael Paige, Leo Papademetre, Angela Scarino (2004)[11] a project published on "Integrated resources for intercultural teaching and learning in the context of internationalization in higher education" Prepared by the Research Centre for Languages and Cultures Education, University of South Australia. In this study the integrated set of resources, presented, intended to be used by individuals or groups of academicians of distinguished disciplines to examine the intercultural teaching and learning and the resources are based on a mapping and analysis of current work and discourses in the areas of the internationalization of education and intercultural teaching and learning.

III. OBJECTIVES

To study the present scenario of business schools education in India with Global trends in business education.

1. To discuss how globalization of business schools education might impact on Business Education in India and the overall educational system as a whole.
2. To identify the forces that has contributed to the globalization of business schools education and the business management educational system as a whole.
3. To identify the overall Industry expectations of the skill sets required of the students in general, so as making them more competent and employable at global platform.
4. To identify the opportunities for advancement through globalization of business schools education in India.
5. To identify the areas and scope of motivational factors and total quality management in Global business education.

IV. HYPOTHESIS

1. *Hypothesis I*: That the globalization of business school's education have no positive impact on business education institutions in India, and the higher educational system as a whole.
2. *Hypothesis II:* That the globalization of business school's education has not have much positive impact in the employment opportunity and competency/skills of the students of India as per the overall Industry expectations at global platform.
3. *Hypothesis III:* That the contribution of motivational factors and total quality management in business education has not have much positive impact in widening the area and scope of global business education in India.

V. RESEARCH METHODOLOGY

A. Measurement: In this research study we have analyzed how globalization of business education and related forces might impact on Business Education in India and the overall educational system as a whole and also tried to made a comparison with present scenario of business education in India with Global trends in the global management education and secondly, we have also analyzed how business education has increased the employment opportunity and competency of the students in India as per the overall Industry expectations at global platform. Thirdly, the analysis is based on the contribution motivational factors and total quality management in business education.

B. Data Collection: In this research, data was collected from various universities/ Institutions both public and private of Delhi and NCR regions of India. India. The questionnaires were distributed among the students of business institutions of the respective universities and request have made to fill them up on priority basis as their precious contribution in the field of business education research. A total of 750 questionnaires were e-mailed as well personally distributed to various universities' respective business institutions among both bachelor and master's level and finally 543 filled questionnaires were collected from the overall distributed student's population.

C. Data Analysis: The data analysis was made through SPSS Software tool. Chi-square test of independence was used to testing of hypothesis and Spearman correlation was used to find the correlation between different variables. Principal Component Analysis (PCA) and Regression is also used for further extension of the research.

VI. DATA ANALYSIS AND INTERPRETATION

From the table it is clear that the number of students those less than 22 years of age is more. The second category belongs to age group from 27 to 30 years. The third category of the students belongs to age group 22 to 26 years. There is no student in our research who has more than 30 years of age in the survey.

The survey result shows that the numbers of bachelor (single) participants are too much in comparison to married one.

Table 1: Personal Factors of the Respondents

Personal Factors	Category	No. of Respondents	%age
Age Group	Less than 22	235	43.3
	From 22 to 26	143	26.3
	From 27 to 30	165	30.4
	From 31 to 34	0	0
	More than 35	0	0
Marital Status	Married	37	6.8
	Single	506	93.2
Educational Level	Finance & Accounting	234	43.10
	Marketing Management	140	25.78
	IT Management	80	14.73
	Human Resource Management	46	8.47
	Business Economics	43	7.92
Discipline	Undergraduate	413	76.1
	Graduate	130	23.9
Preferred Industry of Employment	Finance & Accounting	221	40.7
	Marketing Management	156	28.73
	IT Management	84	15.47
	Human Resource Management	52	9.58
	Business Economics	30	5.52

Source: Survey Questionnaire

The table 1 also shows that Finance & Accounting is the area of first priority of students in which most of the student were studying and further Marketing Management and IT Management, Human Resource management and Business Economics respectively. 76% of the respondents of this survey were from the undergraduate level and 24% are from the graduate level. In case of preferred Industry of Employment the choices. The industry preferences amongst students are Finance & Accounting, Marketing Management, Information Technology, Human Resource Management and Business Economics respectively.

Table 2a shows that the most of variables are showing the value of chi-square test as significant. The correlation result also shows that most of the variable significantly associated with each other. This interprets that the globalizations of business management education have positive impact on business education institutions in India, and the higher educational system as a whole.

Table 2a: Globalization of Business Management Education (GBME)

Reliability Statistics		Cronbach's Alpha : .843			No. of Items: 6	
GBME	GBME-1	GBME-2	GBME-3	GBME-4	GBME-5	GBME-6
c2	635.365[a]	472.020[a]	388.131[a]	856.978[a]	546.333[a]	881.595[b]
Df	3	3	3	3	3	4
Asy. Sig.	.000	.000	.000	.000	.000	.000
Correl.	GBME-1	GBME-2	GBME-3	GBME-4	GBME-5	GBME-6
GBME-1	1.000	.511**	.228**	.650**	.405**	.399**
GBME-2	.511**	1.000	.314**	.452**	.837**	.426**
GBME-3	.228**	.314**	1.000	.272**	.284**	.259**
GBME-4	.650**	.452**	.272**	1.000	.393**	.591**
GBME-5	.405**	.837**	.284**	.393**	1.000	.344**
GBME-5	.399**	.426**	.259**	.591**	.344**	1.000

Correlation: Spearman's rho as data is categorical.

***. Correlation is significant at the 0.01 level; *Correlation is significant at the 0.05 level (2-tailed); Reliability = 0.843; Model=alpha; Scale: All Variables*

Variables= GBME1, GBME2, GBME3, GBME4, GBME5, GBME6;

GBME- Globalization of Business Management Education

Note: GBME 1-To what extent is globalization addressed in the mission and strategic plan of the business school in your country?

GBME-2.Have the Business-schools been adapting quickly enough to the changing demands of the students and their future employers through the globalization of Business Management Education?

GBME-3.How has Institution-Industry relationship changed with the companies that look to you to produce top-notch managers?

GBME-4.Do faculty members and other support staff have access to and take advantage of development opportunities that support the B-school's globalization objectives?

GBME-5.To what extent is business school's portfolio of intellectual contributions includes topics related to globalization that are consistent with its

GBME-6.To what extent is the contribution of government towards the globalization of Business Management education in your country?

Table 2b: Principal Component Analysis (GBME)

KMO and Bartlett's Test			KMO Measure of Sampling Adequacy		.813
Bartlett's Test of Sphericity			Approx. Chi-Square		1372.266
			Df		15
			Sig.		.000
Communalities			**Component Matrix**		Total Variance
	Initial	Extraction		Component Extracted -1	
GBME 1	1.000	.604	GBME 2	.830	56.745
GBME 2	1.000	.690	GBME 4	.824	
GBME 3	1.000	.299	GBME 1	.777	
GBME 4	1.000	.680	GBME 6	.753	
GBME 5	1.000	.566	GBME 5	.752	
GBME 6	1.000	.567	GBME 3	.546	
Extraction Method: Principal Component Analysis, 1 Component Extracted; The solution cannot be rotated.					

Principal components analysis (PCA) is a method of data reduction and is a powerful tool. This is the method of combining 'n' variables and makes them 3 or 4 variables without losing much of the information same as original data. Principal components analysis (PCA) is one of the best methods in case of having lots of Likert data. The interpretation of the principal components explains which variables are most strongly correlated with each component, or can say that which variable is large in magnitude and away from in either positive or negative direction. The value of correlation above 0.5 is deemed significant. Principal components analysis also assumes that each original measure is collected errorless. KMO Measure of Sampling Adequacy and this measure vary between 0 and 1, and values closer to 1 are better. A value of 0.6 is a suggested minimum. Our value is 0.813 which is quite good. The 6 variables remaining in the analysis satisfy the criteria for appropriateness of factor analysis. In our PCA in Table 2b the probability associated with Bartlett's Test of Sphericity should be less than the level of significance. In this case, the probability associated with the Bartlett test is <0.001, which satisfies this requirement. So as per the above results, we can now continue and perform a

valid factor analysis. The number of components extracted is only one and based on the extraction of one components, solution would explain 56.745% of the total variance.

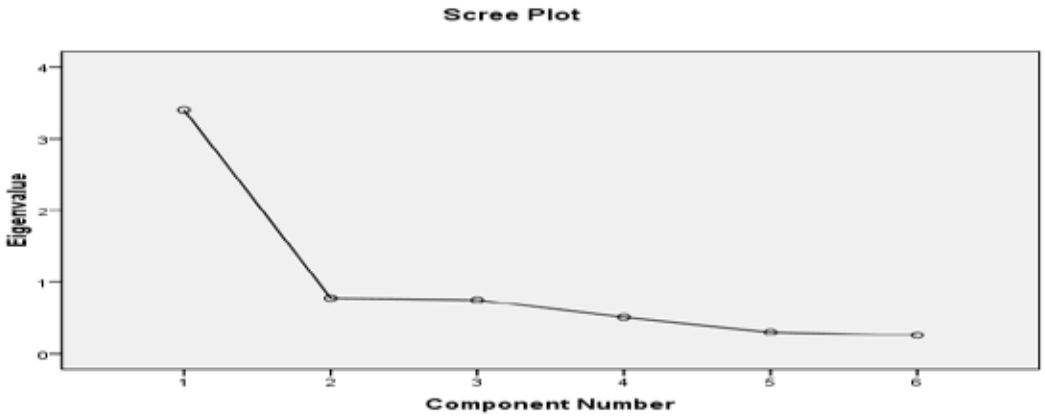

Figure 1: Principal Component Analysis (GBME

It is evident form Table 3a that all of variables are showing the results form chi-square test as significant. The correlation result from the above table also shows that most of the variable significantly associated with each other except only few. This interprets that the Key Drivers of Job Satisfaction of B-School's Students have greater significance on business education institutions in India, and the higher educational system as a whole.

Table 3a: Key Drivers of Job Satisfaction of B-School's Students (KDJS)

Reliability Statistics		Cronbach's Alpha: 0.705			N of Items: 7		
KDJS	KDJS-1	KDJS-2	KDJS-3	KDJS-4	KDJS-5	KDJS-6	KDJS-7
c2	611.497	239.746	314.319	198.707	665.214	547.910	450.967
df	3	2	3	2	3	3	3
Asy. Sig.	.000	.000	.000	.000	.000	.000	.000
KDJS	KDJS-1	KDJS-2	KDJS-3	KDJS-4	KDJS-5	KDJS-6	KDJS-7
KDJS-1	1.000	.285**	.106*	.111**	.122**	.305**	.038
KDJS-2	.285**	1.000	.053	.240**	.159**	.118**	.341**
KDJS-3	.106*	.053	1.000	.124**	.373**	.266**	.068
KDJS-4	.111**	.240**	.124**	1.000	.212**	.357**	.534**
KDJS-5	.122**	.159**	.373**	.212**	1.000	.419**	.349**
KDJS-6	.305**	.118**	.266**	.357**	.419**	1.000	.416**
KDJS-7	.038	.341**	.068	.534**	.349**	.416**	1.000

Correlation: Spearman's rho as data is categorical

***Correlation is significant at the 0.01 level; *Correlation is significant at the 0.05 level (2-tailed); Reliability = 0.705; Model=alpha;*

Variables= KDJS1, KDJS2, KDJS3, KDJS4, KDJS6, KDJA6, KDJS7;

KDJS- Key Drivers of Job Satisfaction of B-School's Students

Scale: All Variables

KDJS 1- Passion for work

KDJS-2 Flexibility in working schedule

KDJS-3 Control as subject matter expert

KDJS-4Autonomy for working independently

KDJS-5 Scope for exercising management skills
KDJS-6 Recognition for myself
KDJS-7 Compensation

Principal components analysis (KDJS) of Table 3b assumes that each original measure is collected errorless and KMO Measure of Sampling Adequacy varies between 0 and 1. Our value is very closer to 1 that is 0.708 which is quite good. The 7 variables remaining in the analysis satisfy the criteria for appropriateness of factor analysis. In our PCA the probability associated with Bartlett's Test of Sphericity should be less than the level of significance is <0.001, which satisfies this requirement. It is clear from the results that we can continue and perform a valid factor analysis. The number of components extracted is 3 and based on the extraction of 3 components; solution would explain 67.565% of the total variance.

Table 3b: Principle Component Analysis (KDJS)

KMO Measure of Sampling Adequacy			.708			Total Variance	65.67		
Bartlett's Test of Sphericity			Approx. Chi-Square			723.483			
			Df			21			
			Sig.			.000			
Communalities			Component Matrix			Rotated Matrix[a]			
Initial	Extraction			Components				Components	
				1	2	3		1	2	3
KDJS 1	1.000	.872	KDJS 6	.749			KDJS 7	.844		
KDJS 2	1.000	.622	KDJS 7	.720		-.480	KDJS 4	.748		
KDJS 3	1.000	.627	KDJS 5	.696	-.345		KDJS 2	.554		.553
KDJS 4	1.000	.616	KDJS 4	.682		-.377	KDJS 3		.792	
KDJS 5	1.000	.630	KDJS 3	.510	-.502	.339	KDJS 5		.743	
KDJS 6	1.000	.605	KDJS 2	.480	.623		KDJS 6	.380	.648	
KDJS 7	1.000	.758	KDJS 1	.336	.529	.692	KDJS 1			.915
Extraction Method: PCA and Rotation Method: Varimax with Kaiser Normalization. 3 components extracted; Rotation converged in 5 iterations.										

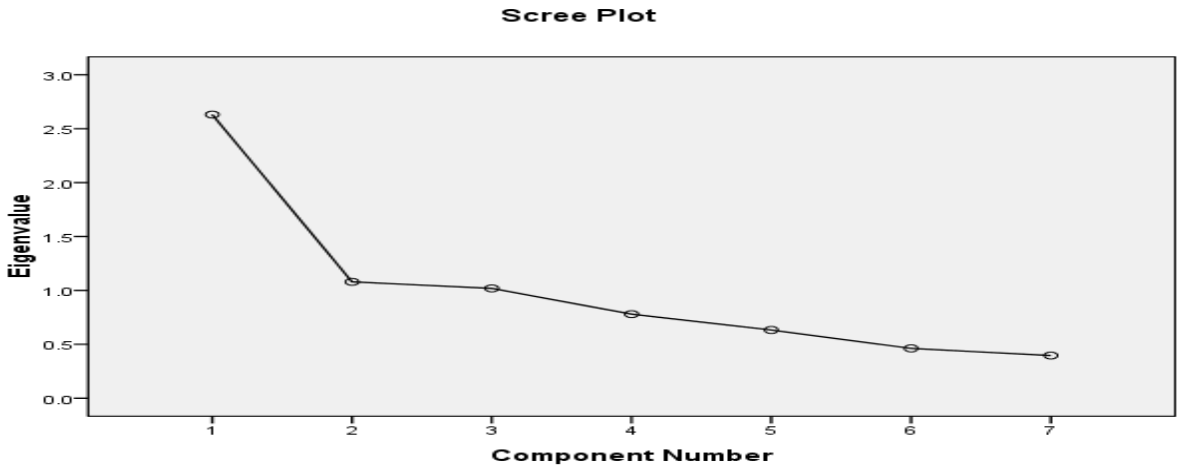

Figure 2: Principal Component Analysis (KDJS)

Table 4: Influential Factors in Choosing Self-Employment Business (IFCSB)

Reliability	Cronbach's Alpha: 0.706			N of Items: 6		
IFCSEB	IFCSEB1	IFCSEB2	IFCSEB3	IFCSEB4	IFCSEB5	IFCSEB6
c2	191.355[a]	229.993[a]	562.405[a]	877.295[b]	552.389[b]	210.711[a]
df	4	4	4	3	3	4
Asy. Sig.	.000	.000	.000	.000	.000	.000
IFCSEB1	IFCSEB1	IFCSEB2	IFCSEB3	IFCSEB4	IFCSEB5	IFCSEB6
IFCSEB1	1.000	.483**	.117**	.108*	.055	.455**
IFCSEB2	.483**	1.000	.154**	.216**	.331**	.498**
IFCSEB3	.117**	.154**	1.000	.159**	.111**	.222**
IFCSEB4	.108*	.216**	.159**	1.000	.292**	.124**
IFCSEB5	.055	.331**	.111**	.292**	1.000	.058
IFCSEB6	.455**	.498**	.222**	.124**	.058	1.000

Correlation: Spearman's rho as data is categorical.

***Correlation is significant at the 0.01 level; *Correlation is significant at the 0.05 level (2-tailed); Reliability = 0.706; Model=alpha;*

Variables-IFCSEB1, IFCSEB2, IFCSEB3, IFCSEB4, IFCSEB5, IFCSEB6

IFCSEB- Influential Factors in Choosing Self-Employment Business

Scale: All Variables

IFCSEB1- Join family business

IFCSEB2- Recognition of ability

IFCSEB3- Generation of Revenue

IFCSEB4- Difficult to Control over all aspects of business

IFCSEB5- Flexibility in Schedule work

IFCSEB6- Autonomy as primary business decision maker

Table 4 shows that the chi-square test of statistic value of all the variables are significant. The Spearman coefficient of correlation results also show that most of the variables are significantly associated with each other except only few. The result interprets that the influential factors are most appropriate in choosing self-employment business and have positive impact on business education institutions in India, and the higher educational system as a whole.

Table 5a pertaining to attendance in class shows that the all of variables (EFSAC 1-7) are showing the value of chi-square test of statistic as significant and the Spearman coefficient of correlation among the variables also show that most of the variable significantly associated with each other except only few.

Table 5a: Dependence of Attendance of Students in Class (EFSAC)

Correlation: Spearman's rho as data is categorical.

Reliability Statistics		Cronbach's Alpha		.725	N of Items		7
c2	EFSAC 1	EFSAC 2	EFSAC 3	EFSAC 4	EFSAC 5	EFSAC 6	EFSAC 7
c2	898.722[a]	840.545[a]	482.466[b]	523.453[b]	699.365[b]	508.779[b]	259.569[c]
df	4	4	3	3	3	3	2
Asy. Sig.	.000	.000	.000	.000	.000	.000	.000
Correlation	EFSAC 1	EFSAC 2	EFSAC 3	EFSAC 4	EFSAC 5	EFSAC 6	EFSAC 7
EFSAC 1	1.000	.195**	.029	-.064	.413**	.023	.033
EFSAC 2	.195**	1.000	.225**	.125**	.171**	.202**	.175**
EFSAC 3	.029	.225**	1.000	.478**	.119**	.864**	.200**
EFSAC 4	-.064	.125**	.478**	1.000	-.020	.510**	.415**
EFSAC 5	.413**	.171**	.119**	-.020	1.000	.059	-.014
EFSAC 6	.023	.202**	.864**	.510**	.059	1.000	.244**
EFSAC 7	.033	.175**	.200**	.415**	-.014	.244**	1.000

***. Correlation is significant at the 0.01 level; *Correlation is significant at the 0.05 level (2-tailed); Reliability = 0.725; Model=alpha; Variables= EFSAC1, EFSAC2, EFSAC3, EFSAC4, EFSAC5, EFSAC6, EFSAC7.*

EFSAC- Effect of Student Attendance in Class

Scale - All Variables

EFSAC 1- Academic quality

EFSAC 2- Co-curricular/ Extracurricular life

EFSAC 3- College facilities

EFSAC 4- Faculty Calibre

EFSAC 5- Student ability/ motivation

EFSAC 6- High cost of education

EFSAC 7- Diversity of Learning

This interprets that the dependence of attendance of student in class over different variables (EFSAC 1-7) are positively related and has significant impact on business management education in India and the higher educational system as a whole.

Table 5b: Principal Component Analysis (EFSAC)

KMO Measure of Sampling Adequacy			.691			Total Variance		59.18
Bartlett's Test of Sphericity			Approx. Chi-Square			1088.072		
			Df			21		
			Sig.			.000		
Communalities			Component Matrix			Rotated Matrix		
				Component		Component		
	Initial	Extraction		1	2	1		2
EFSAC 1	1.000	.671	EFSAC 6	.818	-.304	EFSAC 6	.861	
EFSAC 2	1.000	.505	EFSAC 3	.788	-.322	EFSAC 3	.843	
EFSAC 3	1.000	.724	EFSAC 4	.676	-.350	EFSAC 4	.761	
EFSAC 4	1.000	.580	EFSAC 2	.585	.404	EFSAC 7	.530	
EFSAC 5	1.000	.602	EFSAC 7	.527		EFSAC 1		.817
EFSAC 6	1.000	.762	EFSAC 1	.456	.681	EFSAC 5		.775
EFSAC 7	1.000	.299	EFSAC 5	.410	.659	EFSAC 2	.307	.641
Extraction Method: Principal Component Analysis2 components extracted. Rotation Varimax with Kaiser Normalization; Rotation converged in 3 iterations.								

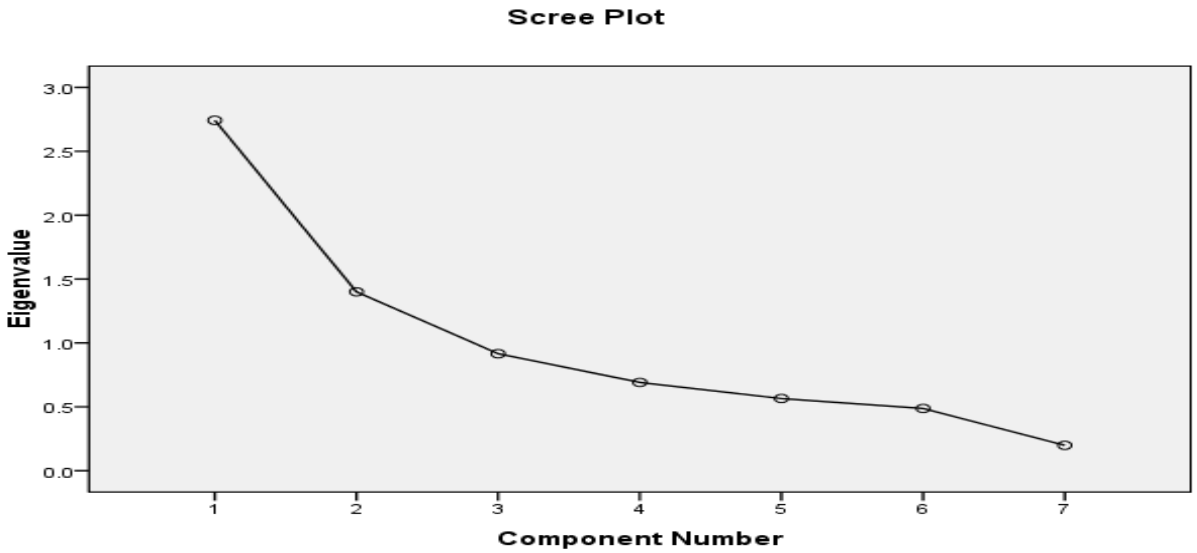

Figure 3: Principal Components Analysis (EFSAC)

Table 5b of Principal components analysis (EFSAC) assumes that each original measure is collected errorless and KMO Measure of Sampling Adequacy varies between 0 and 1. Our value is closer to 1 that is 0.691 which is quite good. The 7 variables remaining in the analysis satisfy the criteria for appropriateness of factor analysis. In our PCA the probability associated with Bartlett's Test of Sphericity should be less than the level of significance is <0.001, which satisfies this requirement. It is clear from the results that we can continue and

perform a valid factor analysis. The number of components extracted is 2 and based on the extraction of 2 components; solution would explain 59.18% of the total variance.

Table 6a: Factors of Motivation to get connected to B-School (FMCB)

Reliability Statistics			Cronbach's Alpha: .726			N of Items: 8		
FMCB	FMCB1	FMCB2	FMCB3	FMCB4	FMCB5	FMCB6	FMCB7	FMCB8
c2	892.28[a]	838.02[a]	760.60[a]	600.05[a]	435.04[a]	884.38[a]	755.96[a]	446.53[a]
Df	4	4	4	4	4	4	4	4
Asy. Sig.	.000	.000	.000	.000	.000	.000	.000	.000
FMCB	FNCB1	FNCB2	FNCB3	FNCB4	FNCB5	FNCB6	FNCB7	FNCB8
FMCB1	1.000	.228**	.096*	.057	-.056	.123**	.124**	-.045
FMCB2	.228**	1.000	.284**	.023	-.163**	.065	.175**	-.157**
FMCB3	.096*	.284**	1.000	.147**	.070	-.039	.441**	.078
FMCB4	.057	.023	.147**	1.000	.254**	.115**	.045	.254**
FMCB5	-.056	-.163**	.070	.254**	1.000	.052	.065	.974**
FMCB6	.123**	.065	-.039	.115**	.052	1.000	.087*	.051
FMCB7	.124**	.175**	.441**	.045	.065	.087*	1.000	.073
FMCB8	-.045	-.157**	.078	.254**	.974**	.051	.073	1.000

Correlation: Spearman's rho as data is categorical.

*** Correlation is significant at the 0.01 level; *Correlation is significant at the 0.05 level (2-tailed); Reliability = 0.725; Model=alpha; Variables= FMCB1, FMCB2, FMCB3, FMCB4, FMCB5, FMCB6, FMCB7, FMCB8.*

FMCB - Factors of Motivation to get connected to B-School

Scale - All variables

FMCB 1- Advancement programs of B-schools

FMCB 2- Opportunity to move in better placement?

FMCB 3- Training and development to date with the B-schools

FMCB 4- Not Giving donation

FMCB 5- Mentoring current/past students

FMCB 6- Campus visits

FMCB 7- Alumni events

FMCB 8- Starting Salary and job Dissatisfaction level

The results form Table 6a shows that the most of variables (FNCB 1-8) are showing the value of chi-square test of statistic as significant and the Spearman coefficient of correlation results also show that most of the variable significantly associated with each other except the only few variables.

This interprets that the influential factors from (FNCB 1-8) have significant effects as factors of motivation to get connected to B-schools and have positively associated with B-schools in India, and the higher educational system as a whole.

Table 6b: Principal Component Analysis (FMCB)

KMO Measure of Sampling Adequacy			.657			Total Variance		59.26
Bartlett's Test of Sphericity			Approx. c2			2174.044		
			Df			28		
			Sig.			.000		
Communalities			Comp. Matrix[a]			Rotated Matrix[a]		
FMCB	Initial	Extraction		Component			Component	
				1	2		1	2
FMCB 1	1.000	.500	FNCB 3	.689		FNCB 2	.775	
FMCB 2	1.000	.610	FNCB 7	.667		FNCB 1	.707	
FMCB 3	1.000	.534	FNCB 2	.572	-.532	FNCB 3	.703	
FMCB 4	1.000	.362	FNCB 1	.570	-.419	FNCB 7	.699	
FMCB 5	1.000	.930	FNCB 6	.551		FNCB 6	.587	
FMCB 6	1.000	.360	FNCB 4	.538		FNCB 5		.964
FMCB 7	1.000	.518	FNCB 5	.558	.787	FNCB 8		.963
FMCB 8	1.000	.927	FNCB 8	.560	.783	FNCB 4		.531
Extraction Method: PCA and Rotation Method: Varimax with Kaiser Normalization; 2 component extracted; Rotation converged in 3 iterations.								

Table 6b of Principal components analysis (FMCB) assumes that each original measure is collected errorless and KMO Measure of Sampling Adequacy varies between 0 and 1. Our value is closer to 1 that is 0.657 which is quite good.

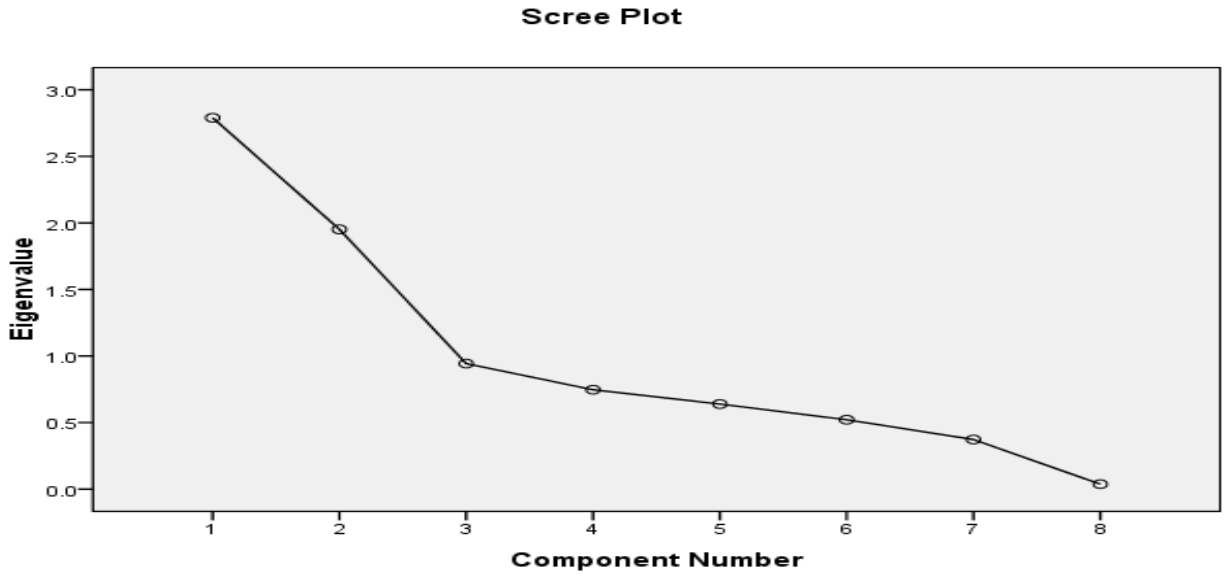

Figure 4: Principal Components Analysis (FMCB)

The 8 variables remaining in the analysis satisfy the criteria for appropriateness of factor analysis. In our PCA the probability associated with Bartlett's Test of Sphericity should be less than the level of significance is <0.001, which satisfies this requirement. It is clear from the results that we can continue and perform a valid

factor analysis. The number of components extracted is 2 and based on the extraction of 2 components; solution would explain 59.28% of the total variance.

Table 7a shows that the results from the all of variables are showing the value of chi-square significant. The spearman correlation result also shows that most of the variable significantly associated with each other. This interprets that the globalizations of business management education have positive impact on overall quality/skills of manpower through Indian business schools and the higher educational system as a whole.

Table 7a: Globalization of management education and its effect on overall quality/ skills of manpower (SBS)

Reliability Statistics			Cronbach's Alpha: .723					Numbers of Items: 11			
SBS	SBS 1	SBS 2	SBS 3	SBS 4	SBS 5	SBS 6	SBS 7	SBS 8	SBS 9	SBS 10	SBS 11
c2	336.663	259.536	448.330	401.978	268.420	653.663	695.033	255.260	375.061	481.536	336.674
Df	2	2	3	2	2	3	3	2	2	2	2
Asy.Sig.	.000	.000	.000	.000	.000	.000	.000	.000	.000	.000	.000
SBS	SBS 1	SBS 2	SBS 3	SBS 4	SBS 5	SBS 6	SBS 7	SBS 8	SBS 9	SBS 10	SBS 11
SBS 1	1.000	.232**	.023	.845**	.210**	.088*	.892**	.195**	-.044	.235**	.600**
SBS 2	.232**	1.000	-.074	.188**	.894**	.004	.224**	.714**	.011	.187**	.345**
SBS 3	.023	-.074	1.000	.005	-.068	.043	.039	-.017	.070	.093*	-.012
SBS 4	.845**	.188**	.005	1.000	.170**	.036	.918**	.167**	-.130**	.193**	.603**
SBS 5	.210**	.894**	-.068	.170**	1.000	-.006	.207**	.702**	-.015	.155**	.338**
SBS 6	.088*	.004	.043	.036	-.006	1.000	.082	.078	.066	.116**	.022
SBS 7	.892**	.224**	.039	.918**	.207**	.082	1.000	.183**	-.107*	.222**	.633**
SBS 8	.195**	.714**	-.017	.167**	.702**	.078	.183**	1.000	.124**	.139**	.197**
SBS 9	-.044	.011	.070	-.130**	-.015	.066	-.107*	.124**	1.000	-.029	-.238**
SBS 10	.235**	.187**	.093*	.193**	.155**	.116**	.222**	.139**	-.029	1.000	.119**
SBS 11	.600**	.345**	-.012	.603**	.338**	.022	.633**	.197**	-.238**	.119**	1.000

*Correlation: Spearman's rho as data is categorical. ** Correlation is significant at the 0.01 level; *Correlation is significant at the 0.05 level (2-tailed); Reliability = 0.725; Model=alpha; Variables= SBS1, SBS2, SBS3, SBS4, SBS5, SBS6, SBS7, SBS8, SBS9, SBS10, SBS11,*

SBS - Skills for B-Schools Students Scale - All Variables

SBS 1- Business skills

SBS 2 - Creative, Analytical, & Logical skills

SBS 3- Entrepreneurship skills

SBS 4 - Ethics & value system

SBS 5- Industry awareness & Industry Dynamics

SBS 6 - Team work skills

SBS 7 - Inter personal Relationships across the border

SBS8 - Leadership & Innovation skills

SBS9 - Learning skills

SBS10 - Presentation skills

SBS11- Problem Solving skills

It is evident form table 7b that Principal components analysis (SBS) assumes that each original measure is collected errorless and KMO Measure of Sampling Adequacy vary between 0 and 1. Our value is very closer to 1 that is 0.783 which is quite good.

Table 7b: Principal Component Analysis (SBS)

KMO Measure of Sampling Adequacy.			.783				Total Variance			59.18
Bartlett's Test of Sphericity			Approx. Chi-Square				3057.195			
			Df				55			
			Sig.				.000			
Communalities			Component Matrix[a]				Rotated Matrix[a]			
				Components			Components			
	Initial	Extraction		1	2	3		1	2	3
SBS 1	1.000	.827	SBS 7	.834	-.435		SBS 7	.923		
SBS 2	1.000	.875	SBS 1	.812	-.401		SBS 4	.918		
SBS 3	1.000	.237	SBS 4	.792	-.460		SBS 1	.879		
SBS 4	1.000	.847	SBS 11	.727			SBS 11	.747		
SBS 5	1.000	.872	SBS 5	.620	.691		SBS 2		.921	
SBS 6	1.000	.277	SBS 2	.642	.677		SBS 5		.920	
SBS 7	1.000	.885	SBS 8	.561	.653		SBS 8		.852	
SBS 8	1.000	.754	SBS 9			.703	SBS 9			.684
SBS 9	1.000	.522	SBS 6			.499	SBS 6			.517
SBS 10	1.000	.309	SBS 3			.464	SBS 3			.470
SBS 11	1.000	.641	SBS 10	.366		.417	SBS 10			.459
Extraction Method: Principal Component Analysis; 3 components extracted Rotation Method: Varimax with Kaiser Normalization.										

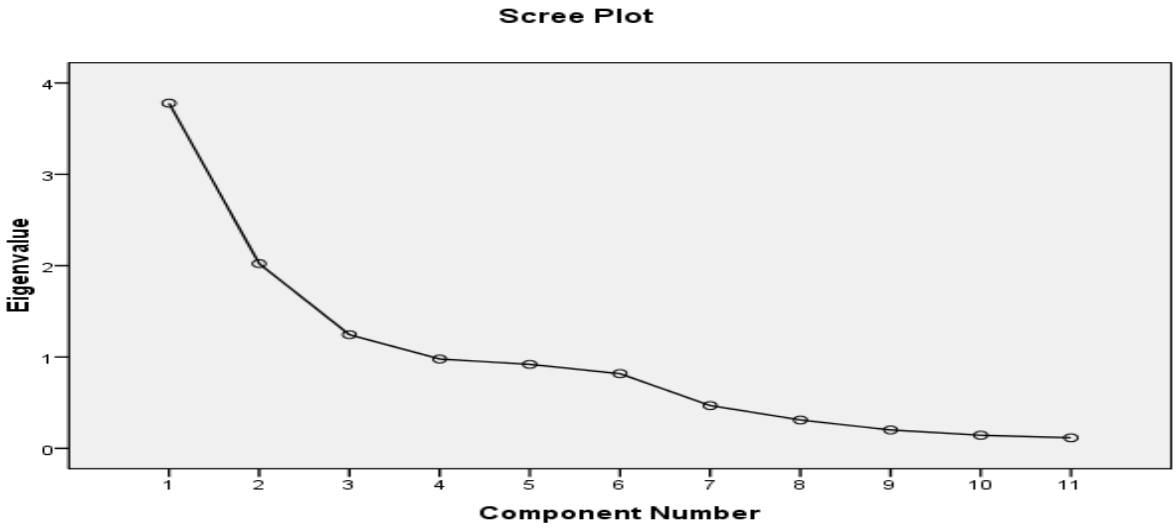

Figure 5: Principal Components Analysis (SBS)

The 11 variables remaining in the analysis satisfy the criteria for appropriateness of factor analysis. In our PCA the probability associated with Bartlett's Test of Sphericity should be less than the level of significance is <0.001, which satisfies this requirement. It is clear from the results that we can continue and perform a valid

factor analysis. The number of components extracted is 3 and based on the extraction of 3 components; solution would explain 59.18% of the total variance.

Table 8: Opportunity for Advancement from the B-School

Opportunities for Advancement	Valid	Freq.	%age	Mean	Standard Deviation	Variance
Opportunities have improved greatly	Yes	505	91	1.07	.255	.065
	No	38	6.9			
Opportunities have improved somewhat:	Yes	501	90.8	1.08	.267	.071
	No	42	7.6			
There has been no change in opportunities	Yes	18	3.3	1.97	.179	.032
	No	525	95.1			
Opportunities have declined somewhat	Yes	60	10.9	1.89	.314	.098
	No	483	89.0			
Opportunities have declined greatly	Yes	35	6.3	1.94	.250	.062
	No	507	91.8			

It is obvious form the table 8 that more than 90% of the surveyed populations from the B- School of India are in favour of that opportunities for the advancement have improved in India through the globalization of business management education. On the other side more than 90% respondents deny that the opportunities have decreased. 95% respondents were against to the statement that there are no changes in opportunities in India thorough globalization of business management education through Indian business schools and the higher educational system as a whole.

The method for selecting variables is derived from some original variables and factors scores from the principle component analysis. In this problem we have taken a dependent variable from original data set and independent variable as principle factor scores from principle component analysis (PCA) and then we have applied multiple regressions.

For further analysis, we here tried to find out to taking assumption null as there is no strong relationship with career outcomes ratings for Business Degree and Students Overall Business Skills Development. The results from the multiple regression analysis are as follows.

Table 9a: Multiple Regression- Model Summaries

Model Summary[b]					
Model	R	R Square	Adjusted R Square	Std. Error of the Estimate	Durbin-Watson
1	.358[a]	.128	.121	.604	1.552

The Multiple R for the relationship between the set of independent variables and the dependent variable is 0.358, which comes under the weak range of correlation. It interprets that the results of correlation are not good. The rule of thumb is as if a correlation less than or equal to 0.20 is characterized as very weak; greater than 0.20 and less than or equal to 0.40 is weak; greater than 0.40 and less than or equal to 0.60 is moderate; greater than 0.60 and less than or equal to 0.80 is strong; and greater than 0.80 is very strong.

The reason could be explained form the value of the Durbin-Watson statistic as resulted from the analysis is 1.552. The Durbin-Watson statistic ranges from 0 to 4. As a general rule of thumb, the residuals are uncorrelated is the Durbin-Watson statistic is approximately 2. A value close to 0 indicates strong positive correlation, while a value of 4 indicates strong negative correlation.

Table 9b: Multiple Regression- ANOVA

ANOVA[b]						
Model		Sum of Squares	df	Mean Square	F	Sig.
1	Regression	20.580	3	6.860	18.789	.000[a]
	Residual	139.839	383	.365		
	Total	160.419	386			

a. Predictors: SBS factor score 1, SBS factor score 2, SBS factor score 3 and *SBS – Skills for B – School Students (3 factors).*

b. Dependent Variable: Career Outcome Ratings for Business Degree (CORBD)

The probability of the F statistic (18.789) for the overall regression relationship of all three independent variables is <0.001, less than the level of significance of 0.05. We reject the null hypothesis that no strong relationship with career outcomes ratings for Business Degree and Students Overall Business Skills Development (R^2 = 0). We support the research hypothesis that there is a strong relationship with career outcomes ratings for Business Degree and Students Business Skills Development.

For further overall analysis, we here tried to find out to taking assumption null as there is no strong relationship with career outcomes ratings for Business Degree and Globalization of Business Management Education (GBME) - one factor, KDJS- Key Drivers of Job Satisfaction of B-School's Students (KDJS) – two factors, Factors of Motivation to get Connected with B-Schools (FMCB) – two factors, Students Business Skills Development (SBS) – three factors (total 8 factors score as independent for multiple regression). The results from the multiple regression analysis are as follows.

Table 10a: Multiple Regression- Model Summaries

Overall Model Summary[b]					
Model	R	R Square	Adjusted R Square	Std. Error of the Estimate	Durbin-Watson
1	.686[a]	.471	.460	.451	2.019

The Multiple R for the relationship between the set of independent variables and the dependent variable is 0.686, which is under the moderate range of correlation. It interprets that the results are quite good.

The rule of thumb is as if a correlation less than or equal to 0.20 is characterized as very weak; greater than 0.20 and less than or equal to 0.40 is weak; greater than 0.40 and less than or equal to 0.60 is moderate; greater than 0.60 and less than or equal to 0.80 is strong; and greater than 0.80 is very strong.

The Durbin-Watson statistic is 2.019. A value of 2 means that there is no autocorrelation in the sample and values approaching to 0.0 indicates positive autocorrelation and values toward 4 indicate negative autocorrelation.

Table 10b: Multiple Regression- ANOVA

ANOVA[b]						
Model		Sum of Squares	df	Mean Square	F	Sig.
1	Regression	68.514	8	8.564	42.028	.000[a]
	Residual	77.026	378	.204		
	Total	145.540	386			

a. Predictors: GBME factor score 1, KDJS factor score 1, KDJS factor score2, FMCB factor score 1, FMCB factor score 2, SBS factor score 1, SBS factor score 2, SBS factor score 3 (total 8 factors).*

b. Dependent Variable: Career Outcome Ratings for Business Skills (CORBD)

The probability of the F statistic (42.028) for the overall regression relationship of all independent variables is <0.001, less than the level of significance of 0.05. We reject the null hypothesis that no strong relationship with career outcomes ratings for Business Degree and Students Overall Business Skills Development ($R^2 = 0$). We support the research hypothesis that there is a strong relationship with career outcomes ratings for Business Degree and Students Business Skills Development.

The further extension of this research could be done for most accurate results through solving the problem of autocorrelation existing at some level here. This could be done through applying the ARIMA model.

VII. CONCLUSION

Industry's changing demand with global changing business environment pay a vital role to understand the sophisticated methodology and business curriculum worldwide, as the global challenges create the forced situations on B-schools to cope with the corporate change worldwide. Global business corporate increasingly recognize the importance of the prominent leaders who can equally comfortable and effective to work anywhere in the world. Business management education and methodology are changing and B-schools have created landmark through research and development. Globalization of business education creates a portfolio through creation of series of new learning skills and using of distinguishing approaches and stat-of-the art technology. Business management education practices are contemporarily required to update and to meet the enhancing Industry and society demand to achieve sustainable growth of the country.

The analysis of results shows the industry preferences amongst students are Finance & Accounting, Marketing Management, Information Technology, Human Resource Management and Business Economics respectively. This means that the Business-schools are adapting quickly enough to the changing demands of the students and their future employers through the globalization of Business Education and the Institution-Industry relationship are changing with the corporate to produce top-notch managers. The faculty members and other support staff also have access and advantage of development opportunities that support the B-school's globalization objectives. The Indian government is also contributing towards the globalization of management education in the country. The results explain very well that the globalizations of business management education have positive impact on business education institutions in India, and the higher educational system as a whole.

The general opinion of the B-school students pertaining to key drivers of job satisfaction explains significantly, Passion for work , Flexibility in working schedule , Control as subject matter expert, Scope for exercising management skills, Recognition for myself, Compensation etc. but not agree with autonomy for working independently. The means our research explains that the most are above factor of job satisfaction are having positive impact on business education institutions in India, and the higher educational system as a whole.

The role of Influential Factors in Choosing Self-Employment Business such as Join family business, Recognition of ability, Generation of Revenue, Difficult to Control over all aspects of business, Autonomy as primary business decision maker are most appropriate in choosing self-employment business explains positive impact on business education institutions in India, and the higher educational system as a whole but the research suggest that the Flexibility in Work schedule are not always right choice as business management professionals. Factors of Motivation to get connected to B-School, such as Advancement programs of B-schools, Opportunity to move in better placement, Training and development to date with the B-schools, Not Giving donation, Mentoring current/past students, Campus visits, Alumni events, Starting salary and job dissatisfaction level have explain significant effects as factors of motivation to get connected to B-schools.

The globalizations of business management education have positive role in enhancing overall quality/ business skills of manpower such as Business skills, Creative, Analytical, & Logical skills, Entrepreneurship skills, Ethics & value system, Industry awareness & Industry Dynamics, Team work skills, Inter personal Relationships across the border, Leadership & Innovation skills, Learning skills, Presentation skills, Problem solving skills through business schools and the higher educational system as a whole.

It is obvious form the student survey of B- School of India that most of the students population are in favor of that opportunities for the advancement have improved in India through the globalization of business education and on the other side highly disagree with the statement that the opportunities for advancement have decreased and there is no change in opportunities through globalization in business education.

The regression results also support the research that there is a strong relationship with career outcomes ratings for students' business degree and overall students' business skills development through globalization Global developing trend in business education.

REFERENCES

[1] GMAC, Graduate Management Admission Council®, The Application Trends Survey Report is a product of GMAC, a global nonprofit education organization of leading graduate business schools and the owner of the Graduate Management Admission Test® (GMAT®), 2013, gmac.com/globalgrads

[2] Prospective Students Survey Comprehensive Data Report, Gregg Schoenfeld, MBA.com PROSPECTIVE STUDENTS Survey, 2011–2012, Graduate Management Admission Council, 2012

[3] GMAC,Corporate Recruiters Survey 2013

[4] GMAC, Alumni Perspectives Survey Report 2013

[5] Mohammed Abdullah Mamun & Ariffin Bin Mohamad , "Management Education for Contemporary Challenges: The Role of Business School", European Journal of Scientific Research, ISSN 1450-216X Vol.30 No.4 (2009), pp.649-661 © EuroJournals Publishing, Inc. 2009, http://www.eurojournals.com/ejsr.htm

[6] M. Mahmood Shah Khan & Nandita Sethi, "Management Education & Corporate Governance: A Case of India and Pakistan© Research Journal of Internatıonal Studıes - Issue 12, 2009.

[7] Mike W. Peng & Hyung-Deok Shin, "How Do Future Business Leaders View Globalization"? 2008, Distinguished Professor of Global Strategy, University of Texas at Dallas, School of Management, Box 830688, mikepeng@utdallas.edu. Published online in Wiley InterScience (www.interscience.wiley.com). © 2008 Wiley Periodicals.

[8] UN Global Impact, "The principles for responsible management education", July 2007 Publication by the UN Global Compact, unglobalcompact@un.org

[9] Henry Gunfield, "The future of business schools Gabriel Hawawini", Chaired Professor of Investment Banking and Dean,INSEAD, Fontainebleau, France, Journal of Management DevelopmentVol. 24 No. 9, 2005pp. 770-782q Emerald Group Publishing,

[10] Deanne Butchey, "The Globalization of Tertiary Business Education", Florida International University, Journal of Academy of Business Education, Vol.6, 2005

[11] M., Papademetre, L. and Scarino, A., n.d., "Integrated resources for intercultural teaching and learning in the context of internationalization in higher education", Report, Research Centre for language and Cultural Education, University of South Austrailia, June 12, 2006, (http://www.unisanet.unisa.edu.au/learning connections/staff/practice/internationalization/document/FINAL-REPORT.pdf.

BIOGRAPHICAL NOTES

Dr. Ajay Singh, origin and nationality from India, presently working as Assistant Professor in Management & Information Department of College of Business Administration, University of Hail, Kingdom of Saudi Arabia since November 2011. He has total work experience is 10.5 years (Industry + teaching) out of which 6 years teaching experience of teaching Masters and Bachelor Classes in distinguishing Institutions. He did his Doctor of Philosophy (Ph.D) in Business Administration in 2008 and Master of Philosophy (M. Phil Economics) in 2003 from Bundelkhand University, Jhansi, India. He did his Master of Business Administration (MBA) in Human Resource Management /Organizational Behaviour from U.P. Technical University, Lucknow (India) in the year of 2002. He has two batcher degrees, one as Bachelor of Science (B.Sc. in Mathematics) and second one as Bachelor of Laws (LL.B in Industrial & Labour Laws) from CSJM University, Kanpur (India). Dr. Singh published many research papers in distinguishing reputed International and National Journals and attended various International conferences, workshops and FDPs in distinguished National & International locations. This research is his original work.

A COMPARATIVE STUDY OF IMAGE ENCRYPTION TECHNIQUES USING CHAOTIC MAPS

Bhagyashri R. Pandurangi[1],Dr.MeenakshiR.Patil[2] ,Vinay Sangolli[3]

[1]AssistantProfessor, Department of Electronics and Communication,

KLS Gogte Institute of Technology, Belgaum (India)

[2]Principal, Jain A.G.M Institute of Technology, Jamkhandi, (India)

[3]Department of Electronics and Communication, Jain College of Engineering, Belgaum (India)

ABSTRACT

For secure image encryption techniques Chaos Based cryptographic algorithms have suggested some new and efficient ways. Image encryption based on chaos became very popular for cryptography since properties of chaos are related to confusion and diffusion, two basic properties of good cipher. In this paper the encryption algorithms using chaotic maps are proposed. The two algorithms proposed are encryption algorithms using compound sine and cosine chaotic map and encryption algorithm based on logistic map. Experiments are performed in Matlab. In order to evaluate performance, the proposed algorithms are tested to measure the security and effectiveness. These tests includes visual test through histogram analysis, correlation coefficient analysis, information entropy test, measurement of encryption quality and time taken analysis.

Keywords*: *Cryptography, Chaotic maps, Decryption, Image processing, Symmetric Encryption

I. INTRODUCTION

Cryptography is the science of information security. It deals with hiding the private information. Cryptography is a method where in the data with useful information referred to as plain image is converted into random image referred to as cipher image with the help of cipher i.e., algorithm and key. Visual images play a vital role in information sharing. Due to extensive use of computers data integrity is of major concern. Chaotic systems are defined on real numbers. Any encryption algorithm which uses chaotic maps when implemented on a computer finite-state machine becomes a transformation from a finite set onto itself. Because of its wide dynamic range, the floating-point implementation seems to be the most appropriate for software implementation of chaotic maps. Conventional image encryption algorithms like DES, AES etc take more computational time and power especially when the image is large. Whereas most of the multimedia applications like image transmission, video etc require less computational time and power. Chaos based encryption algorithms offer good computational efficiency along with the combination of secure image encryption, speed for all the practical purposes. Chaotic systems are defined as dynamical systems with the following three properties: sensitivity to initial conditions, topological mixing, and density of periodic orbits.

Chaos-based encryption algorithms are performed in two stages, confusion and diffusion. Usually a single chaotic map or a set of maps are used for the generation of security keys. Mintu Philip[1] proposed encryption algorithm based on coupled chaotic map. The most important components of image are selected and encrypted.

In [2] the two-dimensional chaotic cat map is generalized to three dimensional for designing a real-time secure symmetric encryption scheme. The most commonly used chaotic maps used for chaotic image encryption are the baker map, tent map, the standard map [3-9]. Paper [9] employs the properties of chaotic systems to design a random bit generator, called CCCBG (Cross coupled Chaotic Based Bit Generator). In [10], image is partially encrypted using phase manipulation and sign encryption. Sign encryption finally provides the partially encrypted image by extracting the sign bits of modified image. In [11], invertible two-dimensional chaotic maps are employed on a torus or on a square for encryption using asymmetric block encryption schemes. Paper [12] describes a symmetric key block cipher algorithm which uses multiple one-dimensional chaotic maps instead of a one-dimensional chaotic map. For gray scale image there is no need of color transformation. Paper [13] describes a data hiding and extraction procedure for AVI videos by inserting the secret message bits in the DCT higher order co efficients. This method is tested for 28 frames by embedding 128 ×128 image.In [15] the Henon chaotic map is used for generation of keys and layered encryption technique for enhanced security along with color transformation technique for separation of color components in RGB images.

II PROPOSED WORK

2.1 Encryption Algorithm Based On Sine and Cosinechaotic Map

The proposed method is simple but highly secured image encryption and decryption algorithm which uses compound sine and cosine maps. The process starts by reading the size of the read image. The image is then prepared for diffusing. The original image is subdivided into three sub images based on the color component that is R, G and B planes. Each sub image is then converted into matrix with the pixel values in them and each pixel is converted into eight bit binary value, thereby resulting in binary matrix. Each pixel will be separated into eight planes corresponding to binary bits, there by resulting in 24 sets of bit plane images represented in matrix forms with single binary number in each pixel, these pixels are further ready for E-XOR with the keys.

The size of the input key is 16 alphanumeric characters which are used to form two set of ASCII codes, X_m and Y_m for setting initial conditions and parameters. The values of m range from 1 to 8. These values are converted into 48 bit binary values which are used in the equations below for the generating initial conditions and the control parameters.

$$R_{Xm} = \frac{(B_{X1} \times 2^0 + B_{X2} \times 2^1 + \ldots + B_{X48} \times 2^{}}{2^{48}} \quad (1)$$

$$R_{Ym} = \frac{(B_{Y1} \times 2^0 + B_{Y2} \times 2^1 + \ldots + B_{Y48} \times 2^{}}{2^{48}} \quad (2)$$

Therefore, the values of initial conditions and parameters are genereated using the R_1 and R_1 values

$$a_m = (R_{Xm} \times R_{Ym}) mod \quad (3)$$

$$b_m = (R_{Ym} \times R_{Ym+1}) mod \quad (4)$$

The value generated by equations are too small to generate the required chaos, therefore they are enhanced by iterating 100 times. These iterated values will be used in the compound sine and cosine chaotic map equations to generate the key

$$x_{n+1}=\cos a x_n+\sin b \quad (5)$$

The initial value of x_n will be 0.5.

These generated chaotic bits from (5) are XORed with the 24 sets of bit planes. The XOR operation gives the result as "0" if two input bits are similar and "1" if the two input bits are different. The result obtained by this XOR operation is 24 matrices with single binary number in each pixel. As a result, the encrypted image is obtained.

The decryption process is exactly the reverse process of encryption with the input image as the encrypted image, and the security keys being shared with the decryption algorithm.

2.2Encryption Algorithm Based On Logistic Map

The proposed encryption algorithm makes use of the logistic map for the generation of initial conditions and parameters.

Step 1: The read color image is divided into three sub images based on R, G & B components.

Step 2: Then value from each sub image is converted into binary value. These values are converted into column matrix and resized by combining with the size of the image.

Step 3: This is repeated for all the sub images, these sub images are concatenated to form one single binary image which is used to do bit XOR with the key.

Step 4: The initial value of the parameter 'a' is chosen as 4 in equation (9). As the signal generated by these values (3.57 to 4) is completely chaotic.

$$\mathbf{Y_{n+1} = a\, X_n (1 - X_n)} \quad (9)$$

Step 5: The input key will be seven bit alphanumeric which will be stored as an ASCII number, this input key will be converted into binary number which is of length 40 bits. Finally by using equation (10) the initial value for starting the execution of the chaotic function logistic map is obtained.

$$U = P_{1,1} \times 2^{39} + \cdots \ldots + P_{5,8} \times 2^0 / 2 \quad (10)$$

Step 6: The image is read part by part, for encrypting the pixels in each part of the image, the initial value of that part and equation (10) are used as follows.

$$\textbf{New value} = \textbf{Round (U)} \oplus \textbf{Old value} \quad (11)$$

The bits generated by the chaotic series are bit XOR ed with the binary images there by resulting in an encrypted binary values.

Step 7: These values are used to reconstruct the image. The first step will be to separate the R, G and components.

Step 8: These components are converted into column vectors and are stored as binary values. These values are stored in their respective planes. This procedure is repeated for green and blue components also. The stored binary values from the respective planes are fetched and are converted into the decimal values.

Step 9: Finally these decimal values of all the planes are concatenated to form the encrypted image.

The decryption algorithm is similar to the encryption algorithm but receiving encryption key and operating with the encrypted image.

III. SECURITY TEST AND COMPARATIVE STUDY

3.1Statistical Analysis

To prove the robustness of the proposed image encryption procedure, Statistical analysis is supported by the histograms, the correlation between two adjacent pixels in the encrypted images and the correlation coefficient for several plain images and their corresponding encrypted images.

3.1.1 Histogram analysis

An image-histogram indicates the image pixel distribution by indicating the number of pixels at each color intensity level. In Fig. 1, the histogram of the original image of Lena of size 256 × 256 and the histogram of corresponding cipher Image has been presented which depicts that the histogram of plain image has certain pattern of R, G, and B components. But in the Cipher image all the pixels are uniformly distributed, thus making the cryptanalysis difficult.

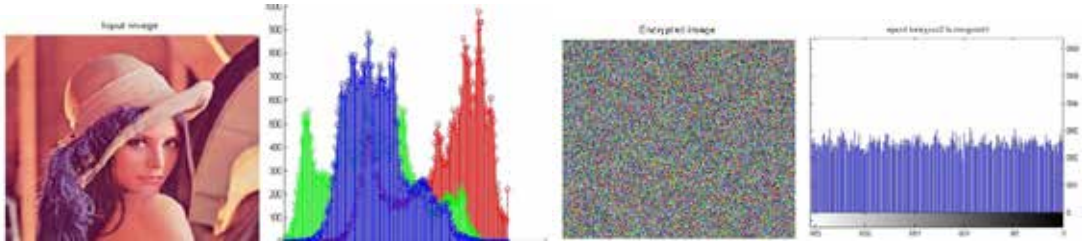

(a) (b) (c) (d)

Fig 1: (a) Plain original image, (b) histogram of original image (c) Encrypted Image, (d) Histogram of encrypted image

This test is conducted for all the three algorithms and satisfactory results were obtained.

3.1.2 Correlation coefficient analysis

In most of the plain images, there exists high degree of correlation among adjacent pixels whereas poor correlation between the neighboring pixels of corresponding cipher image is The correlation coefficient of the the R, G and B componentsfor the encryption algorithm using sine and cosine map, logistic map are shown in the Fig. 2. The correlation between various horizontally, vertically and diagonally adjacent pixels of both the plain and cipher image obtained using Encryption Algorithm based on logistic map are shown in Fig.3.

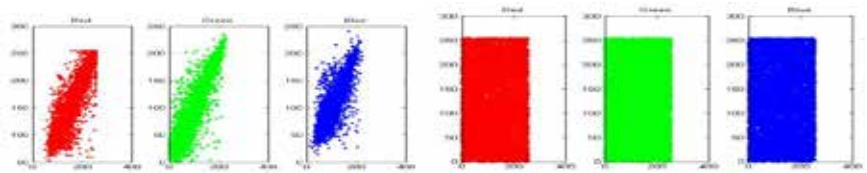

Fig 2: (a) Correlation of adjacent pixels of R, G and B components in plain image, (b) encrypted image

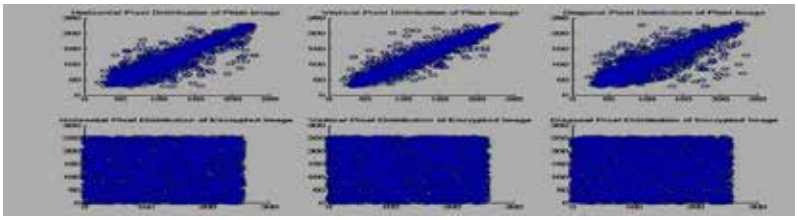

Fig 3: Horizontal, vertical diagonal pixel distribution of plain image and encrypted image.

Table 1.coefficientof horizontal, vertical, diagonal adjacentpixels of original and encrypted images

Image Name	Horizontal Correlation		Vertical Correlation		Diagonal Correlation	
	Plain Image	Cipher Image	Plain Image	Cipher Image	Plain Image	Cipher Image
Lena	0.9453	-0.0012	0.9716	-0.0095	0.9194	0.0078
Jellyfish	0.9669	0.0170	0.9694	0.0150	0.9531	-0.0106

Table1 shows the correlation coefficients between horizontal, vertical, diagonal adjacent pixels of original and encrypted images. Table 2 shows the comparison of correlation coefficient of different encrypted images obtained by encryption algorithms using sine and cosine map (Algorithm1) and logisticmap (Algorithm2).

Table 2.Comparasion of correlation co efficient of Different encrypted images

Image Name	Correlation parameter	Algorithm1	Algorithm2
Lena	Crr	-0.017499	-0.000331
	Crg	-0.015323	0.001827
	Crb	-0.009225	-0.001558
Mandril	Crr	-0.020522	-0.000400
	Crg	-0.008145	-0.004129
	Crb	-0.005235	0.000327
Jelly fish	Crr	-0.029583	0.004773
	Crg	-0.010927	-0.000769
	Crb	0.022440	0.003085

3.2Information Entropy Analysis

Entropy measures the randomness that indicates the texture of an image. The entropy H(s) of a message source s can be calculated as

$$\mathbf{H(s)} = \sum_{i=0}^{2^N-1} p(I_i) log_2 \frac{1}{p} \qquad (12)$$

where $p($ represents the probability of message .When an image is encrypted, the ideal value of entropy should be 8. If it is less than this value, there exists a certain degree of predictability which threatens its security. Table 3 compares the entropy values for plain and encrypted images.

Table 3.Comparison of information entropy

Image Name	Plain Image entropy	Entropy with Algorithm1	Entropy with Algorithm2
Lena	7.44	7.991	7.9991
Jelly fish	6.35	7.998	7.9983
Mendrill	7.48	7.997	7.990

3.3Encryption Quality – NPCR, UACI And Time Taken Analysis

NPCR (number of pixel change rate) and UACI (unified average change in intensity) are generally considered to evaluate the strength of the image encryption algorithm with respect to differential attacks. Opponent can create a small change in the input image to observe changes in the result. By this method, the meaningful relationship between original image and encrypted image can be found. To test the effect of one-pixel change on the image encrypted by the proposed algorithm, two common measures were used – Number of Pixel Change Rate (NPCR) , Unified Average Change in Intensity (UACI) . Consider two cipher-images, Ca(i, j) andCc(i , j) where i = 0,1,2, … , M - 1 and j = 0,1,2, … , N - 1,whose corresponding plain-images have only one pixel difference. Then NPCR and UACI are defined as

$$NPCR = \frac{\sum_{i,j} D(i,j)}{M \times N} \qquad \text{where } D = \begin{cases} 0, \text{if } Ca(i,j) = Cc(i, \\ 1, \text{if } Ca(i,j) \neq Cc(i, \end{cases} \quad (13)$$

$$UACI = \frac{1}{M \times N} \sum_{i,j} |Ca(i,j) - Cc(i, /255 \quad (14)$$

Table 4.Measurement of encryption quality and time taken

Apart from the security consideration, the speed of the algorithm is also an important parameter for a good encryption algorithm. In this paper the encryption/decryption rate of several images of different sizes by using the proposed image encryption algorithms are tested. The time analysis has been done on Intel i3 CPU with 4GB RAM computer. Table 4 depicts the related results.

Image Lena	NPCR	UACI	Time Taken	Image Mandril	NPCR	UACI	Time Taken
Algo1	99.8889	33.6119	2.4694	Algo1	99.9619	30.3741	5.4219
Algo2	99.8489	32.8281	0.3203	Algo2	99.8474	29.5381	0.3202

3.4Sensitivity Analysis

An ideal image encryption procedure should be sensitive with respect to the secret key i.e. the change of a single bit in the secret key should produce a different encrypted image.

For Algorithm1, the encryption and decryption realizes the 16 – character ASCII code “ABCDEFG012345678” as an input key. The resulting eight intial conditions and eight parameters, i.e a total of 16 keys, are represented by 8 – digit floating – point numbers results in 128 uncertain digits, which is greater than the minimum requirement of the 56 bit data encryption standard (DES) algorithm. For Algorithm2, plain image Lena of size 256 × 256 is considered as an example and is encrypted with x_0 = 0.45001, y_0 = 0.54001, μ1 = μ2 = 1.97. In Fig.4,different cipher images of Lena of size 256 × 256 with minor changes in secret keys have been presented.

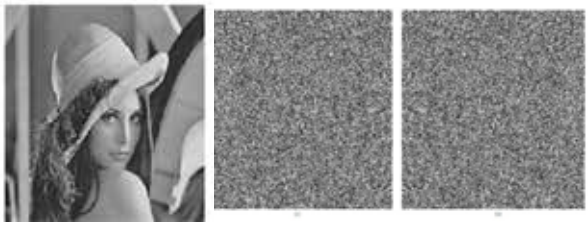

(a) (b) (c)

Fig 4: Key sensitivity test (a)Plain Image Lena of size 256 × 256 (b) Cipher image with chosen key (c) Cipher image with change in x_0 =0.45002, y_0 = 0.54002

In this algorithm, a 40 bit long key is used which produces a key space equivalent to 2^{40} which is a very long

key. In order to test the sensitivity of the key the image is once encrypted with the proposed algorithm, the same image is encrypted once again by changing the initial value of 'a' from to a value lesser than 4 (say 3.9). The encrypted images obtained are different from one another.

IV. CONCLUSION

The experimental results show that chaotic map based encryption algorithms are robust for image encryption. The encryption algorithm using sine and cosine chaotic map offers greater security as compared to the other two methods but takes more time to encrypt and decrypt. The algorithm using logistic map is faster and applicable to colour images but the algorithm with sine and cosine chaotic maps offers high level security hence is used for private data protection.

REFERENCES

[1] M. Philip, "An Enhanced Chaotic Image Encryption" InternationalJournal of Computer Science, Vol. 1, No. 5, 2011.

[2] G. Chen, Y. Mao, CK Chui, "A symmetric image encryption schemebased on 3D chaotic cat maps", Chaos, Solitons and Fractals, Vol.21,1992.

[3] H.K.L. Chang, J.L. Liu, "A linear quad tree compression scheme for imageencryption", Signal Process.vol 4, 279–290, 1997.

[4] J. Scharinger, "Fast encryption of image data using chaotic Kolmogrovflow", J. Electronic Engvol2, 318–325, 1998.

[5] Fridrich Jiri, "Symmetric ciphers based on two dimensional chaoticmaps", Int. Journal of . Bifurcation andChaos, vol 8, 1259–1284,1998.

[6] J.C. Yen, J.I. Guo, A new chaotic key based design for imageencryption and decryption, Proceedings of the IEEE InternationalSymposium Circuits and Systems, vol. 4,. 49–52, 2000.

[7] J.C. Yen, J.I. Guo, "An efficient hierarchical chaotic image encryptionalgorithm and its VLSI realization", IEE Proc. Vis. Image Processing, 167–175,2000.

[8]Fridrich J. "Symmetric ciphers based on two-dimensional chaotic Maps".International Journal of Bifurcation and Chaos,vol8,1259 – 1284, 1998.

[9] Feng Y, Li L J, Huang F. "A symmetric image encryption approachbased on line maps". In: Proceedings of the 1st InternationalSymposium on Systems and Control in Aerospace and Astronautics, 2001.

[10] Parameshachari B D, K M SunjivSoyjaudah, Sumitrha Devi K A,"Secure Transmission of an Image using Partial Encryption basedAlgorithm", International Journal of Computer Applications, vol. 63, no.16,0975 – 8887, February 2013.

[11] Jiri Fridrich, "Symmetric Ciphers Based on Two-Dimensional ChaoticMaps", International Journal of Bifurcation and Chaos, Vol. 8, No. 6, 1998.

[12] N.K. Pareek, VinodPatidar, K.K. Sud, "Cryptography using multipleone-dimensional chaotic maps", Communications in Nonlinear Scienceand Numerical Simulation,vol10 , 715–723,2005.

[13] Vandana Thakur, MonjulSaikia. "Hiding Secret Image in Video" ,International Conference on Intelligent Systems and Signal Processing(ISSP), 2013.

[14] K. Sakthidasan and B.V. Santhosh Krishna, "A New Chaotic Algorithmfor image encryption and Decryption of Digital Color Images",International Journal of Information and Education Technology, Vol. 1,No. 2, June 2011.

[15] Ramesh kumaryadava, Dr. B. K. singh, S. K. sinha, K. K. pandey, "ANew Approach of colour image encryption based on Henon like Chaoticmap", International Conference on Recent Trends in Applied Scienceswith Engineering Applications, Vol.3, No.6, 2013

[16] N.K. Pareek, VinodPatidar, K.K. Sud, Cryptography using Multiple one-dimensional chaotic maps, Communications in Nonlinear Science andNumerical Simulation, 2005.

[17] Kamlesh Gupta, Sanjay Silakari, "New Approach for Fast color imageencryption using chaotic Map", Journal of Information Security,vol 2,139-150, 2011.

[18] G.Chen, Y.Mao, and C.K. Chui,"ASymmetriEncryptionScheme Basedon 3D Chaotic Cat Map", Chao, Solitons& Fractals, 21,749-761,2004

[19] William Stalling, "Cryptography and Network Security", 3rd edition,Prentice Hall of India, 2003.

[20] Narendra K Pareek, VinodPatidar, Krishan K Sud, "A Random BitGenerator using Chaotic maps", International journal of network security Vol.10,No.1,PP.32,Jan2011

A STUDY ON ADVANCEMENTS OF NETWORK CODING IN WIRELESS MESH NETWORK

Dojohn Loyd.B[1], D.Sivakumar[2]

[1]*Research Scholar, Sathyabama University, Chennai,(India.)*

[2]*Professor, Easwari Engineering College, Chennai,(India.)*

ABSTRACT

Wireless Mesh Network is break through architecture in wireless communication that provides improved reliability, simplified link design, last mile coverage, flexible network architecture and minimal setup costs. Network coding proceeds an unconventional compute-and-forward approach rather store-and-forward which improves throughput, robustness, network protection with minimal energy consumption. In this paper we provide a comprehensive study and comparative analysis on the advanced network coding schemes on wireless mesh networks.

Keywords*: *CodeOR, CoMP, CORE,DODE, MIXIT, Network Coding, Proportion Fair Coding, SlideOR, WMN.

I. INTRODUCTION

Wireless Mesh Networks are a low-cost, high efficient, self-organizing and reliable multi hop systems that gains frontier attention from recent advancements of communication.Network coding (NC) is a kind of multicast technology that can encode the received information of the network nodes and then transmit it out [19]. The inherent characteristics of wireless mesh networks such as physical layer broadcast and two way data flow allow it to be appropriate for network coding. Traditional network link recovery method is to re-routing. However, using network coding can reduce the influence of the failure nodes or links to other nodes getting the full data, and effectively improve the robustness of the system.The incorporation of network coding in wireless mesh networks leads to performance improvement of network throughput and robustness.

The impacts of the communication performance of network coding in wireless mesh networks are:

1 **To improve the network throughput**

By using network coding can get the maximum flow of multicast, especially in wireless mesh networks with limited bandwidth, network coding can increase the data flow to a theoretical maximum.

2 **To enhance the network robustness**

In practical applications, wireless mesh networks nodes and links sometimes fail, and it affects the network's robustness.

3 **To reduce the energy consumption**

Network coding contributes vital role in wireless mesh networks in order to save energy. The energy per bit invested in coding/decoding operations can be several orders of magnitude smaller than that used for transmission/reception [15].

4 **To attain the network protection**

In a multi-hop wireless mesh network wireless links are vulnerable due to severe channel fading, interference and physical damage. With network coding, it is possible to achieve 1+N protection which uses the minimum redundant resources to recover any single link/node failure with the minimum delay.

1.1 Wireless Mesh Networks

As a low-cost, high efficiency, "last mile" wireless access system, wireless mesh networks has become the frontier area of academic and industrial research. Wireless mesh networks is a recent broadband wireless network that possesses high-capacity, high speed and distributed network nature. Fig.1 depicts the typical structure of WMN based on 802.11 standards.

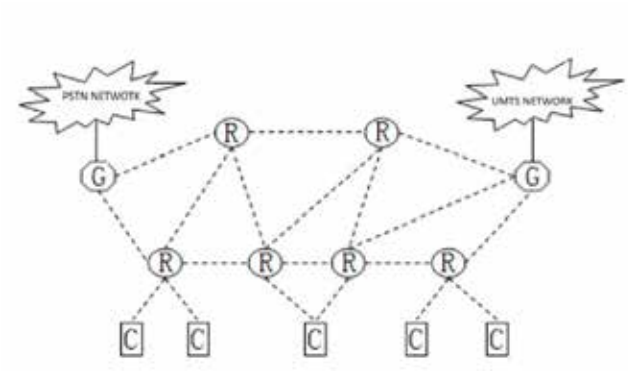

Fig.1 Wireless Mesh Networks Architecture

The network structure is separated into three different layers, the bottom layer constitutes mesh terminal C that can be the terminal equipment, including mobile phones, notebook computers and other devices of 802.11 standard. At the top of terminal layer is the mesh layer, which is composed of mesh gateway G and mesh router R, users can get access to the core network through the meshlayer. The third layer is the "core network layer", which provides diversified network interconnection services. Compared with traditional wireless networks, the advantages of wireless mesh networks: (1) improved reliability; (2) boast the protection mechanisms to conflict; (3) simplified link design; (4) last mile coverage; (5) flexible network architecture; (6) minimal setup costs [12].

1.2 Networks Coding

Network coding is a major advancement in the field of communications, it was proposed in 2000 by Ahlswede et al [19]. Network coding gives an unconventional approach to store-and-forward concept by introducing a compute-and-forward approach.

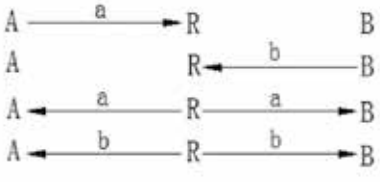

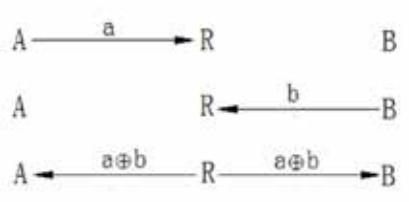

Fig.2 (A) Classical Wireless Communication **Fig. 2(B) Network Coding Approach**

The multicast capacity of wireless networks can be enhanced by mixing up different information in the router. Fig.2 (a) presents a classical wireless communication scenario with two nodes A and B and a relay node R.

Since Nodes A and B are not able to communicate directly, the message is transferred through node R. And arrows indicate directed links, assuming that each link capacity is 1and node A first sends message a to the node R, and node B sends a message b to node R, and then node R broadcasts the message a and b to nodes B and A respectively.

Having completed four such transmission node B received message a, while node A received message b.Fig.2 (b) illustrates network coding approach. In this approach, node R XOR the received messages a and b from nodes A and B and by exploiting shared nature of wireless medium, node R broadcasts the coded message c. Finally node B can recover message a from coded message c. It is apparently shown that it reduces number of transmissions, cost, energy, and increases security. Moreover, network coding can significantly improve the multicast rate consequently throughput of wireless mesh networks. In the early stage approaches of the network coding uses linear coding and advances with introduction distributed random network coding and recent research extends into opportunistic network coding. The simple version of network coding is achieved by XOR entering K packets (x1, x2,⋯,xK), and using y=x1⊕x2 ⊕⋯⊕xK to calculate coded message. COPE is the first network coding approach for wireless mesh networks. It exploits the shared nature of the wireless medium and broadcasts each packet.For adhoc wireless networks, the scheme CATWOMAN that uses unicast instead of broadcast in the MAC layer harness the power of wireless and cooperative networks in order to provide higher throughput and lower energy expenditure.

II. INTER-SESSIONNETWORK CODING

The motivation of inter-session network coding is to enhance the throughput of wireless mesh networks through efficacious usage of spectrum by discovering coding zones and mixing up packets from different sessions. It provides throughput improvement locally since the packets from different sessions are XORed by the minimalistic and localized coding strategies [22]. In the exemplary topology nodes X & Y are connected using relay R. Rather store and forward alone, R broadcasts the coded packets computed from bit-by-bit XOR operation on packets from both X & Y. The fresh coded packets are as same size as the original packets except subtle decoding payload in header. Any node can retrieve the targeted data packets by carrying out a bit-by-bit XOR between stored packet and the incoming coded packet.[22] The coding schemes COPE [21] and CATWOMAN [22] are inter session network coding schemes. Although this coding scheme reduces the number of transmissions from relays in the coding region, it fails to provide protection against packet losses and require special traffic patterns and network topologies to yield gains.

III. INTRA-SESSIONNETWORKCODING

The notion of intra-session network coding is to mix data packets only from the similar session, instead of mixing up packets from diverse sessions. Since this method relies on a computationally rigorous coding at the source node, recoding at relay node and decoding at receiver node. The benefit of this coding method is higher throughput and extends to increased performance in delay, energy, reliability, and security. The well-known strategy that serves as substrate for managing data into generations or batch of packets, with g packets of size L bits. [21] intra-session coding techniques, typically relying in random linear network coding (RLNC) for coding across packets of the same flow in order to provide resiliency against losses in the network. [22]The possibility

to recode packets at intermediate nodes from packets in their buffers using random coefficients allows the system to compensate for losses on a link by link basis, instead of compounding losses end–to–end and, hence, attain higher throughput. RLNC provides a distributed approach to perform intra-flow NC.

IV.COMPREHENSION: ADVANCEDNETWORKCODING

4.1 Symbol Level Network Coding

MIXIT network coding scheme exploits a basic property of mesh networks such that even when no node receives a packet correctly, any given bit is likely to be received by some node correctly. Instead of insisting on forwarding only correct packets, MIXIT [1] routers use physical layer hints to make their best guess about which bits in a corrupted packet are likely to be correct and forward them to the destination. Even though this approach inevitably lets erroneous bits through, it is found that the scheme can achieve high throughput without compromising end-to-end reliability. The core component of MIXIT is a novel network code that operates on small groups of bits, called symbols and each router forwards random linear combinations of the high-confidence symbols belonging to different packets. It allows the nodes to opportunistically route groups of bits to their destination with low overhead. The problems pertained to this approach are scalable coordination that is prevented by randomness from the network code along with a novel dynamic programming algorithm and error recovery problem that is solved by a rateless end-to-end error correcting component that works in concert with the network code . The routers themselves only forward random linear combinations of high-confidence symbols, performing no error handling. The additional technique associated with MIXIT Increased concurrency and congestion aware coding. MIXIT has a throughput gain of 2.8×over MORE and about 3.9×over traditional routing using the ETX metric.

4.2 Online Opportunistic Network Coding

Due to the constraints of computational complexity, a protocol utilizing network coding needs to partition the data into multiple segments and encode only packets in the same segment. However, it is extremely challenging to decide the optimal time to move to the transmissions of the next segment, and existing designs all resort to different heuristic ideas that might harm network throughput. In SlideOR [2], as opposed to segmented network coding, packets are not encoded separately in segments. Instead, the source uses a moving sliding window to determine the set of source packets to be encoded. Hence, in contrast to segmented network coding, where the coded packets in one segment is useless for the decoding of the next segment, the coded packets belonging to different overlapping sliding windows can be helpful to each other.

The challenges associated with slideOR are decision making of how far to advance the sliding window when ACKs arrive and the number of source packets in the re-encoded packet can be significantly larger than the sliding window size, which leads to increased encoding and decoding complexity that is alleviated by removing the coded packets with too many outdated source packets, it can maintain low computational complexity while achieving similar or higher throughput. In particular, SlideOR achieves two-fold performance gain over MORE [22] and 40% gain over CodeOR [11]. Furthermore, SlideOR is as simple as MORE for implementation, and much simpler than CodeOR since advancing sliding windows is much less challenging than scheduling multiple segments in CodeOR. [2].

4.3 Network Coding Multipath Forwarding Scheme

This is a network coding multipath protocol for WMN that extends current state-of-the-art and combines network coding with multipath routing to increase throughput for TCP sessions in WMN. CoMP [4] is situated below TCP/IP in the protocol stack. Typical network coding techniques divide traffic into generations and a coded packet is a linear combination of the packets that belong to the same group. This approach introduces a coding delay, because the source can send coded packets only after it has all the packets from a group, and a receiver can decode native packets only after it receives a number of independent linear combinations. Furthermore, this delay in the coding operations has a negative impact on the TCP performance in wireless environments. The online coding avoid the coding delay where the source mixes the packets from the TCP congestion window and the receiver acknowledges every innovative linear combination it receives, even if it cannot decode a native packet immediately. CoMP scheme is single path and the coding operations are performed end-to-end. Moreover, CoMP is a multipath online network coding scheme that exploits the path diversity in a mesh network, and eliminates the delay problems introduced by coding .It incorporates an algorithm to estimate the loss probability in the network and to adjust online the rate of sending linear combinations .This coding is associated with hybrid credit-based algorithm, where nodes compute the rate of generating linear combinations in a distributed manner and congestion control mechanism based on back-pressure

The study on CoMP shows that it is not only achieves a higher throughput, but it is also more efficient, due to exploiting path diversity and re-encoding packets on a hop-by-hop basis. In terms of efficiency, CoMP outperforms the other protocols for 55% of the flows.

4.4 Network Coding Scheme For N+K Protection

This scheme is a network coding based protection scheme against the average number of failures in a network. In a multi-hop wireless mesh network, wireless links are vulnerable due to severe channel fading, interference and physical damage. Network protection is generally used to handle link or node failures. Traditional network protection schemes can achieve 1:1, 1+1, and 1: N protections against a single node/link failure. With network coding, it is possible to achieve 1+N protection [5] which uses the minimum redundant resources to recover any single link/node failure with the minimum delay. However, the number of failures happening simultaneously in the network varies over time. When the number of failures happening simultaneously in the network is less than kmax, network bandwidth is wasted by the redundant code data packets transmitted in the network which will decrease network throughput.

Since wireless links are vulnerable, this technique exploits network coding to provide protection in which M coded data packets will be generated by linearly combining original data packets and in each time slot one coded data packet will be transmitted on one edge-disjoint path.

In few time slots, the destination may not decode the received coded data packets when the number of failures is more than k. On the other hand, in some time slots, the number of failures may be less than k. In such time slots, if the source encodes partial original packets sent in the previous time slot with the original data packets to be sent in the current time slot, the destination will be able to decode out original data packets sent in the previous

time slot. This network coding method aims to design a linear coding scheme protecting from the average number of failures to improve network throughput. It is shown that as long as the average number of failures is not more than k, the destination can decode and recover the original data packets even if the number of failures in some time slots is more than k with some overhead of sending the feedback to the source.

The network throughput of this scheme is nearly 40% higher than that based on the number of failures in the worst case.

4.5 Distributed Opportunistic Diffused Encoding (Dode)

In the existing network coding schemes, coding chances are inevitably depend on the established route and traffic is strictly coded based on the two-hop coding pattern. In order to overcome these issues DODE [6] combines both the diffused gain from BEND and the generalized coding condition from DCAR. In addition, this scheme includes a routing metric called Shortest Path with Enriched Neighborhood routing Metric (SPENM) which allows DODE to follow the most enriched coding chance path and also to enjoy the diffused gain.

DCAR allows decoders to be more than one hop away from the encoders. Nevertheless, DCAR requires the encoders to be on the routing path of all flows. BEND does not require the later condition because an overhearing node can also be the encoder. However, BEND still insists the encoder and decoders to be neighbors like COPE.

To combine the advantages from the previous architectures, DODE constrains the coding conditions for by integrating of the opportunistic listening and the opportunistic coding features of COPE, the diffused gain by the neighborhood feature of BEND and the generalized coding condition of DCAR. For the traffic to flow through the network with the most potential coding chances, we propose a routing metric called ”shortest path with enriched neighborhood routing metric” (SPENM) which is integrated in the DSDV routing protocol. DODE shows a better performance 16%-33% over the BEND and DCAR

4.6 CORE: COPE With MORE

State-of-the-art in network coding for wireless, meshed networks are suffering from problem of providing reliability for a single session and the problem of opportunistic combination of flows by using minimalistic coding. The CORE [9] protocol brings together these problem and alleviates it efficiently by integrating random linear network coding (RLNC) for intra-session coding and allows nodes in the network to setup inter-session coding regions where flows intersect.

It introduces a mixed approach that allows sources and intermediate nodes to generate RLNC packets for each flow, but also allows the network to identify regions where controlled inter-session coding could take place. It is compulsion that inter-session coding is contained to the identified regions, so the end receivers will not get coded packets with contributions of other flows. A key element of this scheme is that XORed packets at a relay are not discarded if overhearing is unsuccessful. Therefore, the XOR of two coded packets can be used as an additional, richer coded packet that will be useful to recover future linear combinations of packets for a given flow. These advantages are brought forth by performing a more thorough partial decoding at the relays, i.e., not restricted to recovering XORed data. Thus, CORE increases the benefits of XORing by exploiting the

underlying RLNC structure of individual flows. Result shows that the gains of up to 4 fold over COPE-like schemes and it provides median throughput gain of 95 % with routing.

4.7 Proportional Fair Coding

In multihop wireless networks carrying unicast flows for multiple users, each flow has a specified delay deadline, and the lossy wireless links are modeled as binary symmetric channels (BSCs). Since airtime, on the links is shared among flows, increasing the airtime for one flow comes at the cost of reducing the airtime available to other flows sharing the same link. Proportional Fair Coding [10] introduces the joint allocation of flow airtimes and coding rates that achieves the proportionally fair throughput allocation. In the special cases where all links in a network are loss-free or all flow delay deadlines are infinite, it shows that the proportionally fair utility optimization decomposes into decoupled airtime and coding rate allocation tasks. That is, a layered approach that separates MAC scheduling and packet coding rate selection is optimal

However, we show that no such decomposition occurs when one or more link share lossy or one or more flow share finite delay deadlines. Instead, in such cases, it is necessary to jointly optimize the flow airtimes and coding rates. Furthermore, the resulting allocation of airtime and coding rates is qualitatively different from classical results.

The proportionally fair airtime and coding rate allocation results in the allocation of 41% of the airtime for flow, while each flow receive 29.5%.The optimal coding rate is 0.62 for flow and 0.97 for flows and coding rate for flow is much lower than for flows and since a smaller block size must be used by flow in order to respect the delay deadline. Due to the delay deadline, these optimal coding rates yield nonzero loss rates. For flow, the packet loss rate at the receiver, after decoding, is 20%, whereas flows and are loss-free.

4.8 Network Coding with Opportunistic Routing

Opportunistic routing greatly improves unicast throughput in wireless mesh networks and using network coding, opportunistic routing is able to be implemented in a effortless way without resorting to a complex scheduling protocol. Due to limitations of computational complexity, a protocol using network coding is required to carry out segmented network coding, that partitions the data into multiple segments and encode only packets in the same segment. However, previous designs transmit only one segment at any given time while waiting for its acknowledgment, which reduces performance as the size of the network increases. The protocol CodeOR [11] uses network coding in opportunistic routing to improve throughput. This protocol to allow the source to transmit a sliding window of multiple segments using opportunistic routing, and with segmented network coding. CodeOR performs rather than flow control on bytes or packets; it is performed on a sliding window of segments. By transmitting a window of several segments in parallel, it increases the performance by a factor of two on average. CodeOR is in particular appropriate for real-time multimedia applications through the use of a small segment size to decrease decoding delay, and is able to further increase network throughput with a smaller packet size and a larger window size.

V.CONCLUSION

In this paper we studied advancements of network coding from wireless mesh network stand point. The different scenarios where network coding is sought for are illustrated along with performance enhancement details.

REFERENCES

[1] Sachin Katti, Dina Katabi, HariBalakrishnan, and Muriel Medard ," Symbol-level Network Coding for Wireless Mesh Network", SIGCOMM'08, August 17–22, 2008, Seattle, Massachusetts Institute of Technology, Washington, USA. Copyright 2008 ACM.

[2] Yunfeng Lin, Ben Liang, BaochunLif," SlideOR: Online Opportunistic Network Coding in Wireless Mesh Networks",IEEE Communications Society subject matter experts for publication in the IEEE INFOCOM 2010 proceedings.

[3] R. Asorey-Cacheda∗, H. Huang†, F. J. Gonz ´ alez-Casta˜no∗, E. Johnson†, C. L ´ opez-Bravo∗ and F. Gil-Casti˜neira, "A Joint Interchannel and Network Coding Schema for nVoD Services over Wireless Mesh Networks",IEEE Communications Society subject matter experts for publication in the IEEE "GLOBECOM" 2009 proceedings.

[4] StelutaGheorghiu, Alberto Lopez Toledo, Pablo Rodriguez, "Multipath TCP with Network Coding for Wireless Mesh Networks".

[5] Shifang Dai, Xinming Zhang, Member, IEEE, Jin Wang, and Jianping Wang, Member, IEEE,"An Efficient Coding Scheme Designed for N+k Protection in Wireless Mesh Networks",IEEE COMMUNICATIONS LETTERS, VOL. 16, NO. 8, AUGUST 2012.

[6] Thuong-Van Vu, Thi Mai Trang Nguyen and Guy Pujolle, "Distributed Opportunistic and Diffused Coding in Multi-hop Wireless Networks", Workshop on Cooperative and Cognitive Mobile Networks IEEE2012.

[7] Kate Ching-Ju Lin, Member, IEEE, and De-Nian Yang, Senior Member, IEEE, "Multicast With Intraflow Network Coding in Multirate Multichannel Wireless Mesh Networks",IEEE Transactions on Vehicular Technology, VOL. 62, NO. 8, October 2013 3913.

[8] Jin Wang†, Kejie Lu‡, Jianping Wang, and ChunmingQiao," Untraceability of Mobile Devices in Wireless Mesh Networks using Linear Network Coding",2013 Proceedings IEEE INFOCOM.

[9] JeppeKrigslund∗†, Jonas Hansen∗, Martin Hundebøll∗, Daniel E. Lucani∗, Frank H. P. Fitzek†∗,"CORE: COPE with MORE in Wireless Meshed Networks", 2013 IEEE.

[10] KarumbuPremkumar, ,XiaominChen,andDouglasJ. Leith,"Proportional Fair Coding for Wireless Mesh Networks", IEEE/ACM TransactionsonNetworking, vol.23, no.1, February2015.

[11] Yunfeng Lin, Baochun Li, Ben Liang, "CodeOR: Opportunistic Routing in Wireless Mesh Networks with Segmented Network Coding".

[12] Xiaojian Shen1, 2, Zhigang Chen1, Ying Guo1, Hui Ye1," Minimum Cost Routing Based on Network Coding in Wireless Mesh Networks".

[13] Martin Hundebøll, JeppeLedet-Pedersen, Janus Heide, Morten V. Pedersen, Stephan A. Rein, Frank H.P. Fitzek , "CATWOMAN: Implementation and Performance Evaluation of IEEE 802.11 based Multi-Hop

Networks using Network Coding∗",Aalborg University, Department of Electronic Systems, Mobile Device Group.IEEE Magazine 2012.

[14] PeymanPahlevani, AchuthanParamanathan, Martin Hundebøll, Janus Heide, Stephan A. Rein, Frank H.P. Fitzek, "Reliable Communication in Wireless Meshed Networks using Network Coding",Aalborg University, Department of Electronic Systems.

[15] Achuthanparamanathan, Morten v. Pedersen, daniel e. Lucani,and frank h. p. fitzek, " lean and mean: network coding for commercial devices",

[16] Gerg˝oErtliacticom GmbH, Germany AchuthanParamanathan, Stephan Alexander Rein,Daniel E. Lucani, Frank H.P. Fitzek, " Network Coding in the Bidirectional Cross: A Case Study for the System Throughput and Energy"Aalborg University, Department of Electronic Systems.

[17] JeppeKrigslund, Jonas Hansen, Morten V. Pedersen, Daniel E. Lucani, Frank H. P. Fitzek, "Performance Evaluation of Coded Meshed Networks", Department of Electronic Systems, Aalborg University, Denmark.

[18] Qiang Hu 1,2 and Jun Zheng, " CoAOR:An Efficient Network Coding Aware Opportunistic Routing Mechanism for Wireless Mesh Networks",National Mobile Communications Research Laboratory, Southeast UniversityNanjing, Jiangsu 210096, China.

[19] R. Ahlswede, N. Cai, S. Y. Li, and R. W. Yeung, "Network informa-tion flow," IEEE Transactions Information Theo-ry, 2000, 46(4): 1 204-1 216

[20] A. H. Anwar, B. Chadi, T. Thierry, "Network coding for wireless mesh networks: a case study," IEEE Communication Society, 2006: 173-182.

[21] S. Katti et al., "XORs in The Air: Practical Wireless Network Coding," IEEE/ACMTrans. Net., vol. 16, no. 3, 2006, pp. 497–510.

[22] M. Hundebøll et al., "Comparison of Analytical and Measured Performance Results on Network Coding in IEEE 802.11 Ad-Hoc Networks," Proc. 76th IEEE Vehic. Tech. Conf., 2012

A BLEND OF CRYPTOGRAPHY AND STEGANOGRAPHY

[1]Natasha Taneja, [2]Dr. Prinima Gupta

[1]M.Tech Scholar, [2]Assistant Professor, Department of Computer Science,

Manav Rachna College of Engineering, Faridabad (India)

ABSTRACT

Due to increase in demand of internet applications, it is required to transmit data securely from one place to another. The data transmitted is not protected as it can be hampered by hacker or intruder. So, for this purpose we have to use Cryptography and Steganography or the combination of both to enhance the security by providing dual security structure. Cryptography is to hide the data using encryption algorithms. Steganography is used to hide the data into another data or a file known as cover file. In order to make faithful and secure communication, a dual security technique is proposed in this paper. We are merging these two techniques in order to upgrade the security and making communication more reliable.

Keywords: Cryptography, Steganography.

I. INTRODUCTION

Internet is widely used around the world. Its applications are required to send and receive information and their major issue of concern is information security. Transmission of data is not secured in public communication as data can be obstructed by intruder or eavesdropper. In any communication, it is necessary to maintain the integrity of data. With the advancement in technologies, the networks over the long distance may not be reliable to provide the secure communication. To overcome this problem Cryptography and Steganography are the techniques which are used widely. Cryptography is an art of keeping the data secret to ensure that it is unaltered and secure. Steganography is combined with cryptography to enhance the security. Steganography is an art of hiding or embedding file in a cover file to ensure the data confidentiality and authenticity. The blend of these two techniques can ensure the secure transmission of data.

II. CRYPTOGRAPHY

Cryptography means "Hidden Writing". It is one of the techniques which are used to ensure the secure transmission of data between sender and receiver by scrambling the input message to produce the output. In this technique plain text is converted into cipher text by applying several algorithm such as private key cryptography, public key or symmetric and asymmetric algorithm for security of the information. It provides solution to several set of parties but the attacker can easily interpret or modify this text without letting aware of their presence between the communications so to overcome this problem Cryptographic techniques are used.

2.1 Cryptography Schemes

To maintain the security of data, three types of schemes are widely used. These are as follows:

1) *Private / Symmetric Key*: As the name states there should be a same or a secret key used for encryption of plaintext and decryption of cipher text. Plaintext is the original messages send by the sender whereas

Cipher text is the scrambled message which is produced as output at the receiver side. The following diagrams describes two important phases of cryptography: Encryption Phase and Decryption Phase (Figure1.1 and Figure 1.2)

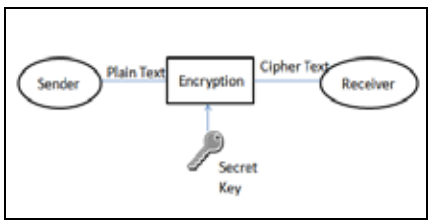

Fig 1.1: Encryption Phase

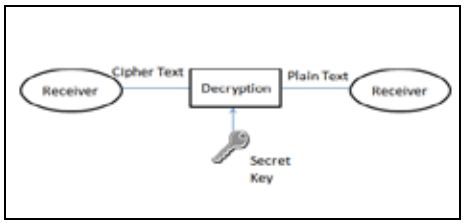

Fig 1.2: Decryption Phase

2) *Public / Asymmetric Key*: In this scheme, different keys are used for encryption and decryption phases. To enhance the security two keys are used: Public Key and Private Key. In Encryption phase, the sender uses public key of receiver to encrypt a message and the receiver uses his private key to decrypt the cipher text. In order to provide authentication, private key of the sender is used to encrypt a message and public key of the sender is used to decrypt the message at the receiver's side.

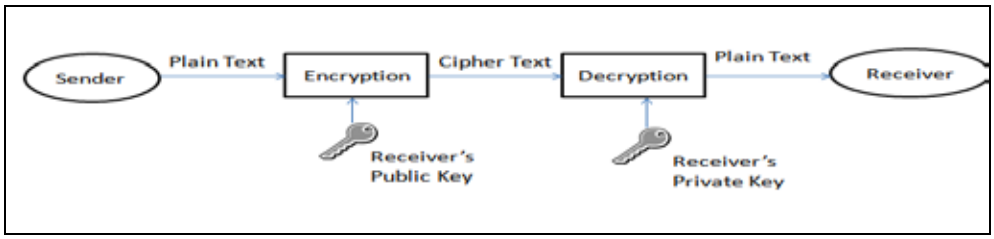

Fig 1.3: Encryption

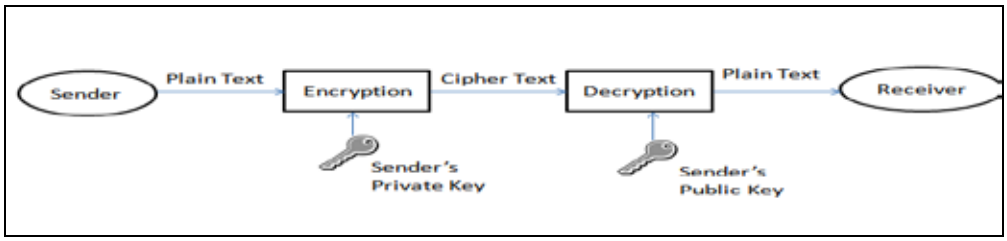

Fig 1.4: Authentication

3) *Hash Functio*n: It is also known as message digest. It maps a message of variable length to a fixed length hash value. This fixed - size output is also known as hash code. It is often used to ensure that file is unaltered or not affected by intruder or hacker.

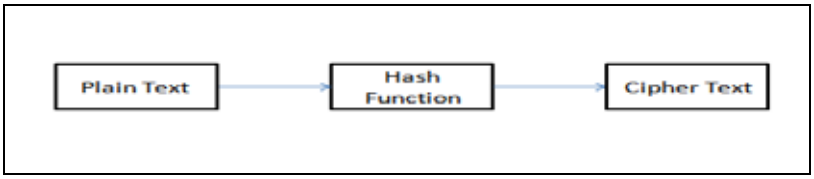

Fig 1.5: Hash Function

One of the most important developments on public key cryptography schemes is Digital Signature. Public key cryptography is being preferred as it is more secure and data integrity is maintained.

Digital Signature is one of the important aspects for securing the content. For that Digital Signature is being used as it overcomes all the limitations of the conventional signature. Now days, it is widely used in email, Credit cards for transaction and many more. The two broad techniques of digital signature are: symmetric key cryptosystem and public key cryptosystem. Cryptosystem here refers to encryption technique.

- *Symmetric Key Cryptosystem*: In symmetric key cryptosystem, secret key is being used which is only known to sender, there only one key or a unique key is used between the sender and receiver or in another words between two users. Its limitation is generation, distribution and keeping track is difficult.
- *Public Key Cryptosystem*: In public key cryptosystem, a pairs of keys is used, private key is only known to a sender and public key is known to all the recipients who are interested in communicating with a sender.

To maintain confidentiality of the message, it should be encrypted with sender's public key on which decryption can be performed by sender's private key.

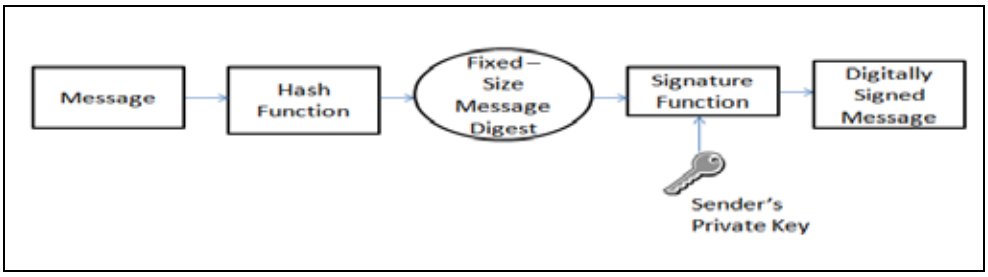

Fig 1.6: Digital Signature

III. STEGANOGRAPHY

Steganography is an art of hiding or embedding one file into another. Cryptography is used to scramble the message but does not to hide the encrypted data whereas in Steganography, message remains unaltered but its presence is hidden by embedding it into a cover file.

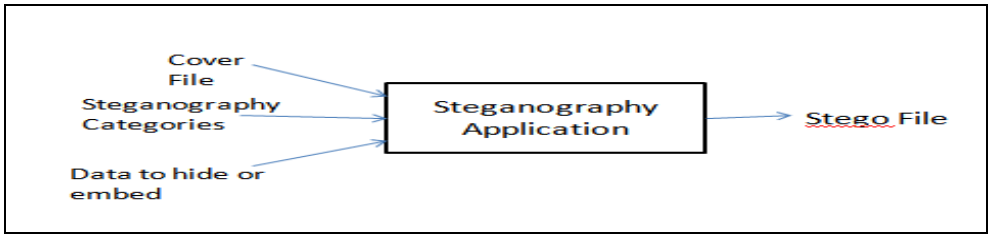

Fig 1.7: Steganography

Fig1.7 describes the following components of Steganography:

- *Cover File*: Data to be concealed is embedded.
- *Data to hide or embed*: Data to be hide.
- *Steganography Categories*: Different categories of Steganography, like text, audio, video etc.
- *Steganography Application*: Is used to hide data within a cover file.
- *Stego File*: It contain cover file along with hidden information.

IV. COMBINATION OF CRYPTOGRAPHY AND STEGANOGRAPHY

Merging these two security approaches provides more privacy and security. Cryptography changes the format of the data that cannot be access by any third party and Steganography on another hand hides this coded data into a cover file. So that no one can easily decrypt the data and also prevent from intruder or hacker.

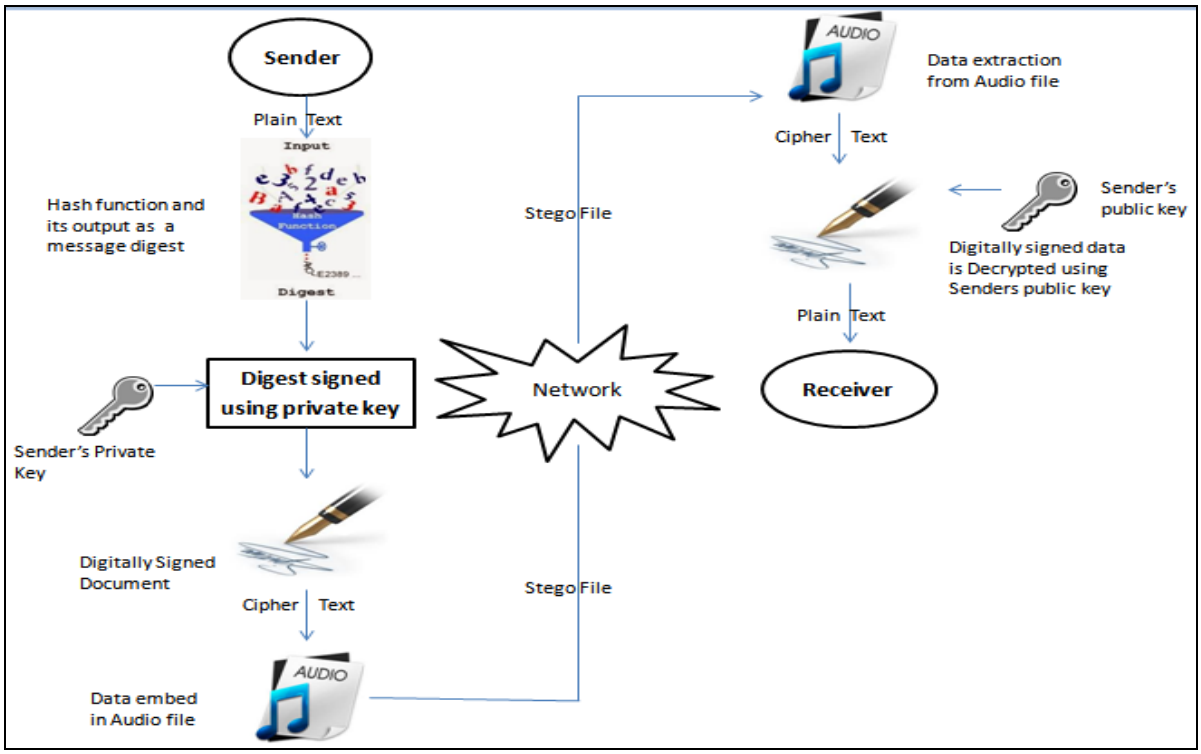

Fig 1.8: Combining Cryptography and Steganography

In Fig 1.8 Sender sends plaintext or original text, this plain text is converted to digitally signed document using hash function and a certificate which further produces a Digitally Signed document. This Digitally Signed document is converted to Stego file using Audio Steganography. The message is decrypted at receiver's end by converting Stego file to Digitally Signed data then to plain text.

If any of these technologies, Cryptography and Steganography is used individually then may lack some security issues which can be achieved by amalgamation of these two. Table 1.1 Depicts the result of combination of these two and how this helps in raising the security against threats.

S.No.	Cryptography	Steganography	Combination
1.	The message is in unreadable format as transformed to Cipher text.	The message is obscured within another medium or Cover file and produces Stego file.	Plain text is transformed to Cipher text then Cipher Text in transformed to Stego file.
2.	The message can be detected and modified easily by anyone.	The message cannot be detect easily as it is hidden within another medium.	The message is encrypted as well as secured from interceptor.
3.	The objective is to prevent unauthorised access.	The objective is to secure the existence of the hidden data from the interceptor.	To prevent from unauthorized attack as well as prevents data from being read by third party.
4.	Data can be discovered easily but extraction of data is complex.	Discovery as well as extraction of data is complex.	Detection as well as extraction of data both are made complex.
5.	Reverse engineering is performed in order to enhance or duplicate the security.	Exchanged data is analyzed and regularly monitored.	Enhancement of security by using Reverse engineering as well as regular monitoring of data.

Table 1.1: Cryptography, Steganography and their combination

However combining both the techniques provides the enhanced security but either of these techniques cannot provide protection as compare to dual protection provided by their combination. Merging of these two is more beneficial as it increases the confidentiality, prevents from unauthorized attacks and improves data secrecy.

V. CONCLUSION

The advantage of Steganography over Cryptography individually is that identity of messages is hidden from phisher. Whereas the objective of Cryptography is to scramble the message to convert it to unreadable by a third party, the objective of Steganography is to conceal the data from a third party. Therefore, combining both Cryptography and Steganography will be a best choice as it will maximize the security, ensures data integrity and provide more authentication as well as privacy.

V1. ACKNOWLEDGMENT

I take this opportunity to express a deep sense of gratitude and thank Dr. Prinima Gupta, Assistant Professor, Department of Information Technology, Manav Rachna College of Engineering for her cordial support, valuable information and guidance in writing this paper.

REFERENCES

[1] Pramendra Kumar and Vijay Kumar Sharma," Information Security Based on Steganography & Cryptography Techniques: A Review", International Journal of Advanced Research in Computer Science and Software Engineering 4(10), October - 2014, pp. 246-250.

[2] Ankit Uppal, Rajni Sehgal, Renuka Ngapal and Aakash Gupta," Merging Cryptography& Steganography Combination Of Cryptography: RC6 Enhanced Ciphering And Steganography: JPEG", Proceedings of 5th SARC-IRF International Conference, 25 May-2014, pp. 62-64..

[3] S.R. Subramanya and Byung K. YI,"Digital signatures", IEEE Potentials, 2006, pp. 5-8.

[4] R.Valarmathi., M.Sc.,M.Phil 1, G.M.Kadhar Nawaz M.C.A., Ph.D 2," Information Hiding Using Audio Steganography with Encrypted Data", International Journal of Advanced Research in Computer and Communication Engineering, Vol. 3, January 2014.

[5] Elżbieta Zielińska, Wojciech Mazurczyk, Krzysztof Szczypiorski,"Development Trends in Steganography", Warsaw University of Technology, Institute of Telecommunications Warsaw, Poland, 00-665, Nowowiejska 15/19.

[6] Abdulaleem Z. Al-Othmani1, Azizah Abdul Manaf2 and Akram M. Zeki3," A Survey on Steganography Techniques in Real Time Audio Signals and Evaluation", IJCSI International Journal of Computer Science Issues, Vol. 9, Issue 1, No 1, January 2012.

[7] Jayram , Ranganatha H, Anupama H," INFORMATION HIDING USING AUDIO STEGANOGRAPHY- A SURVEY", The International Journal of Multimedia & Its Applications (IJMA), vol. 3, no. 3, August 2011.

[8] Erfaneh Noorouzi1 , AMIR REZA ESTAKHRIAN HAGHIGHI ,Farzad Peyravi, Ahmad Khadem zadeh," A New Digital Signature Algorithm", 2009 International Conference on Machine Learning and Computing IPCSIT, vol.3 (2011).

[9] Niels Provos, Peter Honeyman ,"Hide and Seek: An Introduction to Steganography", IEEE Computer Society, IEEE Security & Privacy , 1540-7993.

CENTRALIZED AUTO-TUNED IMC-PI CONTROLLERS FOR REAL TIME COUPLED TANK PROCESS

Ujjwal Manikya Nath[1], Saswati Datta[2], Chanchal Dey[3]

[1,2] *M. Tech Scholar, Department of Applied Physics, University of Calcutta, Kolkata (India)*

[3] *Assistant Professor, Department of Applied Physics, University of Calcutta, Kolkata (India)*

ABSTRACT

Multiple interconnected tanks supplied by more than one pump is a multi-input-multi-output (MIMO) process which is quite common for industrial applications. Presently, Internal Model Control (IMC) technique is widely used in controlling industrial MIMO processes due to its sole tuning parameter. But, as the IMC technique is entirely based on the process model hence in case of any uncertainty in modeling, nonlinear interacting behavior as well as time varying features of the process parameters impose limitations on the performance of IMC controllers. To overcome such limitations, in the proposed work, a simple auto-tuning scheme is incorporated in the conventional IMC based Proportional Integral controller (IMC-PI). In the proposed auto-tuner, the only tuning parameter i.e., the close-loop time constant is continuously varied depending on the instantaneous process error. Performance of the proposed auto-tuned IMC-PI controller (IMC-API) along with conventional IMC-PI controller are verified on a laboratory based real time coupled tank process which is a well known interacting MIMO process. Here, control task is aimed towards maintaining the water levels at the respective desired values under both the set point change and load disturbance. Experimental results substantiate the superiority of the proposed IMC-API compared to conventional IMC-PI controllers.

Keywords : Auto-tuning, centralized control, coupled tank process, IMC-PI controller, system modeling

I. INTRODUCTION

At present, IMC controllers are widely used in various process industries due to their simple approach based on sole tuning parameter and considerable robust performance. In this context, for first order process model, Rivera et al. [1] suggested IMC based PID controller and it was further extended by Chien [2] for second order model. Apart from the simplicity of IMC tuning, the major limitation is that it fails to perform satisfactorily for processes with nonlinear time varying feature. As the IMC based controller design is entirely based on the process model so any type of un-modeled dynamics and interacting behavior of the process parameters are beyond the scope of conventional IMC controllers. To overcome such limitations an online adaptation scheme was first proposed by Datta and Ochoa [3]. They studied the stability of their controller in ideal condition. Silva et al. [4] worked on discrete-time adaptive IMC which showed robust behavior against changes in modeling parameter. Rupp and Guzzella [5] presented an adaptive IMC for stable non-minimum phase single-input single-output (SISO) plant related to air fuel ratio control system. However, those

contributions only focus on SISO system [6] and there is no theoretical assurance for extending SISO adaptive IMC to MIMO system due to interaction among the process parameters. Chi and Zhao [7] proposed adaptive IMC for MIMO system with the help of dynamic decoupler. But, design of a suitable decoupler for a nonlinear MIMO process is not a simple task.

Here, our prime goal is to design an auto-tuning scheme for IMC based proportional integral (IMC-PI) controller which will be capable to provide the desired overall response without using any decoupler for an interacting MIMO process. In the proposed work, our experimental set-up is 'coupled tank' system which is a well known MIMO process with nonlinear behavior. The proposed centralized [8] auto-tuning scheme is quite simple in nature and it provides the necessary variation in the value of only tuning parameter i.e., the close-loop time constant. The online variation of the sole tuning parameter [9] actually results a continuous gain variation for IMC-PI controller [10]. The tuning strategy in the proposed auto-tuner is so designed, for large process error (i.e., when process output is far away from the desired value), a smaller value of close-loop time constant is chosen to achieve good transient response and on the other hand when error becomes small (i.e., process output is close to the desired value), comparatively larger value of close-loop time constant is selected to achieve improved steady state response. Performance of the proposed auto-tuned IMC-PI controller (IMC-API) is tested on a miniaturized coupled tank process manufactured by Feedback Instruments [11]. From the experimental results it is observed that the proposed IMC-API shows superior performance in comparison with IMC-PI under both the set point change and load variation.

II. DESIGN OF IMC-PI CONTROLLER

The block diagram of IMC control technique [9, 10, 12] is shown in fig. 1.

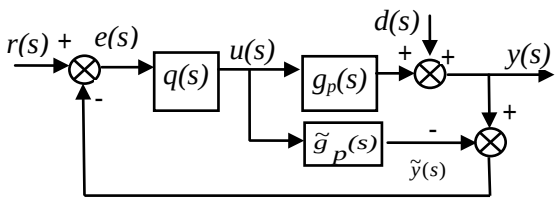

Fig. 1: Block Diagram of IMC Structure.

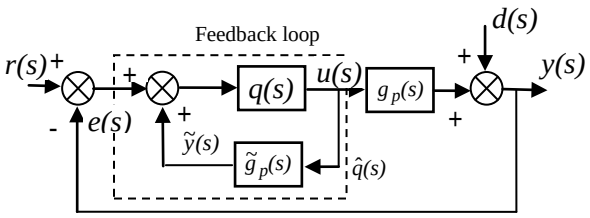

Fig. 2: Feedback form of Equivalent IMC Structure.

The feedback form of IMC based control loop and its equivalent PI structure is shown in fig. 2 and fig. 3 respectively. In fig. 2, $g_p(s)$ is the actual process and $\tilde{g}_p(s)$ is its corresponding model and $q(s)$ is the IMC controller. $r(s)$, $u(s)$, $y(s)$, $\tilde{y}(s)$ and $d(s)$ correspond to set point, control action, output of the actual process, output of process model and disturbance respectively. Here, we consider $g_p(s) = \tilde{g}_p(s) = \frac{k_p}{t_p s + 1}$ i.e., the actual process and process model is identical in nature. The main idea of IMC technique is to design a controller taking the inverse of the process model. So, to design the IMC-PI controller basically three steps are needed as follows:

Step I: Process model is inverted $\tilde{g}_p^{-1}(s)$.

Step II: A filter is added with the inverted process model to make the controller proper. So, the actual IMC controller takes the form $q(s) = \tilde{g}_p^{-1}(s) f(s)$, where $f(s) = \frac{1}{(\lambda s + 1)}$. λ is the close-loop time constant and it is the only tuning parameter of IMC controller.

Step III: To get the equivalent IMC-PI controller, the 'feedback loop' shown in fig. 2 is further simplified and the resultant IMC-PI controller $\hat{q}(s)$ is obtained as shown in fig. 3 and given by equation (1):

$$\hat{q}(s) = \frac{q(s)}{1 - \tilde{g}_p(s) q(s)}. \qquad (1)$$

$$k_c = \frac{t_p}{k_p l}$$

$$t_I = t_p$$

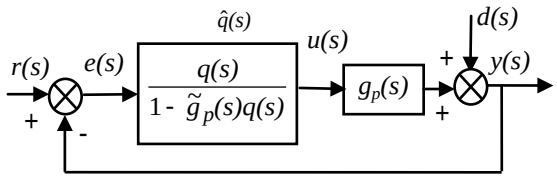

Fig. 3: Equivalent IMC-PI Structure.

k_c and t_I are controller proportional gain and integral time respectively. k_p and t_p are process gain and process time constants respectively.

III. PROPOSED AUTO-TUNER

The proposed auto-tuning scheme for the IMC-PI controller is quite simple and straight forward in nature. It provides continuous variation for the only tuning parameter i.e., the close-loop time constant (λ). When the process output is far away from the desired value (i.e., error (*e*) is large), a smaller value of λ is selected which will provide an enhanced speed of response to nullify the large process error within a smaller duration. On the other hand when the process output is close to the set point (i.e., error (*e*) is small), a larger value of λ will be selected. It results a reduced speed of response, so that an improved steady state behavior may be achieved. Hence, such a continuous modification in the value of close-loop time constant (λ) will provide an overall improved response under both the set point change and load disturbance. The value of close-loop time constant l is varied by the following simple relation

$$\lambda = \frac{1}{1 + |e(k)|} \qquad (2)$$

where $|e(k)|$ is the absolute error calculated at each sampling instant. To make the auto-tuning scheme independent of the process, in equation (2) normalized error value ($|e(k)|$) is used instead of instantaneous error ($e(k)$). The nature of variation in l with $|e(k)|$ is shown in fig. 4.

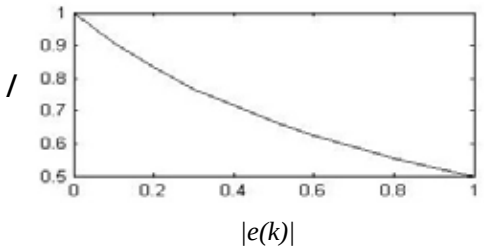

Fig. 4: Relation between / and |e(k)|.

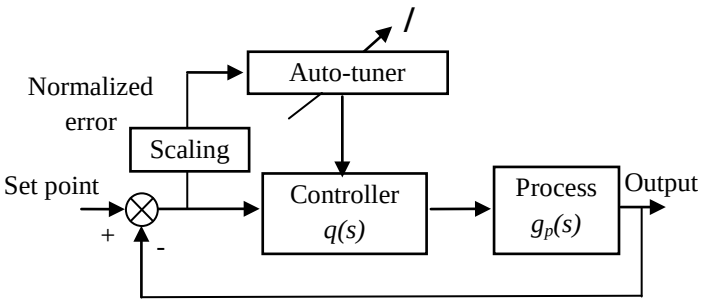

Fig. 5: Proposed Auto-tuned IMC-PI Controller Structure.

IV. COUPLED TANK SYSTEM

The schematic diagram of a coupled tank process is shown in fig. 6.

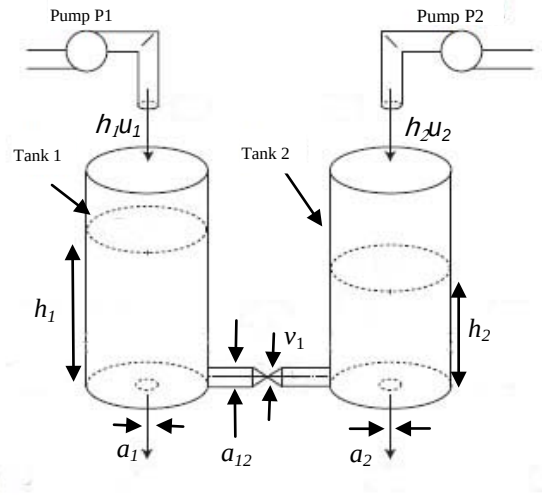

Fig. 6: Coupled Tank Process.

Table 1: Parameters of coupled tank process

Parameter	Description	Value	Unit
η_1	Constant relating the control voltage with the water flow from pump P_1.	2.4×10^{-3}	m/sec-volt
η_2	Constant relating the control voltage with the water flow from pump P_2.	3.262×10^{-3}	m/sec-volt
a_1, a_2	Inlet and outlet area of tanks T_1,T_2.	50.265×10^{-6}	m^2
A	Area of tanks T_1,T_2.	0.01389	m^2
h_1, h_2	Water level at dynamic equillibrium point.	0.15	m
u_{10}, u_{20}	Working point voltage.	2.7	volt
g	Gravitational accelaration.	9.81	m/sec^2

Here, in the experimental set-up as shown in fig. 6, pump P_1 feeds water to tank 1 (T_1) and pump P_2 feeds water to tank 2 (T_2). The controller output u_1 is the driving voltage (0-5volt) to the pump P_1 and the corresponding discharge flow rate is h_1u_1. Similarly, u_2 is the driving voltage (0-5volt) to the pump P_2 and the corresponding discharge flow rate is h_2u_2. The water levels (h_1 and h_2) are the controlled variables which can vary from 0-25 cm for both the tanks T_1 and T_2. The valve v_1 is the interacting element between T_1 and T_2.

V. SYSTEM MODELING

IMC designing is a model based approach and hence modeling of tanks T_1 and T_2 are of primary objective. Based on the Bernoulli's theorem [12] we can find out the dynamic relation for the tanks T_1 and T_2.

Dynamic equation of T_1 is given by

$$\frac{dh_1(t)}{dt} = -\frac{a_1}{A}\sqrt{2gh_1(t)} + \eta_1 u_1(t) \qquad (3)$$

which results the TF of T_1:

$$\frac{\Delta H_1(s)}{\Delta U_1(s)} = \frac{\eta_1}{s + \left(\frac{a_1}{A}\right)^2 \left(\frac{g}{\eta_1 u_{10}}\right)}. \qquad (4)$$

Similarly the TF for T_2 can be given by:

$$\frac{\Delta H_2(s)}{\Delta U_2(s)} = \frac{\eta_2}{s + \left(\frac{a_2}{A}\right)^2 \left(\frac{g}{\eta_2 u_{20}}\right)}. \qquad (5)$$

$\Delta H_1(s)$, $\Delta H_2(s)$, $\Delta U_1(s)$ and $\Delta U_2(s)$ are the liquid levels and their corresponding control actions for tanks T_1 and T_2 respective. By substituting the values of different parameters [11] as given in TABLE 1 we get the TFs for the tanks T_1 and T_2. To validate the tank models obtained from mathematical relations as given by equations (4) and (5), we have also experimentally found the tank models using Process Reaction Curve (PRC) method [9]. The mathematical as well as experimentally obtained models as shown in TABLE 2 are found to be close enough.

The PRC responses for tanks T_1 and T_2 are shown in figs. 7-8.

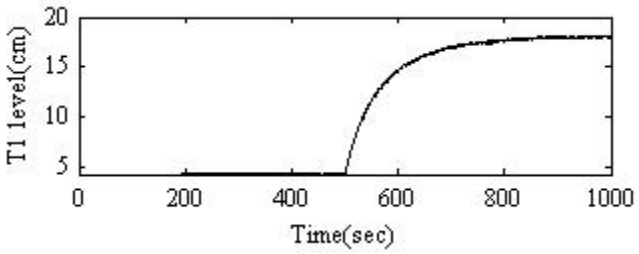

Fig. 7: PRC Response for Tank T_1.

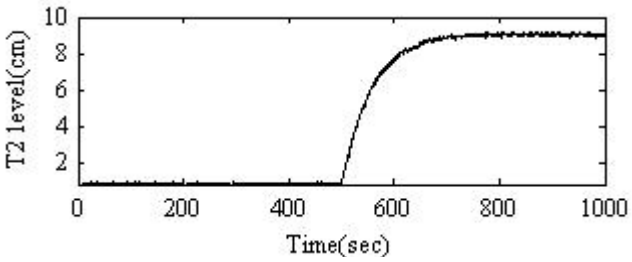

Fig. 8: PRC Response for Tank T_2.

Table 2: Tank models

Tank 1		Tank 2	
Mathematical model	Experimental model	Mathematical model	Experimental model
$\frac{12.12}{(50.50s+1)}$	$\frac{12.70}{(58.00s+1)}$	$\frac{8.40}{(42.03s+1)}$	$\frac{8.10}{(45.00s+1)}$

VI. PROPOSED CENTRALIZED IMC-API CONTROLLER FOR COUPLED TANK PROCESS

In our experimental study, primarily we attempt to design two conventional IMC-PI controllers based on the identified process models to maintain the liquid levels at the respective desired values for the tanks T_1 and T_2. Due to coupling between the tanks, performances of the ordinary IMC-PI controllers are found to be unsatisfactory. As already described that to overcome this limitation two auto-tuned IMC-PI (IMC-API) controllers are designed and their performance will be verified in comparison with IMC-PI controllers.

Tuning parameters and the filter structure for the proposed IMC-PI controller are shown in TABLE 3.

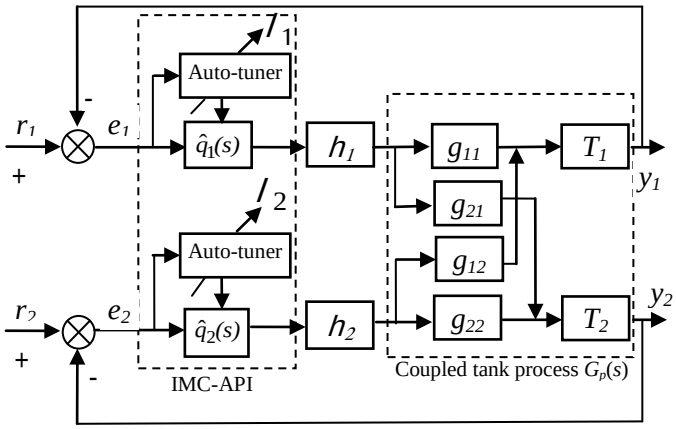

Fig. 9: Close-loop Control of Coupled Tank Process with Proposed Centralized IMC-API Controller.

Table 3: Tuning parameters of IMC-PI

Process	$\tilde{g}_p(S)$	Filter	k_c	t_I
Tank 1	$\frac{12.12}{(50.50s+1)}$	$\frac{1}{(ls+1)}$	$\frac{4.16}{l_1}$	50.50
Tank 2	$\frac{8.40}{(42.03s+1)}$		$\frac{5.00}{l_2}$	42.03

The close-loop schematic structure with IMC-API is shown in fig. 9. Here, $G_p(s)$ represents the coupled tank process and it is expressed as $G_p(s) = \begin{bmatrix} g_{11} & g_{12} \\ g_{21} & g_{22} \end{bmatrix}$ where g_{11} and g_{22} are the TFs of tanks T_1 and T_2 respectively when there is no interaction in between them. The term g_{12} and g_{21} represent the interacting parts among T_1 and T_2. In fig. 9, r_i, y_i, e_i and l_i are the desire level, corresponding response, error signal and close-loop time constant (sole tuning parameter) of T_i, where i = 1,2. $\hat{q}_1(s)$ and $\hat{q}_2(s)$ are two IMC-PI controllers obtained for controlling the water levels of tanks T_1 and T_2 respectively. Auto-tuner block provides the continuous variation in the tuning parameter (l_i) for the individual IMC-PI controller.

VII. REAL TIME EXPERIMENTATION

The laboratory based real time coupled tank system is a product of Feedback Instruments [11] and it is interfaced with computer through Advantech PCI1711 data acquisition interface card. Controllers are developed in PC with help of MATLAB/SIMULINK and the rig is operated in real time using Real Time Workshop (RTW) and Real

Time Windows Target (RTWT). Before we start the experiment both the tanks T_1 and T_2 are need to be filled nearer to desired level (i.e., height at which water levels are to be maintained) and hence a free run for a desired duration is given for both the pumps. During experimentation a step set point change is applied in terms of tank water level and once the level reaches the desired value, load disturbance is introduced. Performance of conventional IMC-PI controllers along with proposed IMC-API controllers are tested with the same set of test signals. Here, load change has been introduced by providing a 20% change in control action once water levels of tanks have reached their desired values. The valve v_1 is always kept open to provide the interaction between T_1 and T_2.

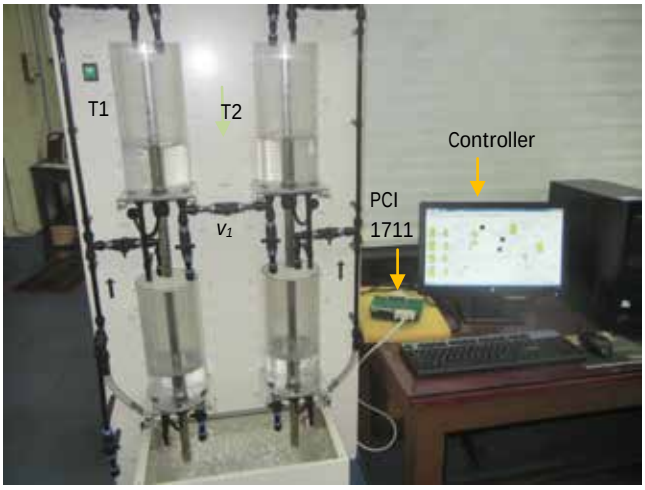

Fig. 10: Experimental Set-up.

VIII. RESULTS

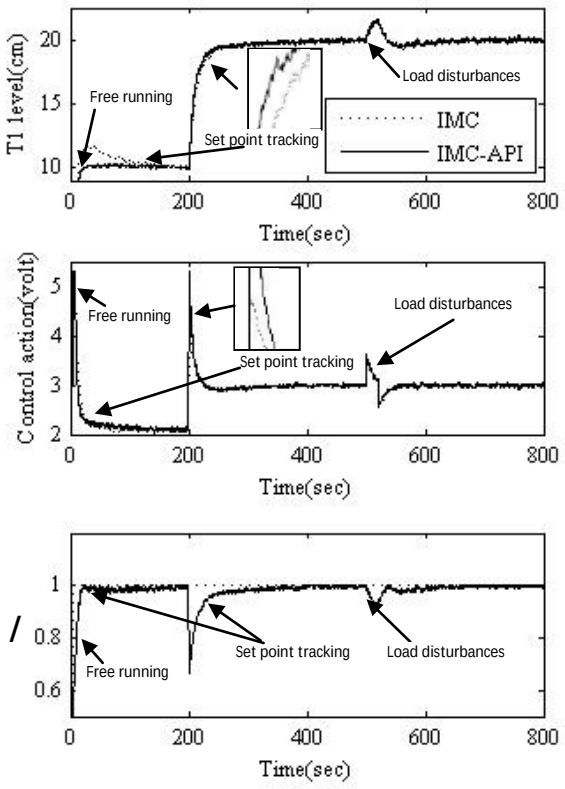

Fig. 11: Performance Study of IMC-PI and IMC-API Controller for Tank T_1.

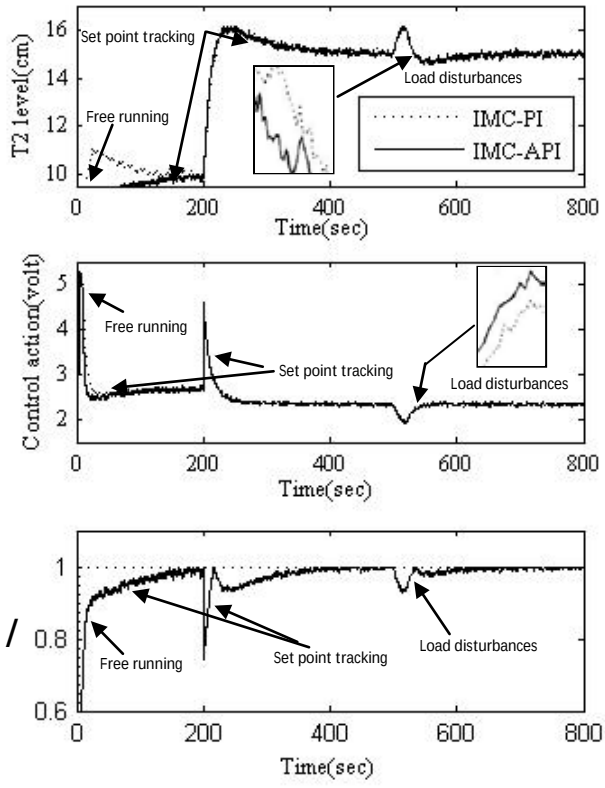

Fig. 12: Performance Study of IMC-PI and IMC-API Controller for Tank T_2.

Table 4: Performance analysis of Tank 1 and Tank 2

Controller	Tank 1 (T_1)		Tank 2 (T_2)	
	IAE	ITAE	IAE	ITAE
IMC-PI	498.80	10.02×10^4	280.00	3.08×10^4
IMC-API	382.80	8.85×10^4	265.00	2.90×10^4

Responses of the conventional IMC-PI and the proposed IMC-API controllers are shown in fig. 11 and fig. 12 for coupled tanks T_1 and T_2 respectively. In each figure IMC-PI responses are plotted with dotted line and for IMC-API solid line is used. Along with the responses the nature of variation of control actions and the corresponding variations of / are also shown in figs. 11-12. To justify the effectiveness of the proposed auto-tuning scheme, controller performance indices are also calculated in terms of Integral Absolute Error (IAE) and Integral Time Absolute Error (ITAE) as depicted in TABLE 4. From the listed values as shown in TABLE 4 it is found that IMC-API controllers result lesser IAE and ITAE values compared to IMC-PI controllers in each case which justify their superiority. For clear visibility of the responses, some sections are zoomed in separate boxes.

IX. CONCLUSION

Conventional and auto-tuned IMC-PI controllers are designed and their performances are evaluated on a laboratory based real time coupled tank process. Coupled tank system is popular nonlinear MIMO process which is difficult to control. To design the IMC-PI controllers, process models are primarily obtained using physical dynamic relations and these models are further validated through experimental study. The main limitation of the conventional IMC-PI controller is that the tuning parameter remains constant and hence fails to perform satisfactorily under both the transient and steady state conditions simultaneously. To overcome such limitations an auto-tuning scheme is incorporated with conventional IMC-PI and named as IMC-API. In IMC-API the only tuning parameter is the close-loop time constant which is varied continuously depending on the absolute value of instantaneous process error. This auto-tuning scheme is very simple in nature and easy to implement. Experimental results substantiate the superiority of the proposed auto-tuning scheme under both the transient and steady state operating conditions. Further, the said auto-tuning scheme may also be implemented in case of PID controller.

REFERENCES

[1] D. E. Rivera, S. Skogested, and M. Morari, *Internal model control for PID controller design*, Industrial Engineering Chemical Process Design and Development, *25(1)*, 1986, 252-265.

[2] I. L. Chien, *IMC–PID controller design-an extension*, IFAC Proceeding Series, *6*, 1988, 147-152.

[3] A. Datta, and J. Ochoa, *Adaptive internal model control : design stability and analysis*, Automtica, *32(2)*, 1996, 261-266.

[4] G. J. Silva, and A. Datta, *Adaptive internal model control: the discrete-time case*, International Journal of Adaptive Control and Signal Processing, *15(1)*, 2001, 15-36.

[5] D. Rupp, and L. Guzzella, *Adaptive internal model control with application to fueling control*, Control Engineering Practice, *18(8)*, 2010, 873-881.

[6] K. Watanabe, and E. Muramatsu, *Adaptive internal model control of siso systems*, SICE Annual Conference, 2003, 1-3.

[7] Q. Chi, Z. Zhao, X. Jin, and J. Liang, *Adaptive internal model controller design using dynamic partial least squares decouple*, International Journal of Innovative Computing, Information and Control, *10(3)*, 2014, 989-1000.

[8] P. Srinivasarao, and P. Subbaiah, *Centralized and decentralized of quadruple tank process*, International Journal of Computer Applications, *68(15)*, 2013, 21-29.

[9] B. W. Bequette, *process control modeling design and simulation* (India: Prentice Hall, 2004).

[10] P. K. Paul, C. Dey, and R. K. Mudi, *Model based PID controller for integrating process with its real time implementation*, UACEE International Journal of Advancements in Electronics and Electrical Engineering, *1(2)*, 2012, 139-144.

[11] Feedback Instruments Ltd., East Sussex, UK, 2010.

[12] D. E. Seborg, T. F. Edgar, and D. A. Melichamp, *process dynamic and control* (NY: Wiley, 2004).

SELECTION OF WORKING FLUID AND EXERGY ANALYSIS OF AN ORGANIC RANKINE CYCLE

Aseem Desai[1], Deepa Agrawal[2],

Sauradeep Datta[3], Sanjay Rumde[4]

[1,2,3,4] *Mechanical Engineering Department, Maharashtra Institute of Technology (India)*

ABSTRACT

There are two degrees of freedom available in designing an Organic Rankine Cycle (O.R.C) - the organic fluid and the evaporator pressure. The upper limit of the latter will be decided by the heat source inlet temperature. The performance of 12 organic fluids including some newly developed silicone oils - D4, MDM, have been analyzed on the basis of thermal efficiency, exergy destruction (neglecting pressure drop) and size of the system required. The optimum evaporator pressure was found for each fluid using power output as the objective function. The source was taken as a flue gas mixture at 150˚C. The exergy destruction due to two irreversibility –heat transfer across a finite temperature difference and pressure drop in a shell and tube heat exchanger was quantified only for R245fa and recalculated for varying source exit temperature. The average tube side heat transfer coefficient and that for liquid-only were obtained from HTRI software for a given geometry. The pressure drop in the shell was obtained using Bell-Delaware method and that in the tube was calculated separately for the single phase and two phase part.

Keywords: Evaporator, Exergy analysis, Organic Rankine Cycle

I. INTRODUCTION

The need for better efficiencies in power plants has never been greater. With drastic climate change occurring all over the world, we need to reduce dangerous emissions into the atmosphere. More than 50% waste heat is unused; converting some of this heat into work can attenuate the problem by reducing the consumption of fossil fuels [1]. Another solution to this problem is the use of renewable sources of energy, like solar and geothermal, which are low grade heat sources. The operation at lower temperatures requires an organic fluid in the power cycle. Organic fluids have much lower normal boiling point than water hence is suitable for low temperature applications. Also organic fluids have lower specific volume as compared to steam hence the corresponding size of the components of the power plant will be considerably smaller.

The importance of exergy is often ignored but as per the Carnot corollary, maximum work is developed only when the irreversibility's are eradicated. Increasing the exit temperature of the source increases the Log Mean Temperature Difference (LMTD) in the evaporator and hence reduces its size. The reduced size and mass flux should give lower pressure drop. Hence, while the exergy destruction due to the temperature difference increases with increase in source exit temperature, the pressure drop irreversibility reduces with the same [2].

Nomenclature

Q	heat transfer rate (KW)
$\dot{m}_h$	mass flow rate of hot fluid (kg/s)
$\dot{m}_c$	mass flow rate of hot fluid (kg/s)
$\dot{m}_{cw}$	mass flow rate of cooling water(kg/s)
h	enthalpy (KJ/kg)
S	entropy (KJ/kgK)
η	efficiency
W	work energy (KJ)
T	temperature (˚C)
T_o	surrounding temperature
Φ	heat Recovery Efficiency
Δ	finite change in quantity
P	pressure (Pa)
N_b	number of baffles
μ	viscosity (Pa-s)
ρ	mean density (kg/m^3)
ρ_i	density at inlet (kg/m^3)
ρ_o	density at outlet (kg/m^3)
G	mass flux (kg/m^2)
l	length of tube (m)
r_h	hydraulic radius (m)
X_{LM}	Lockhart-Martinelli parameter
N	number of tubes in evaporator
U_{avg}	overall heat transfer coefficient
d_o	outer diameter of tube
T_{exit}	flue gas exit temperature
C_{ph}	specific heat at constant pressure for hot fluid (KJ/kgK)
A_s	surface area of evaporator
$\dot{I}$	exergy destruction rate (KW)
x	dryness fraction
f	friction factor
Re	Reynolds Number
Cf	correction factor
Nu	Nusselt number
Pr	Prandtl number

Subscripts

1,2,2s,3,4,4s,5,6,7,8	states in system
e	evaporator
c	condenser
p	pump
LO	liquid only
g	flue gas
l	liquid refrigerant

Another factor is the heat transfer coefficient whose variation may have a drastic effect on the size of the heat exchanger and hence on the exergy destruction.

Many researches have worked on fluid selection for an ORC, Hung et al [3] found the thermal efficiencies of Benzene, Toluene, p-xylene, R113 and concluded that p-xylene had the maximum and benzene has the minimum efficiency. He also found that p-xylene had the lowest overall irreversibility and that maximum irreversibility was present in the evaporator. Wang et al [1] conducted a multi-objective optimization considering heat exchanger surface area per unit power output and the heat recovery efficiency and surmised that R141b is the optimal fluid if the source inlet temperature is greater than 180°C. Lars et al [4] considered the variation of thermal efficiency with critical temperature and found that they had an increasing relationship. Dai et al [5] showed that R236ea had the highest exergy efficiency and that for fixed input source conditions, the maximum power is obtained at a certain optimum evaporator pressure. Larjola et al [6] showed that for a larger two-phase enthalpy drop in the evaporator, the irreversibility in it will be greater. Wei et al [7] analyzed the effect of variation in source parameters like mass flow rate and inlet temperature of the exhaust of an IC engine, on the exergy destruction and thermal efficiency for R245fa.

In this study the fluid selection and exergy analysis (neglecting pressure drop in the evaporator) has been extended to some more fluids like D4, MDM, and R141b etc. The fluids containing chlorine have not been considered in this paper due to their high ODP. In addition the exergy destruction due to pressure drop in a shell and tube heat exchanger was also considered for R245fa. The occurrence of a trade-off has been checked for the given source conditions. The exit temperature of the source was varied and the corresponding exergy destruction in the evaporator was plotted. The effect of increasing the temperature difference between hot and cold fluids in the heat exchanger, on the heat transfer coefficient and size is also shown.

II. MODEL OF AN ORGANIC RANKINE CYCLE

Schematic diagram of the organic rankine cycle as shown in fig. 1 consists of an evaporator driven by low-grade heat source, an expander, a condenser and a working fluid pump. The working fluid is pumped into the evaporator where it is heated and vaporised by the waste heat. The high pressure vapour enters the expander without any superheat, where the vapour gets expanded and power is generated. After this the exhaust vapour enters the condenser while it is still in the superheated state, where it gets condensed by cooling water and then it is pumped back to the evaporator and a new cycle begins.

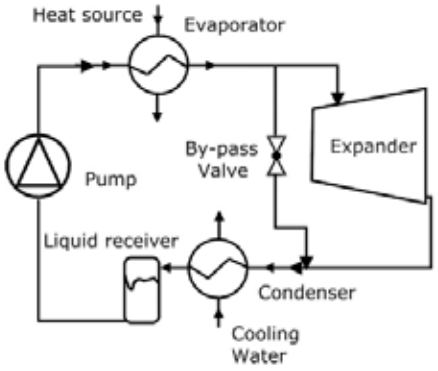

Fig. 1. Schematic diagram of ORC

2.1 Source and Sink Conditions

The waste heat source considered here is a flue gas mixture. The flue gas inlet temperature is assumed constant at 150˚C. A constant pinch of 7˚C was taken between the hot and cold fluid at the point at which two phase flow begins on the cold side. The condenser temperature is kept constant at 50˚C. Since pinch of 5˚C is maintained, cooling water exit temperature is taken as 45˚C. Due to limitations of the cooling tower the cooling water inlet is kept at 35˚C.

2.2 Thermodynamic Analysis

The thermodynamic processes involved in a basic subcritical ORC are illustrated in fig. 2. 1-2 and 3-4 (represented by dotted lines) indicate the actual processes, whereas 1-2s and 3-4s indicate the ideal reversible processes.

Process 4-1: This process represents a constant pressure heat addition in evaporator. The heat absorbed by working fluid in the evaporator is:

$$\dot{Q}_e = \dot{m}_h(h_5 - h_6) = \dot{m}_c(h_1 - h_4) \quad (1)$$

Process 1-2: The high pressure vapour working fluid from the evaporator enters the expander where mechanical power is developed. Power developed by the expander is:

$$\dot{W}exp = \dot{m}_c(h_1 - h_{2s})\eta_e \quad (2)$$

Expander efficiency (η_e) has been assumed as 70%.

Process 2-3: This process represents a constant pressure heat rejection in condenser. The heat rejected by the working fluid in the condenser is:

$$\dot{Q}c = \dot{m}_c(h_2 - h_3) \quad (3)$$

Process 3-4: This process indicates actual pumping process. The power consumed by the pump is:

$$\dot{W}_p = \frac{\dot{m}_c(h_{4s} - h_3)}{\eta_p} \quad (4)$$

The pump efficiency (η_p) has been assumed to 60%.

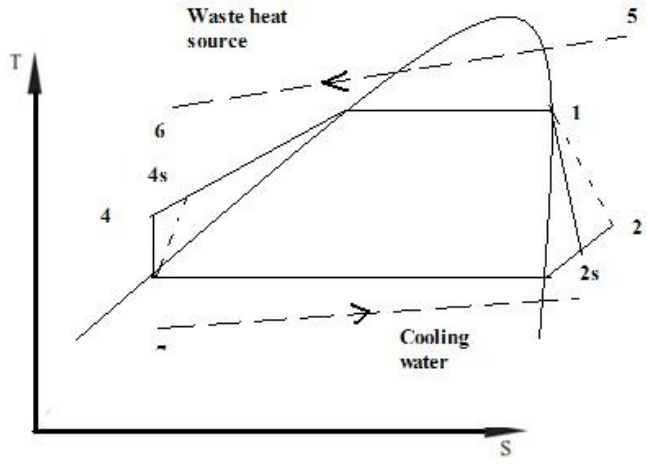

Fig. 2. T-S diagram of ORC system with heat source and cooling water

2.3 Selection of Working Fluid

Selection of correct working fluid is a very important aspect to be considered before designing the ORC. Organic fluids have lower normal boiling points and hence have very high pressures at moderate temperatures facilitating a positive pressure difference in the evaporator. The higher pressure also results in lower specific volumes and hence smaller size of the components. The fluid must also be selected on the basis of the source conditions, as the critical temperature of the fluid may be much smaller or larger than the source temperature.

One of the important thermodynamic attributes of the organic fluid is the slope of the saturation vapour curve. On this basis organic fluids are classified into dry, wet and isentropic fluids. For dry fluids, the slope of the saturated vapour line is positive. Some examples of dry fluids are R245fa, isobutene, R141b, toluene, p-xylene. For wet fluids, the slope of the saturated vapour line is negative. Some examples of wet fluids are water, ethanol, R152. For isentropic fluids, the slope of the saturation vapour curve is infinity. Some examples of isentropic fluids are R134a, R125, R245ca.

Due to the negative slope of saturated vapour curve of the wet fluids in the T-S diagram, the exit state of the fluid from the turbine is often wet. This problem is eliminated for organic fluids since at the exit of the turbine the fluid is always superheated. Another benefit is that the exit temperature of the fluid from the turbine is usually higher than that of the fluid at the exit of the pump. Hence there is some scope for improving the efficiency by introducing regeneration. Unlike the wet fluids no bleed is required from the turbine and hence he fluid expands completely in the turbine. The performance of fluids is evaluated based on three parameters: Thermal efficiency, Maximum power output, Exergy destruction.

2.3.1 Thermal Efficiency Analysis of Various Working Fluids

The thermal efficiency for various working fluids has been calculated based on the thermodynamic model describe previously, using a Matlab program. The fluid properties were obtained by using REFPROP (9.1) software which was linked with Matlab. In this text evaporator temperature refers to the temperature at which boiling starts (T_1, T_9).

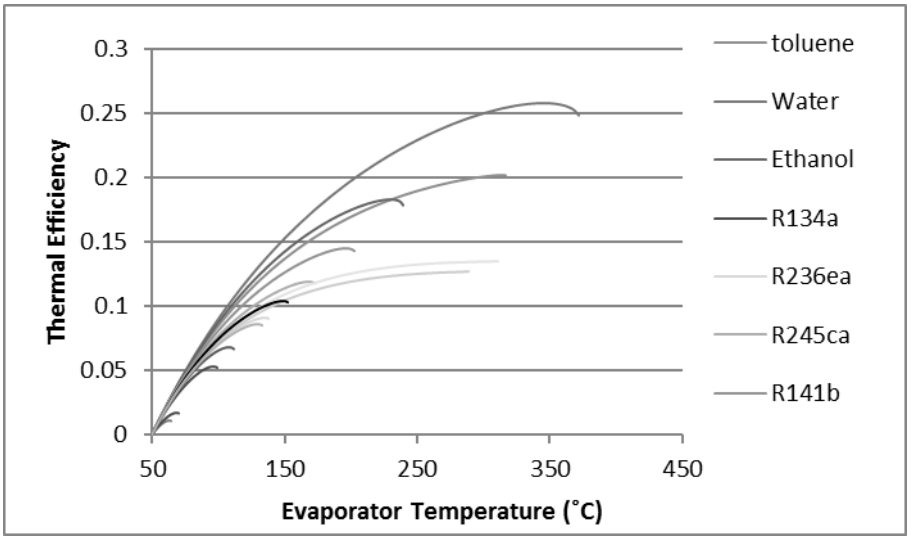

Fig. 3. Thermal efficiency of various fluids plotted against evaporator temperature (at which boiling starts) varying from 50˚C up to the critical temperature of particular working fluid

2.3.2 Analysis of Maximum Power Output for various working fluids

The evaporator temperature adds a restriction on the lowest possible heat source exit temperature. This is because the maximum temperature difference at pinch point is taken as 7˚C. For an ORC, the pinch point is the point at which evaporation begins or the point at which dryness fraction is zero.

The net power output is a product of thermal efficiency and heat duty. As evaporator temperature increases thermal efficiency increases and simultaneously heat duty decreases. Hence it is required to find the evaporator temperature corresponding to which maximum power output is obtained. As the evaporator temperature increases the heat recovery efficiency decreases.

Heat recovery efficiency (Ø) is the ratio of the available energy to the maximum usable energy.

$$\emptyset = \frac{(T5-T6)}{(T5-T4-\Delta TP)} \quad (5)$$

As heat recovery efficiency increases thermal efficiency decreases. Thus, the thermal efficiency and heat recovery efficiency are inversely related.

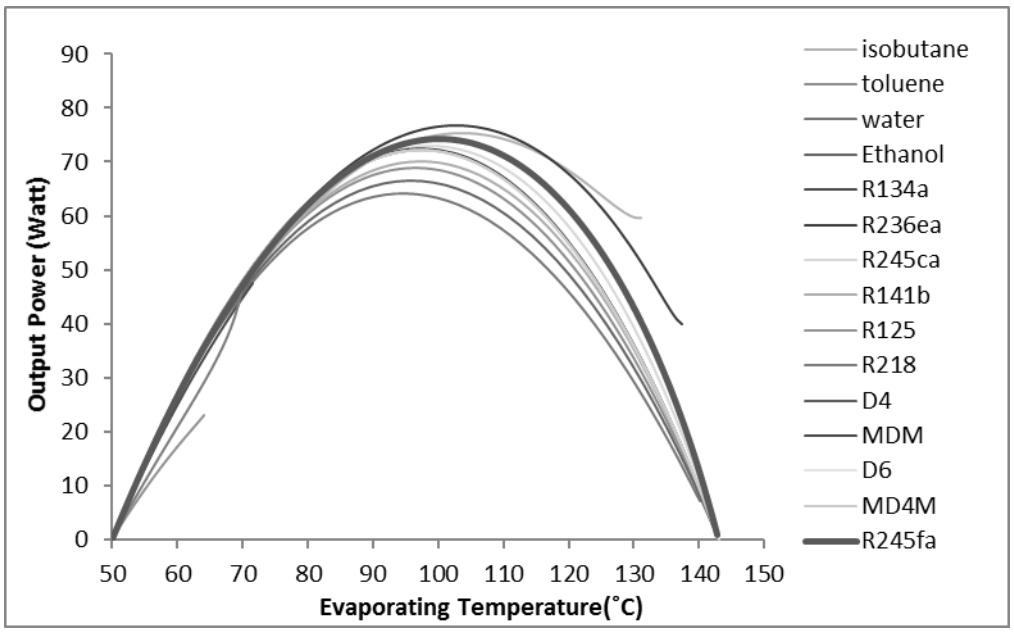

Fig. 4. Shows the variation of output power with change in evaporator temperature for various working fluids

The power output for various working fluids has been calculated using a Matlab program and the temperature for maximum power has been noted.

2.3.3. Exergy Analysis for Entire Cycle

Exergy refers to the total available energy. The efficiency is not an accurate parameter for defining the maximum power producing capacity of an ORC. For this, we need to quantify the irreversibility's by using the exergy destruction. In each of the 4 components, there is some irreversibility.

The exergy destruction is always equal to product of net entropy generation rate and surrounding temperature.

$$I = \dot{S}_{gen} T_o \quad (6)$$

- In the evaporator, there is an exchange of heat between a finite temperature difference (Flue gas and Organic fluid), ideally another heat engine could be added between these two temperature source and sink,

and more work could be extracted. The drop in pressure due to friction in the pipes also results in some work lost in fighting friction.

$$I_{evap} = (\dot{m}_h(S2 - S6) + \dot{m}_c(S4 - S1))T_0 \quad (7)$$

- Similarly the friction between viscous fluid and blades in the turbine also results in some work lost.

$$I_{turb} = \dot{m}_c(S2 - S2s)T_0 \quad (8)$$

- In the condenser, there is net entropy generation due to heat transfer across a finite temperature difference, this time between the organic fluid and cooling water.

$$I_{cond} = (\dot{m}_{cw}(S7 - S8) + \dot{m}_c(S2 - S3))To \quad (9)$$

- Finally the friction between the impeller blades in the pump and the organic fluid results in some entropy generation.

$$I_{pump} = \dot{m}_c(S4 - S4s)T_0 \quad (10)$$

The exergy destruction is defined as the product of environment temperature and the net entropy generation. The net entropy generation is calculated in each component after assuming suitable isentropic efficiencies in the turbine and pump. The pressure drop in the heat exchangers is neglected.

$$I_{total} = I_{pump} + I_{turb} + I_{evap} + I_{cond} \quad (11)$$

As the evaporator temperature increases, the total exergy destruction decreases because the temperature difference between the heat source and the organic fluid reduces along with the mass flow rate of organic fluid in the cycle. Unfortunately the total heat recovered from the source also reduces. Hence lower irreversibility will be obtained at the cost of lower heat recovery efficiency and lower power developed. It can also be concluded that for fluids with higher critical temperature, the two phase enthalpy drop is larger and so is the exergy destruction in the evaporator, yet since the LMTD is larger, a smaller heat exchanger required.

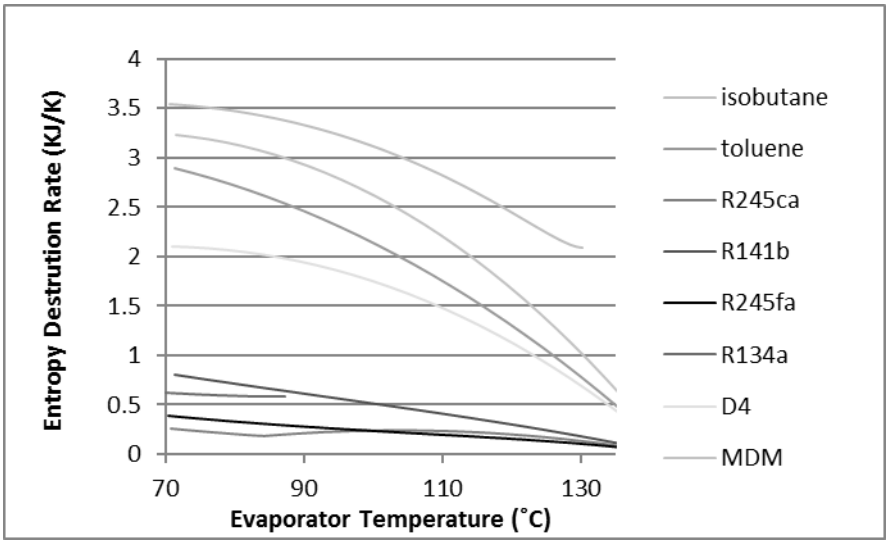

Fig. 5. Represents the overall entropy destruction rate as a function of evaporator temperature for various organic fluids.

Table 1 shows the maximum power output and thermal efficiency for the various working along with certain thermo-physical property

Fluids	Molecular Weight (g/mol)	Slope of Saturated vapour Line $(\frac{dT}{ds})$	Critical Pressure (bar)	Critical Temperature (˚C)	Specific Volume at intermediate temperature of 85˚C (m^3/kg)	Overall Thermal Efficiency for Te=120˚C And Tc=50˚C (%)	Maximum Power output (KW)	Evaporator Temperature at which power is maximum
Water	18.0153	Negative	220.64	373.95	0.1	24.88	64.25	95.07
Isobutane	58.12	Positive	36.29	134.66	0.0262	8.47	75.43	103.729
R245fa	134.05	Positive	36.51	154.01	0.0242	10.35	74.36	99.98
MDM	193.24	Positive	14.15	290.94	0.33	12.72	72.43	97.788
D4	296.62	Positive	13.32	313.34	0.58	13.49	72.22	97.04
R134a	102	Isentropic	37.61	72.71	0.0064	5.26	108.83	99.06
R141b	117	Positive	42.12	204.35	0.0617	14.34	70.02	97.22
R125	120	Isentropic	36.18	66.02	0.0025	1.07	23.15	64.023
R245ca	134.05	Isentropic	39.41	174.42	0.0478	11.78	73.07	98.968
Toluene	92.14	Positive	41.26	318.60	0.4340	20.17	68.82	95.322
R152a	66.1	Negative	45.17	113.26	0.0121	6.63	104.11	111.261
R236ea	152.03	Negative	34.2	139.29	0.0155	8.98	76.87	102.374

III. MODEL OF EVAPORATOR

The evaporator considered is a shell and tube heat exchanger. The working fluid flows through the tubes and the flue gas flows through the shell enclosure. The shell diameter and corresponding tube count has been selected by using 'Heat Transfer Research, Inc. (HTRI)' software after supplying the process condition which includes the constant evaporator temperature of 120˚C. The shell Diameter was taken as 1150 mm, with a pitch of 25 mm for a 45˚ staggered tube configuration, the tube count was 728. The tube diameter was taken as 19 mm and thickness as 1.5mm. The shell type was 'E', Front End-'B', Rear End-'S' and the baffle spacing was taken as 330mm. The source exit temperature was varied from 127˚C up to 147˚C. The corresponding overall heat transfer coefficient and the liquid-only heat transfer coefficient was also obtained from HTRI for a finite number of source exit temperatures.

$$\dot{Q} = \dot{m}_h C_{ph}(150 - T_{exit}) \quad (12)$$

These values take into consideration the effect of heat flux on sub-cooled nucleate boiling region and flow boiling region. The flow boiling process is very complicated as, when the local heat flux reaches a critical heat flux (CHF), the wall starts becoming dry. Based on the region in which CHF is reached the drying out process is called Departure from nucleate boiling (DNB) or Dry-out, the former occurring at low dryness fraction and the latter at higher dryness fraction [10]. In the Matlab program, all geometrical parameters other than length were held constant and the heat transfer coefficient values for intermediate points was found by interpolation. The heat duty reduces along with the mass flow rate and mass flux as the source exit temperature is increased.

$$\dot{m}_c = \frac{Q}{(h_1 - h_4)} \tag{13}$$

The total length and that of the two phase portion and single phase portion was then found using the equations given below:

$$A_s = \frac{Q}{U_{eq} LMTD * Cf} \tag{14}$$

$$l = \frac{A_s}{N \pi d_o} \tag{15}$$

The values of tube side average heat transfer coefficient obtained are plotted against source exit temperature as shown below in fig. 6.

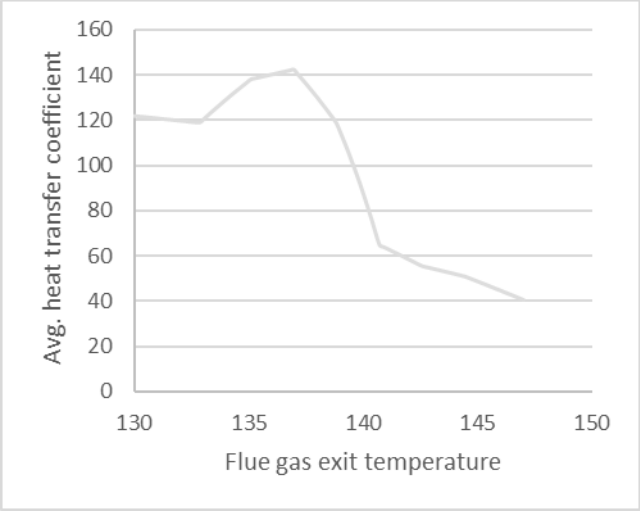

Fig. 6. Shows tube side average heat transfer coefficient versus flue gas exit temperature

The heat transfer coefficient for the flue gas was assumed to be constant since the free flow area in the shell remains unchanged and also because the variation in properties is minimum. It was found using McAdams correlation [9].

$$Nu = 0.36 Re^{0.55} Pr^{0.3} \tag{16}$$

$$h_{shell} = \frac{NuK}{D} \tag{17}$$

Equivalent heat transfer coefficient (Ueq) is calculated considering tube side average heat transfer, shell side heat transfer and conduction through the tube wall, in parallel.

IV. PRESSURE DROP EVALUATION IN EVAPORATOR

4.1 Shell Side

Bell Delaware method has been used to estimate the pressure drop due to friction. The pressure drop evaluation on the shell side of a shell and tube heat exchanger is complicated due to the presence of a cross-flow section, a window section and the inlet and exit sections. The total pressure drop is then the sum of the pressure drops for each window section and each cross-flow section, the number of such sections is decided by the number of baffles or baffle spacing. Empirical correlations for the total pressure drop including the cross-flow, window and the inlet-exit sections [8, 9] are:

$$\Delta p_s = \Delta p_{cr} + \Delta p_w + \Delta p_{i-o} = [(N_b - 1)\,\Delta p_b \zeta_b + N_b\,\Delta p_w]\zeta_l + 2\,\Delta p_b \left(1 + \frac{N_{cw}}{N_{cc}}\right)\zeta_b \zeta_s$$

(18)

A Matlab program has been developed to obtain the pressure drop in the shell using the above equation. This was done after the total length of the heat exchanger was found in each iteration. In fig. 7 based on our process conditions and considering working fluid as R245fa the total pressure drop on shell side is obtained as 73.7Kpa at a source exit temperature of 127˚C. Pressure drop due to static head is also taken into account and the corresponding value obtained is 133Pa.

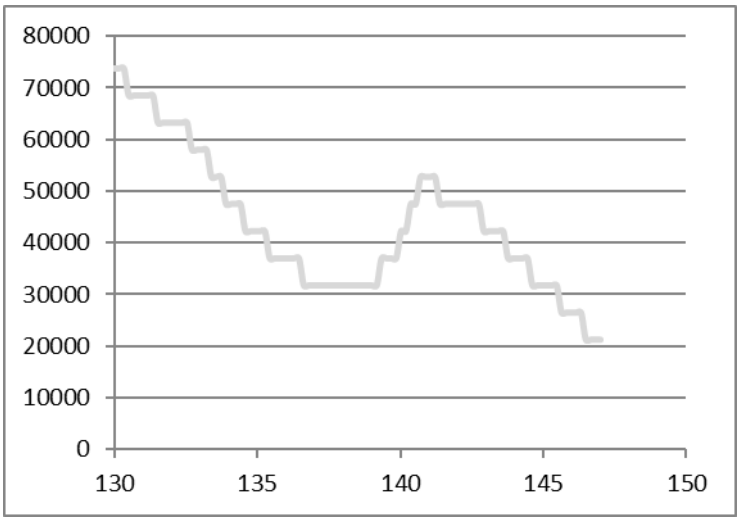

Fig. 7. Total shell side pressure drop with respect to source exit temperature

The step nature of the graph in fig. 7 is because the value of number of baffles can only be a whole number even though the length may vary continuously.

4.2 Tube Side (Single Phase)

The pressure drop inside the tubes is determined by using (19, 20):

$$\Delta p = \frac{G^2}{2\rho_i}\left[(1-\sigma^2+k_c) + 2\left(\frac{\rho_i}{\rho_o}-1\right) + f\frac{L}{r_h}\rho_i\left(\frac{1}{\rho}\right) - (1-\sigma^2-k_e)\frac{\rho_i}{\rho_o}\right] \quad (19)$$

(entrance effect) (momentum effect) (core effect) (exit effect)

Where, Fanning friction factor is:

$$f = (0.079) * Re^{-0.25} \quad (20)$$

The momentum pressure drop has been found to be negligible and has not been considered. Also the combined effect due to the pressure drop at the entrance and exit is very small and has hence been neglected. Hence the

pressure drop in the core is the major contributor to the total tube side pressure drop. A Matlab program has been developed to obtain the pressure drop in tubes, with single phase consideration, using the above equations.

4.3 Tube Side (Two Phase)

For Pressure Drop calculations in tube side considering two phase the following pressure drop correlation [10] has been used:

$$\emptyset_{Lo}^2 = 1 + \frac{C}{X_{LM}} + \frac{1}{X_{LM}^2} \quad (21)$$

$$X_{LM} = \left(\frac{\rho_g}{\rho_l}\right)^{0.5} \left(\frac{\mu_l}{\mu_g}\right)^{0.1} \left(\frac{(1-x)}{x}\right)^{0.875} \quad (22)$$

$$\left(-\frac{d_p}{d_z}\right)_{fr} = \emptyset_{Lo}^2 \left(-\frac{d_p}{d_z}\right)_{fr,Lo} \quad (23)$$

The term $\emptyset_{Lo}^2$ represents the two phase multiplier. The Lockhart- Martinelli method (21, 22) is among the oldest techniques. It assumes that the two phase multipliers are the functions of the Martinelli parameter equation as shown by (23). The phasic frictional gradients depend on the flow regimes of the phases, when each is assumed to flow alone in the channel. A Matlab program has been developed to obtain the pressure drop in tubes with two phase consideration using (21, 22 and 23).

The pressure drop on tube side due to friction (with combined single phase and two phase) is obtained as 4.25Pa for a source of temperature of 127˚C. It is observed that for increase in flue gas exit temperature the tube side pressure drop decreases. Pressure drop is a function of length of the tube and mass flux. In this case the mass flux continuously decreases with increase in flue gas exit temperature but the length fluctuates with respect to the same. The results in fig. 8 shows that the effect of mass flux dominates.

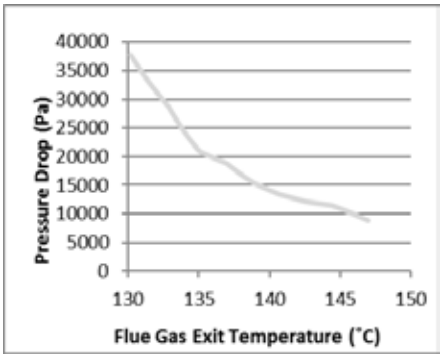

Fig. 8. Represents the total pressure drop in tube side for working fluid R245fa

Pressure drop due to static head has also been taken into account based on our process conditions and working fluid as R245fa.

V EXERGY DESTRUCTION IN THE EVAPORATOR CONSIDERING PRESSURE DROP

The procedure to calculate pressure drop in a shell and tube heat exchanger has been elucidated above. The exit state of the organic fluid in the evaporator is now calculated considering the pressure drop with respect to the inlet and taking the exit state to be saturated vapour (x=1).

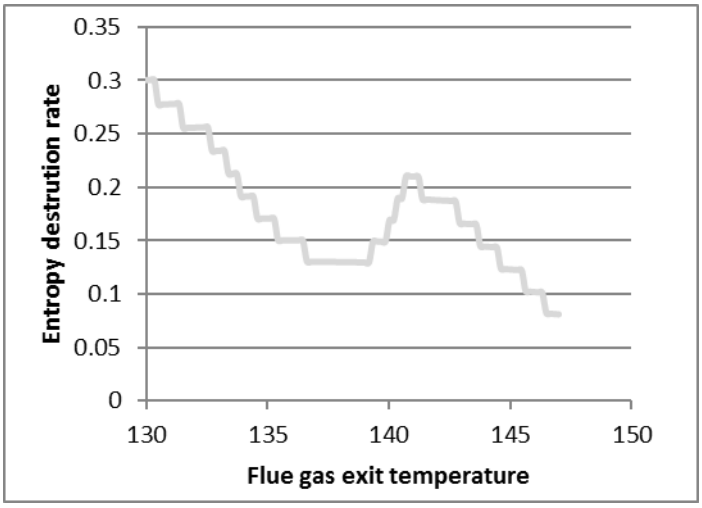

Fig. 9. Represents entropy destruction rate in evaporator versus flue gas exit temperature

The effect of pressure drop on the source exit temperature was not considered and the entropy at the exit was calculated after deducting the pressure drop from the inlet pressure. Comparing the exergy destruction due all three irreversibility's separately, we found that the pressure drop in the shell is the dominant contributor followed by the temperature difference in the evaporator and then the pressure drop in the tube, in descending order.

$$dS_{p,drop} = -\left(\frac{\partial v}{\partial T}\right) dF \tag{24}$$

$$\alpha_v = \frac{1}{v\left(\frac{\partial v}{\partial T}\right)_p} \tag{25}$$

Hence the total exergy destruction has a generally decreasing trend similar to that of pressure drop in shell, with a local minima and maxima. Yet for other heat sources with similar properties (volumetric thermal expansion coefficient) compared to the organic fluid, there might actually be more similar exergy destruction due to temperature difference and pressure drop and hence a trade-off may occur. Further it must be pointed out that there is a lot of flexibility in the rating procedure used, which will have a pronounced effect on the size of the heat exchanger and hence pressure drop. Finally the effect of the temperature difference in the evaporator must be highlighted, as the heat flux increases, sub-cooled nucleate boiling is enhanced along with the heat transfer coefficient but on further increase of heat flux, DNB occurs and the insulating vapour film along the inner periphery of the tube will result in a sharp decrease in heat transfer coefficient. This phenomena in-turn affects the length.

VI. CONCLUSION

- When the heat source parameters are fixed, the selection of the fluid should be based on the power output rather than the thermal efficiency. Maximum thermal efficiency was obtained for Toulene, R141b, D4, MDM, R245ca in decreasing order. Maximum power was obtained for Iso-Butane, Toluene, R236ea, R245fa in decreasing order. Hence even though the thermal efficiency for R245fa is considerably lower than the rest it has a high power output.

- Considering expansion in the turbine, at 85˚C, from 120˚C saturated condition, R125, R134a, R236ea had the lowest specific volumes in increasing order.
- Minimum overall exergy destruction (neglecting pressure drop in the evaporator) was obtained for R245fa, R245ca, R134a in increasing order. The fluids which had maximum power output, i.e. Iso-butane, Toluene and R236ea all had much higher overall exergy destruction. Hence a suitable weightage must be added to each parameter and the sum should be evaluated before selecting the fluid.
- It was found that the exergy destruction for R245fa due to pressure drop in the shell of the heat exchanger, was the much larger, even though the pressure drops are comparable on both sides. The partial derivative $\left(\frac{\partial v}{\partial T}\right)$ is very different for the flue gas and the organic fluid and the mass flow rate is very high. Hence the expected exergy trade-off was not found.

REFERENCES

[1] Z. Q. Wang, N. J. Guo and X. Y. Wang, Fluid selection and parametric optimization of organic rankine cycle for low temperature waste heat, Energy, 40, 2012, 107-115.

[2] Adrian Bejan, George Tsatsaronis and Michael Moran, Thermal Design and Optimization (John Wiley and Sons, Inc., NJ: Hoboken, 1996).

[3] Tzu-Chen Hung, Waste heat recovery of Organic Rankine Cycle using dry fluids, Energy Conversion and Management, 42, 2001, 539-553.

[4] Lars J. Brasz and William M. Bilbow, Ranking of working fluids for organic rankine cycle applications, International Refrigeration and Air Conditioning conference, 2004, 722-780.

[5] Yiping Dai, Jiangfeng Wang and Lin Gao, Parametric optimization and comparative study of organic rankine cycle (ORC) for low grade waste heat recovery, Energy Conversion and Management, 50, 2009, 576-582.

[6] J. Larjola, Electricity from industrial waste heat using high speed Organic Rankine Cycle (ORC), Production Economics, 41, 1995, 227-235.

[7] Donghong Wei, Xuesheng Lu, Zhen Lu and Jianming Gu, Performance analysis and optimization of organic Rankine cycle (ORC) for waste heat recovery, Energy Conversion and Management, 48, 2007, 1113–1119.

[8] Ramesh K. Shah and Dusan P. Sekulic, Fundamentals of heat exchanger design (John Wiley and Sons, Inc., NJ: Hoboken, 2003).

[9] Sadic Kakac and Hongton Liu, Heat Exchangers: selection, rating and thermal design, 2nd ed (CRC Press,NJ: United States of America, 2002).

[10] S. Mostafa Ghiaasiaan, Two-Phase Flow, Boiling and Condensation in Conventional and Miniature Systems (Cambridge University Press, NJ: New York, 2008).

CONTOURLET TRANSFORM FOR FABRIC DEFECT DETECTION

Leena Patil[1], Prof. M.S.Biadar[2]

[1,2] *E & TC, Siddhant College of Engineering, Pune, (India)*

ABSTRACT

Contourlet Transform is the advanced method for the detection of fabric defects. Smooth edge information can be obtained from Contourlet Transform. It has many advantages such as multi directionality, anisotropy, multi resolution over Wavelet Transform. A new filter bank structure is the contourlet filter bank that can provide a flexible multi scale and directional decomposition for images. A new filter bank structure is there which consist of Laplacian Pyramid and Directional Filter Bank. Edges are image points with discontinuity, whereas contours are edges that are localized and regular. So contourlet can be defined as a multi-scale, local and directional contour segment which can be constructed using filter banks.

Keywords: Contourlet Transform, Defect Detection, Directional Filter Bank, Gaussian Pyramid, Laplacian Pyramid

1 INTRODUCTION

Fabric, being a widely used material in daily life, is manufactured with textile fibers. Textile fibers can be made of natural element such as cotton or wool; or a composite of different elements such as wool and nylon or polyester. In particular, defects result from machine faults, yarn problems, poor finishing, and excessive stretching, among others. Examples of some of the defects are netting multiple, warp float, hole, dropped stitches and press-off. A serious defect can render the fabric product unsalable and a loss in revenues. Traditionally, human inspection, carried out in wooden board, is the only means to assure quality. It helps instant correction of small defects, but human error occurs due to fatigue, accuracy is also less and fine defects are often undetected. Hence, automated inspection becomes a natural way forward to improve fabric quality, increased accuracy and efficiency and reduce labor costs. Automated fabric defect detection is therefore beneficial.

Minh N. Do and Martin Vetterli in the paper “Wavelet Based Texture Retrieval Using Generalized Gaussian Density and Kullback- Leibler Distance,” have proposed statistical view of texture retrieval by combining Feature Extraction and Similarity Measurement. Wavelet based texture retrieval is based on accurate modeling of marginal distribution of wavelet coefficients using Generalized Gaussian Density.

Minh N. Do and Martin Vetterli in the paper “The Contourlet Transform: An Efficient Directional Multi resolution Image Representation,” have proposed double filter bank structure, named the pyramidal directional filter bank, by

combining the Laplacian Pyramid with a directional filter bank The result is called the Contourlet Transform, which provides a flexible multi resolution, local and directional expansion for images.

Mohand Said Allili in the paper "Wavelet Modeling Using Finite Mixtures of Generalized Gaussian Distributions: Application to Texture Discrimination and Retrieval" have addressed statistical based texture modeling using wavelets. He proposed that the new method for representing the marginal distribution of wavelet coefficients is finite mixture of generalized Gaussian distributions which captures wide range of histogram shapes which provide better description and discrimination of texture.

Wavelet Transforms can be used as a means of feature detection. After the wavelet decomposition at each level, the image will be divided into four sub-images which are the approximate, horizontal, vertical, and diagonal coefficients. In order to obtain the approximate coefficients, the rows and columns are passed through the low-pass filter which resembles the original image, albeit at a sub sampled resolution. Next the horizontal coefficients are obtained by passing the rows through the low-pass filter and the columns through the high-pass filter, which will emphasize the horizontal edges. The vertical coefficients are obtained by passing the columns through the low-pass filter and the rows through the high-pass filter that will stress the vertical edges. Lastly, when both the columns and rows are passed through the high-pass filter, this will produce the diagonal coefficients which accent the diagonal edges. Some of the benefits of using wavelet decomposition are that multiscale analysis; salient features of original image are preserved in the approximate coefficients, real-time implementation, and can be developed for a parallel computer. One disadvantage with wavelet decomposition is that wavelets are not shift invariant; therefore, wavelets are not able to change with the translation operator. Also the wavelet transform is incapable of providing directionality and anisotropy. These disadvantages of wavelet transform are overcome by contourlet transform.

The Contourlet Transform is a 2-D transform technique recently developed for image representation and analysis. Also referred to as the pyramidal directional filter bank, it consists of two filter banks. The first filter bank, known as the Laplacian pyramid, is utilized to generate a multiscale representation of an image of interest. Subsequently, the subband images from the multiscale decomposition are processed by a directional filter bank to reveal the directional details at each specific scale level. The output values from the second filter bank are called "contourlet coefficients."

II PROPOSED METHOD

In this paper we are going to use contourlet transform and MoGG for fabric defect detection. First the preprocessing is done on original image (image with defect). In preprocessing there can be color to gray conversion or noise removal in the image is done.

Then contourlet transform is used to extract the features in the image. Then using MoGG modeling of contourlet coefficients the fabric defect detection is done.

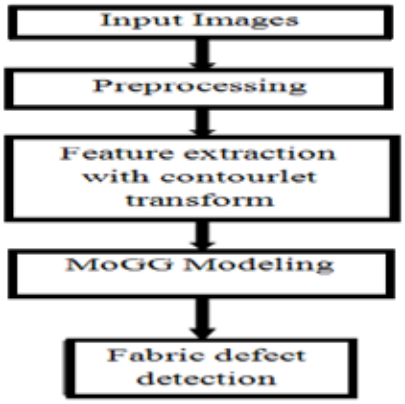

Fig: 2.1: Block Diagram of Proposed System

2.1 Contourlet Transform

The transform uses a double filter bank structure for obtaining sparse expansions for typical images having smooth contours. In the double filter bank structure: Laplacian Pyramid (LP) and Directional Filter Bank (DFB). In particular, the Contourlets have elongated supports at various scales, directions and aspect ratios. This allows Contourlets to efficiently approximate a smooth contour at multiple resolutions. In the frequency domain, the contourlet transform provides a multiscale and directional decomposition. The Contourlet transform uses a double filter bank structure to get the smooth contours of images. In this double filter bank, the Laplacian Pyramid (LP) is first used to capture the point discontinuities, and then a Directional Filter Bank (DFB) is used to form those point discontinuities into linear structures as shown in Fig.2.2.

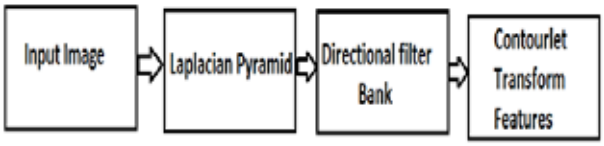

Fig. 2.2: Contourlet transform procedure

The Laplacian Pyramid (LP) decomposition only produces one band pass image in a multidimensional signal processing, which can avoid frequency scrambling. And DFB is only fit for high frequency since it will leak the low frequency of signals in its directional subbands. This is the reason to combine DFB with LP, which is multiscale decomposition and remove the low frequency. Therefore, image signals pass through LP subbands to get band pass signals and pass those signals through DFB to capture the directional information of image. This double filter bank structure of combination of LP and DFB is also called as Pyramid Directional Filter Bank (PDFB), and this transform is approximate the original image by using basic contour, so it is also called discrete contourlet transform.

2.2 Laplacian Pyramid

One way to obtain a multiscale decomposition can be obtained by using the Laplacian Pyramid. The LP decomposition at each level generates a down sampled low pass version of the original and the difference between the original and the prediction, resulting in a band pass image.

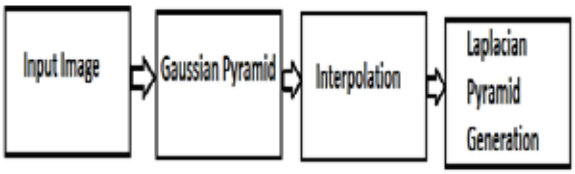

Fig. 2.3: Basic steps in Laplacian pyramid generation

The original image is convolved with a Gaussian kernel. The resulting image is a low pass filtered version of the original image. The Laplacian is then computed as the difference between the original image and the low pass filtered image. This process is continued to obtain a set of band-pass filtered images (since each one is the difference between two levels of the Gaussian pyramid). Thus the Laplacian Pyramid is a set of band pass filters. By repeating these steps several times a sequence of images, are obtained. If these images are stacked one above another, the result is a tapering pyramid data structure as shown in Fig. 2.4

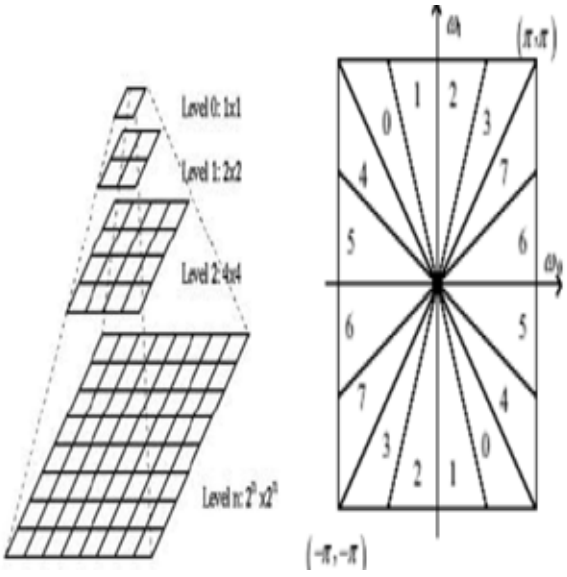

Fig. 2.4: Laplacian Pyramid structure & DFB Frequency Partitioning [9]

2.3 Directional Filter Bank (DFB)

DFB is designed to capture the high frequency content like smooth contours and directional edges. This DFB is implemented by using a k-level binary tree decomposition that leads to 2k directional sub-bands with wedge shaped frequency partitioning as shown in Fig.2.4 The DFB divides a 2-D spectrum into two directions, horizontal and

vertical. The second one is a shearing operator, which amounts to the reordering of image pixels. Due to these two operations, directional information is preserved. The scheme is flexible since it allows for a different number of directions at each scale.

2.4 Gaussian pyramid

The first step in Laplacian pyramid coding is to low-pass filter the original image g_0 to obtain image g_1. We say that g_1 is a "reduced" version of g_0 in that both resolution and sample density are decreased. In a similar way we form g_2 as a reduced version of g_1, and so on. Filtering is performed by a procedure equivalent to convolution with one of a family of local, symmetric weighting functions. An important member of this family resembles the Gaussian probability distribution, so the sequence of images g_0, g_1, g_2, ------- g_n, is called the Gaussian pyramid.

2.4.1 Gaussian Pyramid Generation

Suppose the image is represented initially by the arrays g_0 which contains C columns and R rows of pixels. Each pixel represents the light intensity at the corresponding image point by an integer I between 0 and K - 1. This image becomes the bottom or zero level of the Gaussian pyramid. Pyramid level 1 contains image g_1, which is a reduced or low-pass filtered version of g_0. Each value within level 1 is computed as a weighted average of values in level 0 within a 5-by-5 window. Each value within level 2, representing g_2, is then obtained, from values within level 1 by applying the same pattern of weights. A graphical representation of this process in one dimension is given in Fig.2.5. The size of the weighting function is not critical. We have selected the 5-by-5 pattern because it provides adequate filtering at low computational cost. The level-to-level averaging process is performed by the function REDUCE.

g_k = REDUCE (g_k- 1)

Which means, for levels $0 < l < N$ and nodes i, j, $0 < i < C_l$, $0 < j < R_l$.

$$g_l(i, j) = \sum_{m=-1}^{1} \sum_{n=-1}^{1} w(m, n) * g_{l-1} * (2i + m, 2j + n)$$

Here N refers to the number of levels in the pyramid, while C and R, is the dimensions of the l^{th} level.

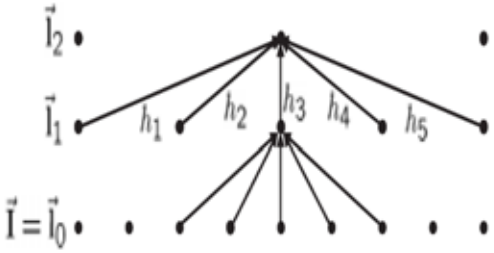

Fig.2.5: One-dimensional graphic representation of the process which generates a Gaussian Pyramid [9]

III EXPERIMENTAL RESULTS

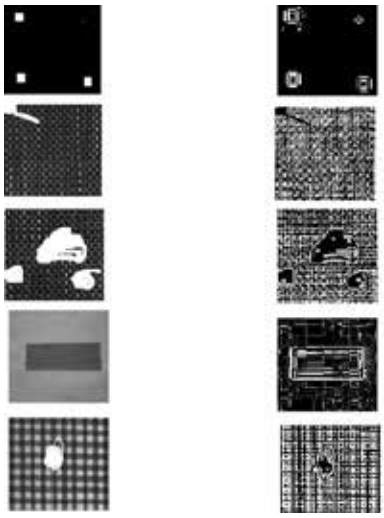

(a) **(b)**

Fig.3.1: (a) Original images with defects (b) Detected defect in images

IV CONCLUSION

The drawbacks associated with the 2-D wavelet transform such as multiresolution, localization, directionality and anisotropy are overcame by contourlet transform. Contourlet transform is capable of capturing the smooth edges information. A new filter bank structure is the contourlet filter bank that can provide a flexible multiscale and directional decomposition for images.

Contourlet transform is good at detecting texture directions. Accuracy of classification is higher than wavelet related methods. Only simple norm-based metric is required for texture classification.

REFERENCES

[1] M. S. Allili and N. Baaziz, "Contourlet-based texture retrieval using a mixture of generalized Gaussian distributions," in Proc. Int. Conf. Computer Analysis of Images and Patterns, 2011, no. 2, pp. 446–454.

[2] N. Baaziz, "Adaptive watermarking schemes based on a redundant contourlet transform," in Proc. IEEE Int. Conf. on Image Processing, 2005, pp. I-221–I-224.

[3] P. J. Burt and E. H. Adelson, "The Laplacian pyramid as a compact image code," IEEE Trans. Commun., vol. 31, no. 4, pp. 532–540, 1983.

[4] E. J. Candes and D. L. Donoho, "New tight frames of curvelets and optimal representations of objects with piecewise-C2 singularities," Commun. Pure Appl. Math., vol. 57, pp. 219–266, 2002.

[5] M. N. Do and M. Vetterli, "Wavelet-based texture retrieval using generalized Gaussian density and," IEEE Trans. Image Process., vol. 11, no. 2, pp. 146–158, 2002.

[6] M. N. Do and M. Vetterli, "Rotation invariant texture characterization and retrieval using steerable wavelet-domain hidden Markov models," IEEE Trans. Multimedia, vol. 4, no. 4, pp. 517–527, 2002.

[7] M. N. Do and M. Vetterli, Contourlets, Beyond Wavelets, G. V. Wellard, Ed. New York, NY, USA: Academic, 2003.

[8] Z. He and M. Bystrom, "Color texture retrieval through contourlet based hidden Markov model," in Proc. IEEE Int. Conf. Image Processing, 2005, pp. 513–516.

[9] M. N. Do and M. Vetterli, "The contourlet transform: An efficient directional multiresolution image representation," IEEE Trans. Image Process., vol. 14, no. 12, pp. 2091–2106, 2005.

[10] Z. Yifan and X. Liangzheng, "Contourlet-based feature extraction on texture images," in Proc. Int. Conf. Computer Science and Software Engineering, 2008, pp. 221–224.

[11] Mohammad H. Rohban, and Shohreh Kasaei, "Skin Detection using Contourlet-Based Texture Analysis," IEEE Fourth International Conference on Digital Telecommunications, pp. 59-65,2009

[12] Ali Mosleh, Farzad Zargari, Reza Azizi,"Texture Image Retrieval Using Contourlet Transform," IEEE conference on Image Processing, 2009

[13] Sherin M. Youssef, Ezzat A. Korany, Rana M. Salem, "Contourlet-based Feature Extraction for Computer Aided Diagnosis of Medical Patterns," 11th IEEE International Conference on Computer and Information Technology, pp. 481-487, 2011

[14] Zhiling Long, and Nicolas H. Younan, "Contourlet Spectral Histogram for Texture Classification," IEEE conference on image processing, pp. 31 -36, 2006

PATTERNED FABRIC DEFECT DETECTION USING BOLLINGER BAND METHOD

Jyoti Nikam[1], Prof. M.S.Biadar[2]

[1,2] *E & TC, Siddhant College of Engineering, Pune, (India)*

ABSTRACT

This paper analyses how the Bollinger Band method is used to represent defective objects and repeated patterns in fabric images. Regularity is one of the main features for many Patterned texture material inspection. This study shows the new approach called Bollinger Band (BB) method which is used to outline the shape of the defective region. In the proposed method the Bollinger Band is calculated based on standard deviation and moving average. The Bollinger Band method is shift invariant approach and hence immune of the alignment. In this paper the upper Bollinger band and lower Bollinger bands are developed to indicate defective areas in patterned fabric. Abnormal changes in the pattern lead to large variation in the standard deviation. Its mathematical definition was simple. For defect detection on patterned texture application of Bollinger Band is divided into training stage and testing stage.

Keywords : Bollinger Band, Defect Detection, Histogram Equalization, Moving Average, Patterned Fabric, Standard Deviation.

I INTRODUCTION

Nowadays automated fabric inspection is a more effective technique in the production of automation. In automated industry defect inspection is the most effective technique because on-loom machine material will move around a speed of 200dpi/ meter so human inspection is not possible with this speed. Errors are caused by human fatigue. Quality assurance and quality control is necessary to retain the stability in the market and maintain the quality. Quality control is nothing but the manufacturing the fabric without defect. Defect is nothing but the flaw on the fabric. So due to automated inspection human errors are minimized and increase the efficiency, reduce the labor cost and computational time which is most effective measures for the improvement of fabric quality. Textures are broadly classified into patterned regular textures and irregular textures. This paper analyses the patterned texture inspection. Fabric is a 2-D pattern texture and is underlined lattice with its symmetry properties governed by its 17 wallpaper groups. In mathematical algebra the wallpaper groups also known as the crystallographic groups. Pattern texture of such a wallpaper group can be generated by at least one of its symmetry rules on lattice among translational, rotational, reflectional and glide reflectional symmetries [1]. These 17 wallpaper groups are named as p1, p2, pm, pg, cm, pmm, pmg , pgg, cmm, p4, p4m, p4g, p3, p3m1, p3mp6, and p6 while letter p refers to primitive and c is a centered cell. The integer that follows p or c denotes the highest order of symmetry that is 1-fold, 2-fold, 3-fold, 4-fold, or 6-fold. Where symbol m indicates

a reflectional symmetry and g is a glide reflectional symmetry. Generally the patterned fabric inspection methods depend upon the spectral, statistical, model based, learning and structural. This is a natural study about the underlying patterned fabric and the geometrical defective objects in fabric images. For defect detection some previous methods will not give correct result for dot, star, and box patterned fabric which is a complicated patterned fabric [7]. Whereas for the grey relational analysis, (DT) Direct Thresholding, (WGIS) Wavelet Golden Image Subtraction [2], (LBP) Local Binary Pattern, (BB) Bollinger band methods are developed for complicated pattern fabrics. Out of that Direct Thresholding, and Local Binary Pattern belongs to spectral approach and Bollinger Band, Wavelet Golden Image Subs traction belongs to mixture of statistical and filtering approach. In this the BB having a regularity property in the patterned texture which is further used to detect the defects in the simple patterned texture of (p1 wallpaper group) that means all above approaches are classified under non –motif based approach which treat whole input image for fabric inspection. Bollinger Band consists of Lower Band, Upper Band, and Middle band. By the principle of the Bollinger Band method that is the patterned rows (columns) will generate periodic upper and lower bands. Any defective region in patterned fabric means that there would be break of periodicity in the pattern. Abnormal changes in the Upper Band and Lower Band leads to large variation in standard deviation.

II PROPOSED METHOD

2.1 Bollinger Band Method

Mostly it is used for financial technical analysis based on moving average and standard deviation. It provides a relative definition of high and low prices mainly in stock market for oversold and over brought shares.[8]. Bollinger band consists of Middle band with only moving average, lower band and upper band having moving average and standard deviation. It was extended from 1-D approach to 2-D approach for jacquard fabric inspection. The detection accuracy achieved is 98.59% in good quality from three groups (pmm, p2 and p4m). Bollinger band method was shift invariant across patterned fabric material in addition it was able to outline the shape of defects [3]. [4].

Fabric defect detection Bollinger Band mainly consists of two stages:-

1) Training stage 2) Testing stage

2.1.1 Training Stage

Training stage consists of defect free image the threshold values are determined from the Bollinger band of the reference defect free image. The flow diagram for training for reference free image is shown in Fig1.

Step1. Histogram equalization helps in reducing the noise on the images and makes the later threshold process more reliable. Mainly this block is used for contrast enhancement to show equalization of the signal. Which is shown in Fig 2 **(**a) Defect-free sample of star-patterned fabric without histogram equalization, (c) the histogram of (a), (b) defect-free sample of Star- patterned fabric with histogram equalization, (d) the histogram of (b). it shows a comparison of two defective samples with and without histogram equalization as a preprocessing step. The resultant image show better results with histogram equalized preprocessing than those without histogram equalization. Defect on the fabric is usually characterized by high frequency changes in pixel intensities within an image.

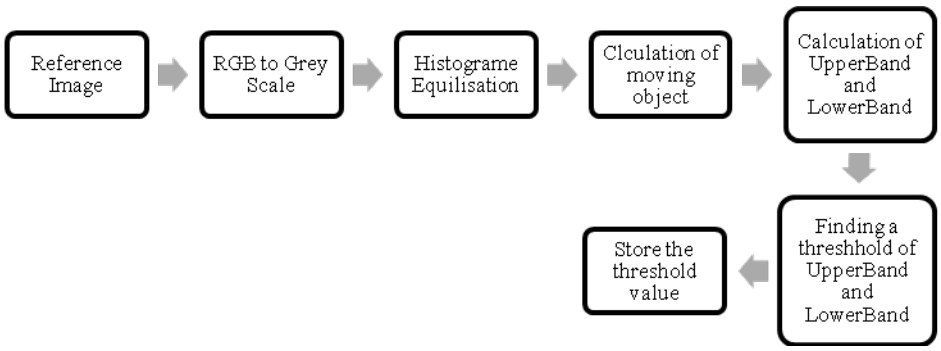

Fig1. Flow diagram for training of fabric defect detection using Bollinger Band

Step2. Calculation of moving average or mean

The input image is first converted into the 1-d vector, then the moving average is calculated for the period of n=20 where n denotes the row dimension of repetitive unit.

$$M_r = \frac{\sum_{j=r1}^{rn} x_j}{n}$$

Where Mr= is moving average for input image, n=period, x_j = Value of image pixel for the given period. The moving average for n=20 is shown in Fig.2(e).

Step3. Calculation of Upper band and Lower band

For input image calculation of Upper band and Lower band depends upon the moving average and standard deviation which is calculated by following formula and shown in Fig .2(f) and (g)

Upper band is defined as

$$UB_r = M_r + d * \delta_r$$

Lower band is defined as

$$LB_r = M_r - d * \delta_r$$

The standard deviation is defined as

$$\delta_r = \sqrt{\frac{\sum_{j=r1}^{rn} (X_j - M_r)^2}{n}}$$

Step 4: Obtained the threshold values

In this calculation of Upper band is maximum (UBmax1) and Minimum of (UBMin1), and for lower band is Maximum of (LBMax1) and Minimum of (LBMin1). Combination of Upper Band, Lower Band and Moving average is shown in Fig.2 (h) which is computation of all.

2.1.2 Testing Stage

The testing stage consists of similar stages of training stage. Here for the calculation of Bollinger band, the threshold values of Upper band of testing stage are compared with the threshold values of upper band of training stage(reference image) and the testing stage threshold values of lower band are compared with threshold values

of lower band of training stage(reference image). But for testing take a defected image. The flow diagram for testing stage is shown in Fig.3.

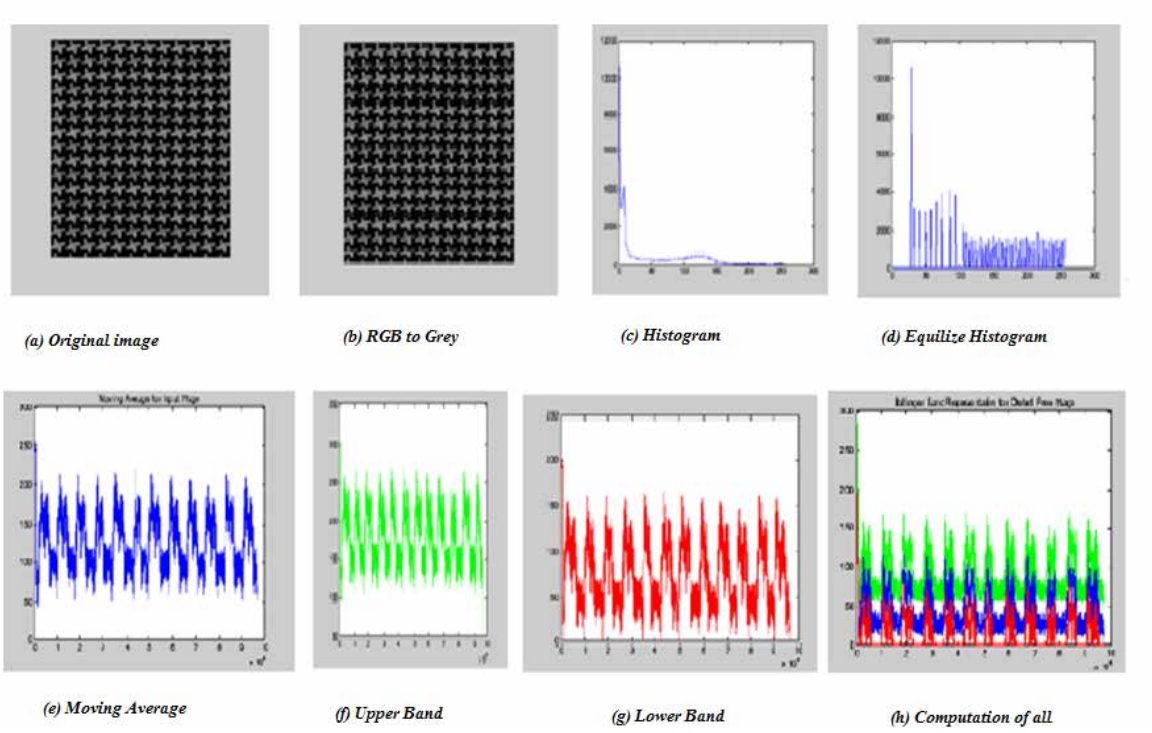

Fig2. Training stage Results

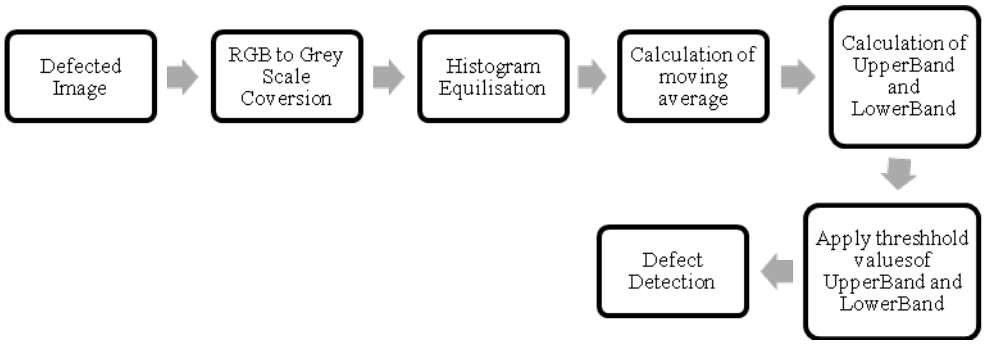

Fig 3: Flow diagram of testing stage of defected image for the representation of Bollinger Band.

Step1:-Histogram equalization of input images

The defected images with hole or any defect take its histogram, the histogram equalized image and its histogram is given in Fig.4. **(**a)Defected sample of star-patterned fabric without histogram equalization, (c) the histogram of (a), (b) Defected sample of Star-patterned fabric with histogram equalization, (d) the histogram of (b).

Step2. Calculation of moving average or mean is shown in Fig.4 (e).

Step3. Calculation of the upper band and lower band is shown in Fig.4. (f) and (g). In this the value of upper band and lower band of the Bollinger band representation of the defected image is shown. In this the value of upper band and lower band will cross the threshold value (determined in training stage) at the position of defect.

Step4. Threshold the Upper band and Lower band with corresponding threshold values determined during testing stage as shown in Fig.4 (h).

f (x) = 1 UB Max1 > UB Max

Step5. Detect the defect in defected image using comparison of threshold values in the testing stage and training stage.

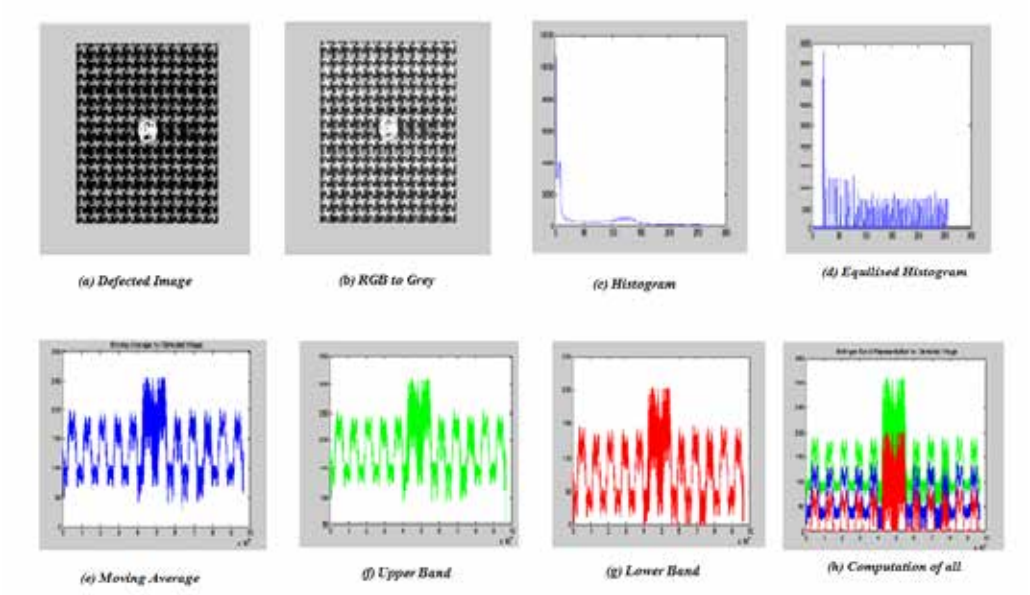

Fig 4: Testing Stage Results

III EXPERIMENTAL RESULTS

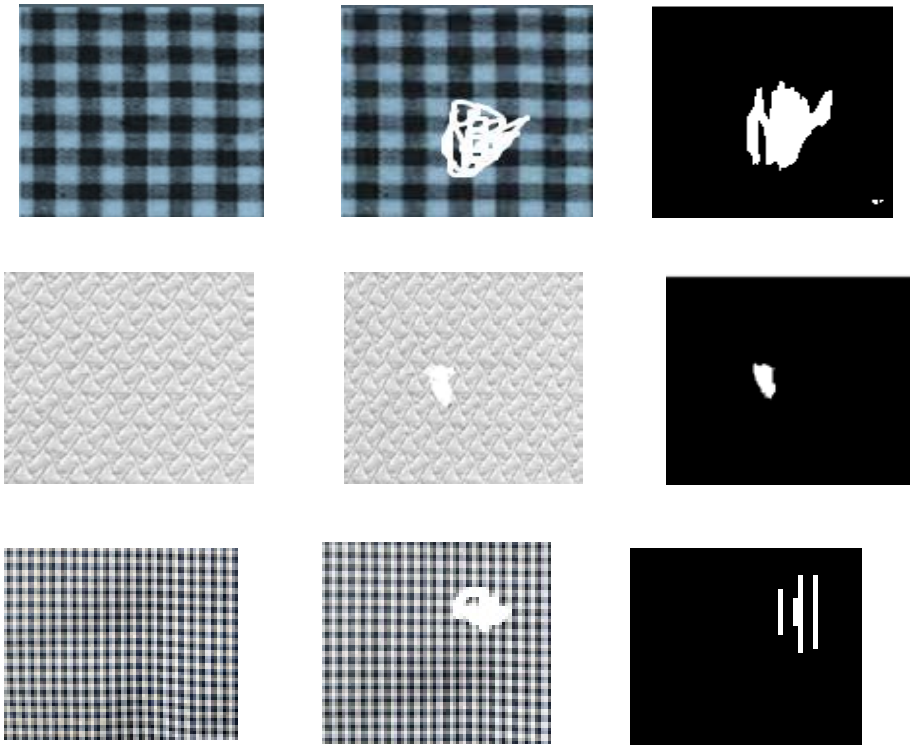

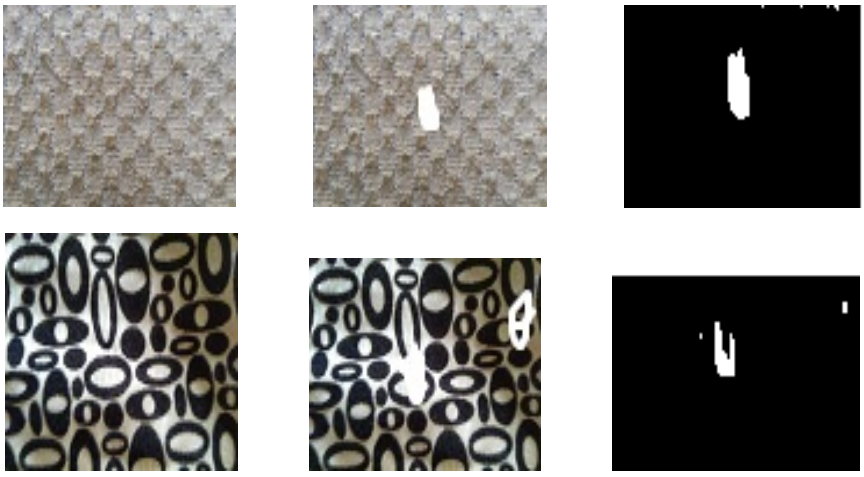

(a) (b) (c)

Fig5. (a) Original Image (b) Defected Image (c) Detected defect.

IV CONCLUSION

In this paper the Bollinger band method used for patterned fabric defect detection is very effective and robust for regular patterned fabric. Its strength is periodic in nature and any change in the periodic signal will affect the output. As compared to other patterned fabric defect detection methods its 1-D approach is suitable to optimizing the period lengths (that is n) if it select a larger than repetitive unit. By using BB the alignment problem occurred in wavelet Subtraction method is solved. It require less computation time. It is simple to implement and the mathematical definition was very simple. Its efficiency is also high as compared to DT and WGIS. While using BB method light color differences such as light shade not detected by the Bollinger Band method because it is only applicable for gray scaled images not to the RGB scaled images.

REFERENCES

[1] Henry Y.T. Nagan, Grantham K. H. Pang and Nelson H. C. Yung. “Automated fabric defect detection-A review”. Image Vision Computing. Vol. 29, No 7, pp. 442-458, in 2011

[2] Henry Y.T. Nagan, Grantham K. H. Pang, S. P. Yung, Michael K. Ng. “Wavelet based methods on patterned fabric defect detection”. Pattern Recognition, Vol. 38, No 4, pp. 559-576, 29 July 2004.

[3] Henry Y.T. Nagan, Grantham K. H. Pang. “Regularity Analysis for Patterned Texture Inspection”, IEEE Transactions Aut. Sci. and eng, Vol 6, No1, pp.131-144, 2009.

[4] Henry Y.T. Nagan, Grantham K. H. Pang. “ Novel method for patterned fabric inspection using Bollinger Bands” Opt Eng, Vol 45, No 8, Aug 2006.

[5] Henry Y.T. Nagan, Grantham K. H. Pang and Nelson H. C. Yung. “ Motif based defect detection using patterned fabric” Pattern Recognition, Vol. 41, No. 6, pp. 1878-1894, 12 Nov. 2007.

[6] Henry Y.T. Nagan, Grantham K. H. Pang and Nelson H. C. Yung “ Patterned fabric defect detection using a motif-based approach” IEEE Transaction, 2007.

[7] Michal K. Ng, Henry Y. T. Nagan, Xiaoming Yuan, and Wenxing Zhang. Patterned fabric inspection and visualization by the method of image decomposition. IEEE Transactions on Aut. Sci. and Eng, Vol. 11, No. 3, 2014

[8] Roland T. Chin, Charles A. Harlow "Automated visual inspection: A Survey" IEEE Transaction on Pattern Analysis and Machin Intelligence, Vol.PAMI-4, No. 6,November 1982.

[9] Henry Y.T. Nagan, Grantham K. H. Pang," Pattern Fabric defect detection Using A Motif-Based Approach" IEEE The University of Hong Kong, 2007.

[10] Anil K. Jain," Texture Analysis", The Handbook of Pattern Recognition and computer vision(2nd Edition), 1998.

[11] Henry Y.T. Nagan, Grantham K. H. Pang," Performance Evaluation for Motif-Based Patterned Texture Defect Detection", IEEE Transaction on Automation Science and Engg, Vol. 7, No 1, Jan 2010.

[12 H. Sari-Sarraf and J.S. Goddard, "Vision System for on-loom fabric inspection",IEEE Trans.Ind,Appl.35(6), in 1999.

[13] Michal K. Ng, Xiaoming Yuan, and Wenxing Zhang," Coupled Variational Image Decomposition and Restoration Model for Blurred Cartoon-Plus-Texture Images With Missing Pixels", IEEE Transaction on image Processing, VOL.22,NO.6,JUNE 2013.

[14] Xue Zhi Yang, Grantham K. H. Pang and Nelson H. C. Yung, " Discriminative Fabric Defect Detection Using Adaptive Wavelets", Society of Photo-optical instrumentation Engineers, December 2002.